

**REMOVAL OF CONTAMINANTS IN USED LUBRICATING OIL  
WITH CHEMICAL ACTIVATED CARBONS FROM PALM KERNEL  
AND COCONUT SHELLS**

**BY**

**BOADU, KWASI OPOKU  
BSc. (UCC, Ghana), MSc. (UAS, Germany)  
G2017/Ph.D/ACE-CEFOR/FT/ 076**

**DEPARTMENT OF CHEMICAL ENGINEERING  
FACULTY OF ENGINEERING  
UNIVERSITY OF PORT HARCOURT,  
PORT HARCOURT, RIVERS STATE, NIGERIA**

**IN COLLABORATION WITH WORLD BANK AFRICA CENTRE OF  
EXCELLENCE FOR OIL FIELDS CHEMICALS RESEARCH  
UNIVERSITY OF PORT HARCOURT**

**JANUARY, 2020**



# CERTIFICATION

UNIVERSITY OF PORT HARCOURT

SCHOOL OF GRADUATE STUDIES

**REMOVAL OF CONTAMINANTS IN USED LUBRICATING OIL WITH  
CHEMICAL ACTIVATED CARBONS FROM PALM KERNEL AND COCONUT  
SHELLS**

BY

**KWASI OPOKU BOADU**

**G2017/Ph.D/ACE-CEFOR/FT/ 076**

The Board of Examiners certifies that this Thesis is accepted in partial fulfilment of the requirements for the award of the degree of Doctor of Philosophy (PhD) in Chemical Engineering.

DESIGNATION	NAME	SIGNATURE	DATE
Supervisor (1)	Prof. O. F. Joel	-----	-----
Supervisor (2)	Prof. D. K. Essumang	-----	-----
Supervisor (3)	Dr B. O. Evbuomwan	-----	-----
Centre Leader	Prof. O. F. Joel	-----	-----
Dean, Faculty of Eng.	Prof. O. F. Joel	-----	-----
Chairman, Departmental Graduate Board	Prof. A.O. Kuye	-----	-----
External Examiner	Prof. E.O. Ekumankama	-----	-----
Dean, School of Graduate Studies/Chairman of Board of Examiners	Prof. A.A Okeregwo	-----	-----

## **DEDICATION**

This research work is dedicated to my mother Abena Nyantakyiwaa, wife Mrs Mavis Opoku Boadu and children Ama Nyantakyiwaa Opoku Boadu, Naana Abena Opoku Boadu, Yaa Ntiwaa Opoku Boadu and Kofi Opoku Boadu.

## **ACKNOWLEDGEMENTS**

I wish to express my ultimate gratitude to my supervisors Prof. Ogbonna .F. Joel; Prof. David K. Essumang and Dr Benson O. Evboumwan for their guidance, timely discussions, suggestions, corrections, constructive criticism and encouragement throughout my research work. This enabled me to accomplish my task on time. My esteemed supervisors made my research work very pleasant and enjoyable by making available all the resources needed.

I did appreciate their advice and inputs right from day one, which helped to move this work forward as planned.

My profound appreciation also goes to the University of Cape Coast (UCC) and World Bank African Centre of Excellence for Oil Field Chemicals Research (ACE-CEFOR) for granting me the scholarship opportunity, providing the resources (research grants, stipends and study leave in the case of UCC etc.). Without their assistance, this project would not have been accomplished.

I am particularly grateful to the ACE-CEFOR Centre Leader and my principal supervisor Prof. Ogbonna .F. Joel, for his constant motivation, encouragement, support and care, which always kept me on track. My sincere gratitude is also extended to all other Professors in ACE-CEFOR, especially Prof. Ajienka.

To my fellow students, the staff of ACE-CEFOR and POCEMA, I say a big thank you for your warm friendship and most in-depth support. It was a great opportunity, a pleasant and valuable experience working with you. Indeed, you all made me feel at home throughout my studies.

## ABSTRACT

This research work examined the heavy metals contaminants and physico-chemical parameters of virgin and used lubricating oils using Atomic Adsorption Spectrometer for copper, cadmium, zinc, lead, magnesium, iron and chromium elements using various ASTM D methods. The results obtained shows that there were significant differences in the virgin and used lubricating oils. Comparative studies of the physicochemical properties of chemically activated carbon from palm kernel (PKS) and coconut (CNS) shells were investigated. From the results obtained, the chemically activated carbon prepared from palm kernel and coconut shells showed good physicochemical properties and adsorption capacity. For instance palm kernel shells were able to reduce the following metals Zinc, 28.7%; Cadmium, 75.1%; Chromium, 67.3% and Magnesium, 97.5% respectively. In the case of coconut shells the reduction were as follows, Zinc, 64.9%; Cadmium, 96.1%; Magnesium, 91.65% and 0.6% increase in Chromium. It was observed that the coconut shell activated carbon was effective in the removal of lead (Pb), 60.50% metals while palm kernel shell could not but increase its concentration by 59.2%. However, coconut shell with BET surface area of 1177.520 (m<sup>2</sup>/g) and pH 7.5, performed better as an adsorbent than palm kernel shell with BET surface area of 717.142(m<sup>2</sup>/g) and pH 8.7 respectively. Also, coconut shell has a specific gravity of 1.42 and moisture content of 19.7% compared to palm kernel shell with the specific gravity of 1.61 and moisture content of 20.4% respectively. In contrast, the activated carbons produced from palm kernel and coconut shells are not suitable for the removal of both copper and iron metals. The fit of this isotherm model to the equilibrium adsorption data were determined, using the linear coefficient of determination (R<sup>2</sup>). The following R<sup>2</sup> values were obtained; Copper (0.8185), Cadmium (0.8347), Lead (0.9349), Chromium (0.9378), Iron (0.9927), Zinc (0.9953), and Magnesium (0.9997) respectively. The results obtained revealed that the Langmuir model shows a better fit due to the high coefficient of determination (R<sup>2</sup> ≈ 1). The recovered oil could be used again.

## **TABLE OF CONTENTS**

DECLARATION	ii
CERTIFICATION	iii
DEDICATION	iv
ACKNOWLEDGEMENTS	v
ABSTRACT	vi
TABLE OF CONTENTS	vii
LIST OF TABLES	xi
LIST OF FIGURES	xii
LIST OF PLATES	xiii
LIST OF ABBREVIATIONS/SYMBOLS	xiv
<b>CHAPTER ONE: INTRODUCTION</b>	<b>1</b>
1.1 Background to the Study	1
1.2 Statement of the Problem	1
1.3 Used Oil Recycling	2
1.4 Environmental Concerns of Used Oil	4
1.5 Aim and Objectives of the Study	7
1.6 Scope of the Study	8
<b>CHAPTER TWO: LITERATURE REVIEW</b>	<b>9</b>
2.1 Characteristics of Palm Kernel and Coconut Shells	9
2.2. Adsorption Isotherms	13
2.2.1 Langmuir Isotherm Model	13
2.2.4 Toth Isotherm Model	15
2.2.5 Tempkin isotherm	15
2.2.6 Freundlich-Jovanovic Isotherm Model	16
2.2.7 Linear Isotherm Models	16
2.3 Used lubricating oils (ULOs)	18
2.3.1 Conventional Methods	21
2.3.2 Acid-clay	21
2.3.3 Solvent Extraction	22
2.3.4 Vacuum distillation	23
2.3.5 Hydrogenation	24

2.3.6	Membrane Technology	25
2.3.7	Catalytic Process	25
2.4	Combined Technologies/methods	26
2.4.1	Vaxon process	26
2.4.2	Chemical Engineering Partners (CEP) process	27
2.4.3	Ecohuile process	27
2.4.4	Cyclon process	28
2.4.5	Studi Technologie Progetti S.p.A (STP) method	29
2.4.6	Interline process	29
2.4.7	Propak thermal cracking process	29
2.4.8	Hylube process	30
2.4.9	Snamprogetti process/ IFP technology	31
2.4.10	Revivoil process	32
2.4.11	Mineral Oil Raffinerie Dollbergen (MRD) solvent extraction process using N-methyl-2-pyrrolidone	33
2.5	Modern Technologies for Used Oil Re-refining	35
2.6	Knowledge Gap	40
 <b>CHAPTER THREE: MATERIALS AND METHODS</b>		 41
3.1	Activated Carbon Samples Collection, Preparation and Characterization	41
3.1.1	Chemical Activation and Carbonization	43
3.2	Determination of the Physiochemical Properties of the Activated Carbon Samples.	43
3.2.1	pH Measurement	43
3.2.2	Determination of Moisture Content	44
3.2.3	Ash content Determination	44
3.2.4	Pore Volume Measurement.	45
3.2.5	Bulk Density and Porosity Determination	45
3.2.6	Surface Area Determination by Brunauer, Emmett and Teller (BET) (2015 Model ASAP 2020 Micromeritics Analyzer)	46 46
3.2.7	Fourier transform infrared spectra (FTIR)	46
3.2.8	Scanning Electron Microscopy (SEM)	47
3.2.9	Determination of Heavy Metals Present	47
3.3	Samples Collection, Preparation and Characterization	47
3.3.1	Preparation of Samples	48
3.3.2	Characterization of Samples	48



3.3.2. 1 pH Measurement	48
3.3.2.2 Specific gravity	48
3.3.2.3 Dynamic viscosity	48
3.3.2.4 Kinematic viscosity	49
3.3.2.5 Water content	49
3.3.2.6 Sediment content	49
3.3.2.7 Digestion and Elemental Analysis	49
3.5 Methods for Data Analysis and Presentation	50
<b>CHAPTER FOUR: RESULTS AND DISCUSSION</b>	<b>51</b>
4.0 Introduction	51
4.1 Presentation of Results	51
4.2. Discussions of Results	77
4.2.1. The physicochemical and concentration of heavy metals analyses in virgin and used lubricating oils: a spectroscopy study	77
4.2.1.2 Specific Gravity:	78
4.2.1.3 Dynamic viscosity:	78
4.2.1.4 Kinematic Viscosity:	78
4.2.1.5 Water and sediment contents:	79
4.2.1.6 Elemental Metals:	79
4.3.2. Comparative Studies of the Physicochemical Properties and Heavy Metals adsorption Capacity of Chemical Activated Carbon from Palm Kernel and Coconut shells	81
4.3.2.1 pH.	81
4.3.2.2 Moisture (%):	82
4.3.2.3 Ash content (%):	82
4.3.2.4 Pore Diameter (nm):	83
4.3.2.5 Bulk density (g/cm <sup>3</sup> ):	83
4.3.2.6 Porosity (%):	84
4.3.2.7 Specific gravity:	84
4.3.2.8 BET Surface area (m <sup>2</sup> /g):	85
4.3.2.9 Heavy Metals (ppm):	85
4.4 Surface morphology of chemically activated carbons produced from palm kernel and coconut shells	86
4.4.1 Fourier transform infrared (FTIR) analyses on the chemically activated carbon samples from coconut and palm kernel shells	89
4.4.2 Surface Area Data Summary	93

4.4.3	The properties of the filter beds	94
4.4.4	Adsorption capacities of the filter beds.	94
4.5	Adsorption of Heavy Metals in Used Lubricating Oil using Palm Kernel and Coconut Shells as Adsorbents.	95
4.6	Adsorption Isotherms	103
<b>CHAPTER FIVE: SUMMARY, CONCLUSIONS AND RECOMMENDATION</b>		<b>108</b>
5.1	Summary	108
5.2	Conclusions	109
5.3	Recommendations	110
5.4	Contributions to Knowledge	110
REFERENCES		112
APPENDICES		133
APPENDIX A: EXPERIMENTAL RAW DATA		133
APPENDIX B: STATISTICAL ANALYSIS		137
APPENDIX C: GRAPHS / ISOTHERMS (HEAVY METALS)		142
APPENDIX D: EQUATION OF THE MODEL (HEAVY METALS)		164
APPENDIX E: BET DATA AND THEORY		177
APPENDIX F: FTIR SPECTROSCOPY		190
APPENDIX G: SCANNING ELECTRON MICROSCOPY (SEM)		191
APPENDIX H: ATOMIC ABSORPTION SPECTROSCOPY (AAS)		193

## LIST OF TABLES

Table		Page
2.1	Types of Linear Isotherm Model	17
2.2	Previous studies conducted on the preparation of activated carbon from coconut and palm shells and their applications in removal of pollutants from wastewater and used lubricating oil	39
4.1	Physicochemical parameters of the virgin and used lubricating oil samples	51
4.2	Concentration levels of various elements present in virgin and used lubricating oil samples	52
4.3	Physico-Chemical Characteristics of Chemical Activated Carbons of Coconut and Palm Kernel Shells	53
4.4	Concentrations of heavy metals present in Coconut and Palm Kernel Shells	54
4.5	One-way ANOVA in SPSS Statistics of the activated carbons from coconut and palm kernel shells	55
4.6	Functional groups and the classification of compounds identified in chemically activated carbon from palm kernel shell by FTIR analysis	56
4.7	Functional groups and the classification of compounds identified in chemically activated carbon from Coconut shell by FTIR analysis	57
4.8	Surface Area Data Summary	58
4.9	Properties of the filter beds for the activated carbons from palm kernel and coconut shells	59
4.10	Volume of samples adsorbed by various filter beds, after filtration process and adsorption capacity	60
4.11	Mean, $\pm$ SD, of virgin and used lubricating oil samples before filtration with palm and coconut shells activated carbons	61
4.12	Mean, $\pm$ SD of virgin and used lubricating oil samples after filtration with Palm Kernel Shell Sample	62
4.13	Mean, $\pm$ SD of virgin and used lubricating oil samples after filtration with Coconut Shell Sample	63
4.14	Summary (LS means) - Filtration process	64
4.15	Analysis of Variance of Variables and Summary for all Y's for the various Heavy Metals	65

## LIST OF FIGURES

Figure		Page
4.1	Concentration of various heavy metals present in virgin and used lubricating oil samples	60

## LIST OF PLATES

<b>Plate</b>	<b>Page</b>
2.1 Palm Kernel Shells	10
2.2 Coconut Shells	12
2.3 Typical Recycling Process Cycle	20
3.1 Carbolite HT F17/5 High-Temperature Laboratory Chamber Furnace (5 litres 17000C)	42
4.1 SEM micrograph of Palm Kernel Shell	67
4.2 SEM micrograph of Coconut Shell	68
4.3 Picture of FTIR spectra of Palm Kernel Shells	69
4.4 Picture of FTIR spectra of Coconut Shells	70

## LIST OF ABBREVIATIONS/SYMBOLS

$q_{e,exp}$	Measured adsorbate concentration at equilibrium(mg/g)
$(q_e)_{mod}$	Calculated adsorbate concentration at equilibrium (mg/g)
$a_K$	Khan isotherm model exponent
$A_T$	Tempkin isotherm equilibrium binding constant (L/g)
$a_T$	Toth isotherm constant (L/mg)
$b$	Langmuir isotherm constant (L/mg)
$b_K$	Khan isotherm model constant
$b_T$	Tempkin isotherm constant [(J/mole)
$C_0$	Adsorbate initial concentration (mg/L)
$C_e$	Equilibrium concentration of adsorbate(mg/L)
<b>D. W. T.</b>	Durbin-Watson Test
$K_F$	Freundlich isotherm constant [(mg/g)
$(L/g)^n]$	Related to adsorption capacity
$K_{FJ}$	Freundlich-Jovanovic isotherm equilibrium constant (L/mg)
$K_T$	Toth isotherm constant (mg/g)
<b>M</b>	Adsorbent mass (g)
<b>MRPE</b>	Mean relative percentage error
<b>n</b>	Adsorption intensity
<b>N</b>	Number of experiments
$n_{FJ}$	Freundlich-Jovanovic isotherm exponent
$Q_0$	Maximum monolayer coverage capacity (mg/g)
$q_e$	Amount of adsorbate on the adsorbentat equilibrium (mg/g)
$q_{FJ}$	Maximum monolayer coverage capacities (mg/g)
$q_s$	Theoreticalisotherm saturationcapacity (mg/g)
<b>R</b>	Universal gas constant (8.314 J/mol K)
$R^2$	Co-efficient of determinant
<b>T</b>	Temperature (K)
<b>t</b>	Toth isotherm constant

<b>V</b>	Solution volume (L)
<b>HT</b>	High temperature
<b>FTIR</b>	Fourier-transform infrared spectroscopy
<b>BET</b>	Brunauer, Emmett and Teller
<b>SEM</b>	Scan electron microscopy
<b>ASTM D</b>	American Society for Testing and Materials
<b>PKS</b>	Palm kernel shells
<b>CNS</b>	Coconut shells

# **CHAPTER ONE**

## **INTRODUCTION**

### **1.1 Background to the Study**

Lubricating oils (LOs) are conventionally obtained from crude oil. Chemical composition of LOs consists, on average, of about 80–90% base oil and about 10–20% chemical additives and other compounds (Sonibare and Omoleye, 2018). Lubricating oils mainly help in reducing friction, dust, corrosion, protection against wear and tear and provision of the heat transfer medium in various equipment or machinery (Kannan *et al.*, 2014). During the operation period, LOs deteriorate, as well as their additives, and its physical and chemical properties become unsuitable for further use (Tsai, 2011). In the process of usage of lube oil, temperature build up occurs which breaks down the oil and weakens its properties such as pour point, flash point, specific gravity, viscosity etc. (Udonne and Bakare, 2013). These render the oil unsuitable for regular usage as a result of the presence of contaminants in the lube oil such as water, wear metals, carbon residue, ash content, gums, varnishes etc. Chemical changes in the oil occurred due to thermal degradation and oxidation. Europe represents 19% of the total worldwide market volume of lubricants, consuming around 6.8 million tons in 2015 (Kupareva *et al.*, 2013a).

### **1.2 Statement of the Problem**

The statement of the problem for these research work are the following

1. Improper disposal and management of used oils lead to health issues and environmental pollutions
2. The present practice of indiscriminate dumping of palm kernel, groundnut and coconut shells leads to economic losses and environmental pollution



3. From API data, 42 gallons of light, fresh crude oils generate approximately 0.5 gallons of lubricating oils, but 42 gallons of used lube oils produce 34 gallons lubricating oils. Therefore improper disposal of used lube oil leads to substantial economic losses.

### **1.3 Used Oil Recycling**

In contrast to the above, used lubricating oils can be considered as valuable resources because it is possible to recover energy or useful materials for further use(Guerin, 2008). Thus, gross calorific value of used lubricating oils is estimated to be around 40 MJ/kg (Botas *et al*, 2017) and 1L of motor oil can be produced by using only 1.6L of recycled used lubricating oils(Durrani *et al*, 2011). Used lubricating oil management has a global impact on crude oil consumption, and local as well as regional implications because of environmental, economic and social issues. At present, globally, different automotive and industrial sources generate large amounts of used lubricating oils, which poses a severe pollution problem.

An analysis of regional and global lubricant demands found that Western Europe accounts for only 13 percent of the global market, while North America and Asia accounts for 22 percent and 30 percent, respectively, with remaining for other parts of the world. Compare with other regions due to the widespread use of cars (Kupareva *et al.*, 2013a).Nigeria in recent times averages about 400,000,000 litres yearly of the total consumption of lubricating oil(Joel, 2013). Majority of these used lube oil is wastefully disposed of in the country and this contaminate the water, land and air which goes on to cause a lot of public health problems. Due to high lube oil consumption, various countries have designed their systems for the management of waste oils.

The main path for used lubricating oils recycling is what is called re-refining, which consists of recovering the original base oil from being reused in the formulation of brand new

products. The re-refining industry has become an important industry in many countries, such as USA, Australia, and Saudi Arabia. It is estimated that about 400 oil re-refining plants using a variety of technologies, with an overall capacity of 1.8 million tons/year (Kupareva *et al.*, 2013a). The number of re-refining plants in Europe is 28, of which 17 produce base oil. The industry has a theoretical nameplate capacity of 1.3 million tons corresponding to the total turnover of between €200 and 250 million per year (Giovanna, 2009).

According to European Commission resources, (Pinheiro *et al.*, 2018) about 5.7 million tons of lubricating oils are consumed in Europe annually, with automotive and industrial sectors accounting for 65% and 35% respectively. Such a scale of operation generates approximately 2.7 million tons of used oil, or in words around 48% of the total lube oil consumption. Of the latter quantity, only about 73% or 2.0 million tons, is collected; therefore, about 0.7 million tons or 23% is assumed to be lost or illegally burnt or dumped in the environment. Engine oil represents more than 70% of the collectable waste oil, and industrial oils comprise the balance of 30%. About 35% of the collected oil is re-refined into base oil; the remaining 65% is burnt replacing coal (10%), or used as heavy fuel oil (45%) and unknown other products (10%) (Kupareva *et al.*, 2013a).

With the increasing number of vehicles and industrial plants, the volume of used lubricating oil produced each year is also increasing. Due to the necessity for environmental protection and stricter environmental legislation, the disposal and recycling of used lubricating oils has become very important. Recycle of used oil has been carried out by several methods. Concentrated sulphuric acid has been used to remove asphaltenic material. The product is then clay treated (Ossman and Farouq, 2015). The sludge could be used as fuel which leads to the production of acidic gases. Use of acid could be avoided by treating used oil with natural polymers. The product is vacuum distilled then decolourised (Kamal *et al.*, 2014). The recycled oil contains a higher amount of metals.

The inorganic membrane has been used to extract the oil followed by adsorption which requires high pressure and specialised inorganic composite membrane (Examiner and Fortuna, 2000) and (Kamal and Khan, 2009a). Use of radiations has been reported (Kamal and Khan, 2009b). Alkali (NaOH/KOH) with ammonium salt or ethylene glycol has also been used to recover the oil (Taylor *et al.*, 2010).

#### **1.4 Environmental Concerns of Used Oil**

Some of the factors that affect the environmental quality, the discharge of heavy metals has exposed millions of people to their harmful effects, and it is one of the biggest environmental challenges faced by the world (Barakat, 2011). Heavy metals are persistent, bioaccumulative and able to disrupt the metabolic functions and vital organs in humans and animals (Tchounwou *et al.*, 2012). The biological function of heavy metals in trace concentrations is considered essential for plants and animals, but the chemical or physical transformation to which these metals are subjected to will determine their toxicity and environmental behaviour (Jiménez-Castañeda and Medina, 2017).

For examples, Chromium (Cr) causes severe respiratory, cardiovascular, gastrointestinal, haematological, hepatic, renal and neurological damage and has been suggested to be carcinogenic (Fu and Wang, 2011). Cadmium (Cd) is considered a human carcinogen with an impact on the respiratory system; its other effects include damage to the liver as well as the cardiovascular, immune and reproductive systems (Islam *et al.*, 2016). Lead (Pb) causes poor development of the brain and the nervous system. It is particularly dangerous to foetuses and young children. Exposure to lead (Pb) damages the kidneys, the reproductive and nervous systems. It accumulates in the teeth and the bones (Jiménez-Castañeda and Medina, 2017). Zinc (Zn) is an essential trace element that is considered to be relatively nontoxic to humans,

but overexposure can cause stomach cramps and irritation, vomiting, nausea, anaemia or even death(Cazetta *et al.*, 2011).

Heavy metals are removed from used lubricating oils by applying adsorbents such activated clay, acid-activated clay, bentonite, acid-activated bentonite, date palm kernels powder etc. (Abdel-Jabbar *et al.*, 2010). Adsorption is extensively applied due to the flexibility of the process and, accordingly, many adsorbents with high adsorption capacity, including zeolites and clays have been thoroughly investigated(Jiménez-Castañeda and Medina, 2017).

Adsorption is a surface phenomenon in which adsorptive (gas or liquid) molecules bind to a solid surface. However, in practice, adsorption is performed as an operation, either in batch or continuous mode, in a column packed with porous sorbents. Under such circumstances, mass transfer effects are inevitable. The complete course of adsorption includes mass transfer and comprises three steps(Zacaroniet *al.*, 2015):

Step 1: Film diffusion (external diffusion), which is the transport of adsorptive from the bulk phase to the outer surface of the adsorbent.

Step 2: Pore diffusion [intraparticle diffusion (IPD)], which is the transport of adsorptive from the external surface into the internal pores.

Step 3: Surface reaction, which is the attachment of adsorptive to the internal surface of the sorbent.

Also, adsorption involves the up taking and immobilising of contaminants on an adsorbent and the related mechanisms, such as surface adsorption, partition, surface precipitation and structural adsorption (Tan and Hameed, 2017). Tertiary treatment involves physicochemical separation techniques such as carbon adsorption, flocculation/precipitation, and membranes for advanced filtration, ion exchange, dechlorination and reverses osmosis. Among the standard tertiary treatment methods, adsorption had been reported as an efficient and

economical option (Onundi *et al.*, 2010a) especially when the source of the adsorbent is cheap. Also, the adsorption process provides an attractive alternative treatment, especially if the adsorption is inexpensive and readily available (Tabassi *et al.*, 2017). The adsorbents that are mostly used in recent times are agrowastes such as date palm kernel powder, egg shale and oil adsorbent (Anyika *et al.*, 2017). The economic availability of these adsorbent materials is the major obstacle to their use in used lubricating oil treatment.

Activated carbon is a form of carbon that has been processed to make it extremely porous with an extensive surface area available for adsorption or chemical reactions. It is produced from organic based materials such as in this case palm kernel and coconut shells. The raw material is carbonised to obtain the char or carbonaceous material, which is activated to yield the highly porous final product. The activated carbon particle has two types of pores existing in it by which adsorption take place, that is, macropores ( $>10^1 \mu\text{m}$ ) and the micropores ( $10^{-3} - >10^{-1} \mu\text{m}$ ). The macropores provide a passageway to the particle's interior and to the micropores but do not contribute substantially to the particle surface area. The micropores, on the other hand, are responsible for the large surface area of activated carbon particles and are created during the activation process. It is in the micropores that adsorption mainly takes place (Ling *et al.*, 2010). It has been the appropriate low-cost technology for the treatment of wastewater used lubricating oil (Kwakyee-Awuah *et al.*, 2018).

The high cost of industrial manufactured activated carbon such as silica gel has stimulated interest in examining the feasibility of using affordable locally raw materials. Substitute materials tested include palm kernel and coconut shells. Indigenous researchers have been investigating the adsorption capacity of some local materials such as palm kernels (Udonne and Bakare, 2013), mango seed shells (Akpen and Leton, 2014), coconut shells (Gopalswami *et al.*, 2010), raffia palm seeds (Akpen *et al.*, 2017) among others. Notably, these adsorbent

materials are agricultural by-products commonly viewed, creating problems to the environment and having no economic value.

The palm kernel and coconut shells are in abundance in many parts of Nigeria. They have not been investigated as a possible precursor for the production of chemically activated carbons for removal of heavy metals and other pollutants in used lubricating oil. The use of chemically activated carbons produced from palm kernel and coconut shells would serve many purposes: It will provide an opportunity for the utilisation palm kernel and coconut shells hitherto regarded as waste. Also, the manufacture of activated carbon from a local agricultural waste available material will reduce its cost. Besides, the use of palm kernel and coconut shells to remove heavy metals and pollutants in used lubricating oil create jobs for the teeming youths in agriculture and by extension trade. In addition to the above, it will prevent the pollution of the environment by the discharged of these heavy metals in used lubricating oil.

### **1.5 Aim and Objectives of the Study**

This work aims to study the removal of heavy metals and other contaminants in used lubricating oil using chemically activated carbon from palm kernel and coconut shells.

The specific objectives are to:

1. ascertain the physicochemical properties of virgin and used lubricating oils,
2. analyse the physicochemical properties of the chemically activated carbons from palm kernel and coconut shells,
3. determine that chemically activated carbons produced can be effectively used in the adsorption process,

4. set-up a simple plant to remove heavy metals and other pollutants in used lubricating oil, and
5. validate experimental results with the model equation

### **1.6 Scope of the Study**

In this research work, chemically activated carbons adsorbents from palm kernel shells (PKS) and coconut shells (CNS) were investigated for their suitability to remove heavy metals and contaminants in used lubricating oil. The type of lubricating oil was selected because it is suitable for use in gasoline and diesel engines, particularly commercial cars and light industrial vehicles. It can also be used in all lubricating operating conditions. For example, light and heavy-duty generators, road and motorways equipment irrespective of the season. This type of lubricating oil is perfectly suitable for vehicles equipped with catalysts and using unleaded fuel or liquefied petroleum gas. The work relied on extensive studies conducted earlier on, that have shown the excellent physicochemical and adsorptive properties of chemically activated carbons from palm kernel and coconut shells as suitable adsorbents in the treatment of wastewater, dyes, polluted water, underground water etc. The ultimate aim would be to use mathematical modelling to explain all the laboratory data obtained.

## **CHAPTER TWO**

### **LITERATURE REVIEW**

#### **2.1 Characteristics of Palm Kernel and Coconut Shells**

Activated carbon is a particular type of carbonaceous substance. It has a highly crystalline form and extensively developed internal pore structure. Due to activation, the internal pore network is created which imparts specific surface chemistries (functional groups) inside each particle. Thus carbon gets its unique characteristics leading to the high surface area, porosity and greater strength. The absorptivity of the adsorbent depends on both the size of the molecule being adsorbed and the pore size of the adsorbent. The organic material which has high carbon content can be utilised as the raw material for the synthesis of activated carbon. There are many cheap, readily available materials such as palm kernel shell and coconut shell which have been used as the source for the synthesis of activated carbon. They are used in the reduction of hazardous contaminants in used lubricating oil.





**Plate 2.1 Palm Kernel Shells**

Oil Palm (*Elaeis guineensis*) is the most prominent species in the *Elaeis* genus which belongs to the family Palmae. It is cultivated in West Africa and all tropical areas, especially in Malaysia, Indonesia and Thailand. The oil palm fruit is reddish and has a size of a large plum and grows in large bunches. A bunch usually has a weight of 10 to 40kg. Each fruit consists of a single seed (the palm kernel) and surrounded by a soft oily pulp mesocarp. Oil is extracted from both the fruit pulp and the nut. The oil extracted from the fruit pulp is used for edible purposes while the extracted oil from the kernel is mainly used for manufacturing of soap. Palm oil is one of the world's largest source of edible oil with 38.5 million tonnes or 25% of the world's total oil and fat production (Evbuomwan *et al.*, 2013).

Though the oil palm industry has been recognised for its contribution towards rapid economic growth and development, it has also accounted for substantial environmental pollution due to the production of large amounts of by-products from the extraction process. The waste products from oil palm processing consist of oil palm trunks, oil palm fronds, empty fruit bunches, and palm pressed fibres, palm kernel shells, less fibrous material such as palm kernel cake and liquid discharge palm mill effluent (Das *et al.*, 2015).



**Plate 2.2 Coconut Shells**

The coconut tree (*Cocos nucifera*) is a member of the family Arecaceae (palm family) and the only living species of the genus *Cocos*. The term coconut can refer to the whole coconut palm or the seed, or the fruit, which, botanically, is a drupe, not a nut. Coconuts are known for their versatility ranging from food to cosmetics. They form a regular part of the diets of many people in the tropics and subtropics. Coconuts are distinct from other fruits for their endosperm containing a large quantity of water (also called "milk"), and when immature, may be harvested for the potable coconut water. When mature, they can be used as seed nuts or processed for oil, activated carbon from the hard shell, and coir from the fibrous husk. When dried, the coconut flesh is called copra. The oil and milk derived from it are commonly used in cooking and frying, as well as in soaps and cosmetics. The husks and leaves can be used as material to make a variety of products for furnishing and decorating. The coconut also has cultural and religious significance in certain societies, particularly in India, where it is used in Hindu ritual (Promdeeet *et al.*, 2017).

## **2.2. Adsorption Isotherms**

### **2.2.1 Langmuir Isotherm Model**(Ghorbanian *et al.*, 2018).

Langmuir adsorption isotherm describes gas–solid-phase adsorption onto activated carbon. The model is based on two assumptions that the forces of interaction between adsorbed molecules are negligible, and once a molecule occupies a site, no further sorption takes place. In its derivation, Langmuir isotherm refers to homogeneous adsorption, with no movement of the adsorbate in the plane of the surface(Tan and Hameed, 2017)and (Ghorbanian *et al.*, 2018).

$$q_e = \frac{Q_0 b C_e}{1 + b C_e} \quad (2.1)$$

where  $q_e$  is the amount of adsorbed solute per weight of adsorbent at equilibrium;  $C_e$  is the equilibrium concentration of adsorbate;  $Q_0$  is the maximum monolayer coverage capacities, and  $b$  is Langmuir isotherm constant.

### 2.2.2 Freundlich Isotherm Model

(Baeten *et al.*, 2019)

Freundlich isotherm is one of the known model describing the non-ideal and reversible adsorption, not restricted to the formation of a monolayer. This empirical model can be applied to multilayer adsorption, with non- uniform distribution of adsorption heat and affinities over the heterogeneous surface(Tan and Hameed, 2017)(Baeten *et al.*, 2019).

$$q_e = K_F C_e^{1/n} \quad (2.2)$$

where  $K_F$  is the Freundlich isotherm constant related to adsorption capacity, and  $n$  is the adsorption intensity.

### 2.2.3 Khan Isotherm Model

(Baeten *et al.*, 2019)

Khan isotherm is another empirical model recommended for the pure solutions, that  $a_K$  and  $b_K$  are the model exponent and model constant, respectively(Baeten *et al.*, 2019)

$$q_e = \frac{q_s b_k c_e}{(1 + b_k c_e)^{a_k}} \quad (2.3)$$

where  $a_K$  is the Khan isotherm model exponent;  $b_K$  is the Khan isotherm model constant, and  $q_s$  is the theoretical isotherm saturation capacity.

#### 2.2.4 Toth Isotherm Model

(Foo *et al.*, 2010)

Toth isotherm model is also an empirical equation derived to improve upon the Langmuir isotherm. This model is useful in describing heterogeneous adsorption systems, which satisfying both low and high-end boundary of the concentration (Foo *et al.*, 2010). It reduces to Henry's law at deficient levels (Ghorbanian *et al.*, 2018).

$$q_e = \frac{K_T C_e}{(a_T + C_e)^{1/t}} \quad (2.4)$$

where  $a_T$ ,  $K_T$ , and  $t$  are isotherm constants.

#### 2.2.5 Tempkin isotherm (Baeten *et al.*, 2019).

Tempkin isotherm is the simple type of adsorption isotherm model. The isotherm holds a factor that explicitly takes into the account of adsorbent–adsorbate interactions. The model assumes that heat of adsorption (the function of temperature) of all molecules in the layer would decrease linearly rather than logarithmic with coverage except in deficient and high concentrations (Baeten *et al.*, 2019).

$$q_e = \frac{RT}{b_t} \ln(A_T C_e) \quad (2.5)$$

where  $A_T$  is the Tempkin isotherm equilibrium binding constant,  $b_T$  is the Tempkin isotherm constant,  $R$  is the universal gas constant, and  $T$  is temperature.

### 2.2.6 Freundlich-Jovanovic Isotherm Model

(Shahbeig *et al.*, 2013) and (Tan and Hameed, 2017)

Further to the same assumptions ascertained in the Langmuir model, the Freundlich-Jovanovic model studies the possibility of some mechanical contacts between the adsorbing and desorbing molecules. In addition to, this isotherm was utilised for heterogeneous surfaces without lateral interactions (Shahbeig *et al.*, 2013)(Tan and Hameed, 2017).

$$q_e = q_{FJ} \{1 - \exp(-K_{FJ} C_e^{n_{FJ}})\} \quad (2.6)$$

where  $q_{FJ}$  is the maximum monolayer coverage capacities,  $K_{FJ}$  is the equilibrium constant, and  $n_{FJ}$  is the Freundlich-Jovanovic isotherm exponent.

### 2.2.7 Linear Isotherm Models

(Chen, 2015).

Linear types of isotherms models are extensively used to determine the isotherm parameters and the most suitable model for the adsorption system due to the mathematical application. The linear types of the Langmuir, Freundlich and Dubinin-Radushkevich isotherms models are shown in Table 2. The Langmuir isotherm model can be linearised into four different types, as shown in Table 2 type's I–IV. Among the four linear forms which will result in different parameter estimates, the type I is the most prevalent linear forms used in works of literature, due to the minimal deviations from the suitable equation (Chen, 2015). Hence by plotting  $C_e/q_e$  against  $C_e$  it is possible to obtain the value of the Langmuir constant  $K_L$  and  $q_m$ ; by plotting  $\ln(q_e)$  against  $\ln(C_e)$ , the Freundlich constant of  $K_F$  and  $n$  can be determined; and by plotting  $\ln(q_e)$  against  $\varepsilon^2$ , the Dubinin-Radushkevich constants of  $K_D$  and  $q_s$  can be obtained.

**Table 2.1 Types of linear isotherm model**

<u>Isotherm models</u>	<u>Linear form</u>
I	$\frac{C_e}{q_e} = \frac{1}{q_m K_L} + \frac{C_e}{q_m}$
II	$\frac{1}{q_e} = \left[ \frac{1}{q_e K_L} \right] \frac{1}{C_e} + \frac{1}{q_m}$
Langmuir (Akpen <i>et al.</i> , 2018) (2.2.7.a)	III $q_e = q_m - \left[ \frac{1}{K_L} \right] \frac{q_e}{C_e}$
IV	$\frac{q_e}{C_e} = K_L q_m - K_L q_e$
Freundlich (Akpen <i>et al.</i> , 2018) (2.2.7.b)	$\forall \ln q_e = \ln K_F + \frac{1}{n} \ln C_e$
Dubinin-Radushkevich (Tabassiet <i>et al.</i> , 2017) (2.2.7.c)	VI $\ln q_e = \ln q_S - K_D \varepsilon^2$

Several model parameters were analysed with both non-linear regression and linear least-squares method using XLSTAT-2014-5.03 software. The standard errors (S.E.) for each parameter were used to determine the goodness-of-fit. Besides S.E., the coefficient of determination ( $R^2$ ) was also used to determine the suitable isotherm model to the experimental data, illustrated as Equation (7).

$$R^2 = \frac{\sum(q_m - \bar{q}_e)^2}{\sum(q_m - \bar{q}_e)^2 + \sum(q_m - \bar{q}_e)^2} \quad (2.8)$$

where  $q_m$  is the constant obtained from the isotherm model,  $q_e$  is the equilibrium capacity derived from experimental data and  $\bar{q}_e$  is the average of  $q_e$ .



### 2.3 Used lubricating oils (ULOs)

Used lubricating oils (ULOs) are classified as hazardous wastes, and constitute a severe pollution problem not only for the environment, but also for human health due to the presence of harmful contaminants, such as heavy metals, polychlorinated biphenyls (PCBs) and polycyclic aromatic hydrocarbons (PAHs) (Boadu *et al.*, 2019). Improper management and haphazard disposal of used lube oils can have an adverse effect on the environment (Lam *et al.*, 2016). Research scientists have reported that in West Africa, the dispersion of the air pollutants could travel at a speed of 10-12 m/s (Emetere *et al.*, 2019). The implication of this report is that air pollution from the burning of waste lubricant is not localised to the source of pollution but could travel with time to other locations. For example, it was recently reported that black soot covered a metropolitan city of Port Harcourt while remote sources were at the suburb settlement ( about 22 km away from the town) (Sonibare and Omoleye, 2018) and (Boadu *et al.*, 2019).

Alternatively, ULOs can be considered as valuable resources, in the sense that it is possible to recover energy or useful materials for further use (Oladimeji and Sonibare, 2018). The best environmental options, for the management of used oils, follow the 'waste hierarchy' by recycling, recovering and then disposing-off. Used lube oils can be used as an alternative fuel in a variety of engine configurations and other applications. Its gross calorific value is greater than 42.9 MJ/kg (Pelitli, 2017). The principal objective of any waste management plan is to ensure safe, efficient and economical collection, transportation, treatment and disposal of waste as well as satisfactory operation for current and foreseeable future scenarios (Diphare *et al.*, 2013). The treatment of used lubricating oil is vital because it is energy-efficient and affordable compared to conventional refining of crude oil, it helps in improving air quality, land and water pollution in the environment. The most preferred option by experts in the reuse of the used lubricating oil generated by consumers (Jafari and Hassanpour, 2014). In

this study, a thorough review of various removal or treatments techniques for used lubricating oil were considered starting from conventional to the most modern methods and their limitations; further improvement of these fields was also touched. Also, environmentally friendly and affordable adsorbents were developed to remove contaminants such as heavy metals in used lubricating oil.



**Plate 2.3 Typical Recycling Process Cycle**

### **2.3.1 Conventional Methods**

The conventional methods of treating contaminants such as heavy metals in used lube oil either demand an expensive technology such as vacuum distillation or the use of toxic solvents such as sulphuric acid, benzene, toluene, 2-propanol, methyl ethyl ketone, propane etc. These methods also produce contaminating by-products which have high sulphur levels, especially in the Kurdistan region/Iraq(Hamawand *et al.*, 2013a).

### **2.3.2 Acid-clay**

Assessment of different contaminants removal processes in used lube oils indicates that acid-clay method had the highest environmental risk and lowest cost. This method, involve treatment of used oil with acid and clay(Udonne and Bakare, 2013)(Ossman and Farouq, 2015) and (Abu-Ellella *et al.*, 2015). The clay was used as an adsorbent to remove the odour and dark colour. What makes acid-clay method distinct from others are; its simple process, less capital investment, low operating cost and does not need skilled operators (Dalla *et al.*, 2003); (Nwachukwu, 2012) and (Pinheiro *et al.*, 2018).

However, this method has many disadvantages; it also produces a large number of pollutants and even unable to treat modern multigrade oils, and it's challenging to remove asphaltic impurities (Das *et al.*, 2015). To address this problem, the acid treatment stage of the process can be done under atmospheric pressure to remove the acidic products, oxidized polar compounds, suspended particles and additives(Hani and Al-Wedyan, 2011). Josiah and Ikiensikimama, 2010observed that high recovery rate of treated lubricating oil from used lubricating oil depends mostly on the source of the used lubricating oil, pre-treatment mechanisms, extent of contamination and the grade of the acid used. He also showed that the

volume of the adsorbent (clay) used could affect the rate at which contaminants are removed and the percentage of recovery of the method.

Abu-Elella *et al.*, 2015 worked on used motor oil. They treated used motor oil with phosphoric acid, sulphuric acid, methanoic acid and acetic acid. They observed that methanoic acid, sulphuric acid and acetic acid have a significant impact on the kinematic viscosity while phosphoric acid was not affected by the used lubricating oil. They, therefore, concluded that treatment with acetic acid showed better results than formic acid-clay.

### **2.3.3 Solvent Extraction**

This method has replaced acid-clay treatment as the preferred method for improving the oxidative stability and viscosity as well as temperature characteristics of the base oils. Base oils obtained from solvent extraction are of good quality and contains fewer amounts of contaminants. In contrast to acid-clay treatment, it operates at higher pressures, requires a skilled operating system and qualified personnel (Islam, 2015). The solvent selectively dissolves the undesired aromatic components (the extract), leaving the desired saturated parts, especially alkanes, as a separate phase [the raffinate](Pinheiro *et al.*, 2018).

Different types of solvents have been used for solvent extraction such as 2-propanol, 1-butanol, methyl ethyl ketone (MEK), ethanol, toluene, acetone, propane etc.(Rincón *et al.*, 2007) used propane as a solvent. They found out that the propane was capable of dissolving paraffinic or waxy materials and intermediately dissolved oxygenated materials. Asphaltenes which contain heavy condensed aromatic compounds and particulate matter which are insoluble in liquid propane. These properties make propane an ideal solvent for recycling used engine oil, but, there are other issues to be considered. Propane is hazardous and flammable, therefore making this process regarded as a dangerous method.

Sterpu *et al.*, 2013, found out that methyl ethyl ketone has the highest performance due to its low oil percentage losses and high sludge removal. Also, (Hussein *et al.*, 2014) used butan-1-ol solvent for the extraction and which produced the highest sludge removal rate. Oladimeji and Sonibare, 2018 used a composite of methyl ethyl ketone and 2-propanol solvents; the treated oil from this process was comparable to that produced by acid-clay method; however, it was costly.

In general, solvent extraction leads to solvent losses and demands high operating maintenance. Also, it occurs at pressures higher than 10 atm and requires high pressure sealing systems which make solvent extraction plants expensive to construct, operate and the method also generates remarkable amounts of hazardous by-products (Hamawand *et al.*, 2013b).

#### **2.3.4 Vacuum distillation**

Numerous research works have been done on vacuum distillation on used oil by the following (Emam and Shoaib, 2012); (Hamawand *et al.*, 2013a) and ((Kannan *et al.*, 2014). In this process, used lube oil collected is heated at a temperature of 120<sup>0</sup>C to remove the water generated in the oil during combustion. Then the dehydrated oil is subjected to vacuum distilled at a temperature of 240<sup>0</sup>C and pressure of 20 mmHg. This process leads to the production of light fuel oil at a temperature of 140<sup>0</sup>C (the light fuel oil can be used as a fuel source for heating) and lubricating oil at 240<sup>0</sup>C. The lubricating oil vapour is condensed and sent for the next stage (Kannan *et al.*, 2014). The advantages of vacuum distillation process compared to atmospheric pressure distillation are: columns can be operated at lower temperatures; more economical to separate high boiling point components under vacuum distillation; avoid degradation of properties of some species at high temperatures hence thermally sensitive substances can be handle with ease.

In contrast to the above, the remaining oil generated at this temperature (240<sup>0</sup>C) contains the dirt, degraded additives, metal wear parts and combustion products like carbon and is collected as residue. The residue obtained, is in the form similar to that of tar, which can be used as a construction material. For example, on the road and bitumen production (Dalla et al., 2003) and (Kupareva et al., 2013a). The disadvantage of this process is that, high investment cost and the use of toxic materials such as sulphuric acid (Kupareva *et al.*, 2013a).

### **2.3.5 Hydrogenation**

To prevent the formation of harmful products and environmental issues resulted from the above methods, some modern processes have been employed, and the most suitable one is the hydrotreating method (Ossman and Farouq, 2015). This method immediately follows vacuum distillation. In this process, the distillate from vacuum distillation is hydrotreated at high pressure and temperature in the presence of a catalyst for the purpose of removing chlorine, sulphur, nitrogen and organic components. The treated hydrocarbons resulted in products of improved odour, chemical properties and colour (Oladimeji *et al.*, 2018).

Other significant advantages of these methods are Production of high Viscosity Index lube oil with strong oxidation resistance; right solid colour and yet having low or no discards. At the same time, it takes care of flouxy quality feed. Further, this method has an advantage to the extent that, all of its hydrocarbon products have suitable applications and product recovery with no (or very low) disposals. Other hydrocarbon products are: In an oil refinery, the light – cuts can be used as fuel in the plant itself. Gas oil may be consumed after being mixed with heating gas oil. The distillation residue can be blended with bitumen and destroyed as the paving asphalt because it improves immensely its rheological properties. Also, it can be used as a concentrated anti-corrosion liquid coating. For instance, in vehicles frames to prevent rusting (Durrani, 2014).

However, the disadvantages of this method are that the residue obtained from the process is of high boiling range of hydrocarbon product. The hydrocarbon product, when fractionated yields neutral oil products with varying viscosities which can also be used to blend lube (Nicholas and Hussein, 2018).

### **2.3.6 Membrane Technology**

Membrane technology is another method for removal of contaminants of used lubricating oils. In this process, three types of polymer hollow fibre membranes [polyethersulphone (PES), polyvinylidene fluoride (PVDF), and polyacrylonitrile (PAN)] were investigated. (Liew *et al.*, 2018) and (Boadu *et al.*, 2019) researched the use of membranes for recycling of used engine oils. Their process was carried out at 40 °C and 0.1 MPa pressure. Their method was a continuous operation as it removed metals, particles and dust from the used lube oil. It also improved the recovered oils liquidity and flash point (Manyuchi, 2018).

Besides the aforementioned advantages, the expensive membranes may get damaged and fouled by large particles with time (Hamawand *et al.*, 2013a).

### **2.3.7 Catalytic Process**

For example Hylube process from Germany. This method allows the production of mainly base oils. The Hylube process is a proprietary process developed by Universal Oil Products (UOP) for the catalytic processing of used lube oils into re-refined lube base stocks for re-blending into marketable lube base oils (Kapustina *et al.*, 2014). This is a unique re-refining process, in which as received used oil is treated, without any pre-treatment, in a pressurised hydrogen environment. In a typical HyLube process, the feedstock consists of a blend of used lube oils containing high concentrations of particulate matter such



as iron and spent additive contaminants such as zinc, phosphorus, and calcium (Epelle *et al.*, 2016).

The Hylube process unit operates with reactor section pressures of 60–80 bar and reactor temperatures in the range 300–350<sup>0</sup>C (Geyer *et al.*, 2013). The Hylube process achieves more than 85% of lube oil recovery from the lube boiling range hydrocarbon in the feedstock (Kupareva *et al.*, 2013a). Besides the advantages of this process, this method is costly. This method requires high-level personnel due to its high temperature and pressure operations.

## **2.4 Combined Technologies/methods**

These are advanced methods that combine two or more generic techniques in their technology. Due to the sophisticated nature of removal of contaminants in used lube oils, using a single approach may not yield the desired standard emission controlled process required. Therefore some companies have developed specific combined processes for treatment and removal of contaminants in used lube oils (Mekonnen, 2014), these methods require sophisticated technologies, equipment and processes. Many a time, these combined methods yield the desired results. Some of these complex processes are briefly discussed below;

### **2.4.1 Vaxon process**

This process contains chemical treatment, vacuum distillation and solvent refining units. The advantage of the Vaxon process is the particular vacuum distillation unit, where the cracking of oil is sharply decreased (Epelle *et al.*, 2016).

The final chemical stage does not, however, allow the production of high-quality base oils; although in Spain, the Catalonia refinery produces base stocks accepted by an original equipment manufacturer (OEM). In connection with this fact, the lube distillate obtained

from the Vaxon process (Denmark) or North Refining (Netherlands) are precursors for the Avista Oil base (Kupareva *et al.*, 2013b).

#### **2.4.2 Chemical Engineering Partners (CEP) process**

This technology combines thin film evaporation and hydroprocessing. In this method, the used oil is chemically pre-treated to avoid precipitation of contaminants which can cause corrosion and fouling of the equipment. The pre-treating step is carried out at temperatures within 80–170<sup>0</sup>C. The chemical treatment compound comprises sodium hydroxide, which is added in a sufficient amount to give a pH of about 6.5 or higher (Boadu *et al.*, 2019).

Heavy materials such as residues, metals, additive, degradation products, etc. are sent to the dense asphalt flux stream. The distillate is hydro-purified at high temperature (315<sup>0</sup>C) and pressure (90 bar) in a catalytic fixed bed reactor (Boadu *et al.*, 2019). This process removes nitrogen, sulphur, chlorine and oxygenated organic components. In the final stage of the process, three hydrotreating (Hydrofinishing) reactors are used in series to reduce sulphur to less than 300 ppm and to increase the number of saturated compounds to over 95%, to meet the critical specifications for API Group II base oil. The final step in this process is vacuum distillation to separate the hydrotreated base oil into multiple viscosity cuts in the fractionator. The yield of base oils is about 70% (Kupareva *et al.*, 2013a).

#### **2.4.3 Ecohuile process**

The re-refining process was based on vacuum distillation and acid-clay treatment steps until the end of 2000 (Ani *et al.*, 2015). Acid-clay adsorption was banned in 2001, and the plant was modified and upgraded to the Sotulub process (Kilmer, 2010). Moreover, the addition of injection facilities of so-called Antipoll-additive (1–3 wt. % of pure sodium hydroxide) has been provided and has allowed solving the following fundamental problems:

- corrosion of dehydration column and cracking column top section due to the organic acidity of the used oil;
- plugging of equipment and piping due to polymer formation in the cracking section;
- high losses of base oil in the oily clay due to the high consumption of clay.

The Sotulub process (Kilmer, 2010) is based on the treatment of the used oil with an alkali additive called Antipoll and high vacuum distillation. The used oil is pre-heated to about 160<sup>0</sup>C and mixed with a small amount of Antipoll-additive, which decreases equipment fouling (Boadu et al., 2019). This process allows a final product to be obtained with acceptable quality without any additional finishing stage. The oil obtained is additionally fractionated to get various base oil cuts. The process provides base oils with a yield of 82–92 % (Kupareva *et al.*, 2013b).

#### **2.4.4 Cyclon process**

This method combines the technology of vacuum distillation and hydro-finishing (Kupareva *et al.*, 2013a). The processing licence belongs to Kinetic Technology International (KTI) (Kajdas, 2000). In this technology, used oils taken from storage tanks are dewatered, and the light hydrocarbons are removed by distillation. The heavier fraction is sent to high vacuum distillation, where the majority of base oil components are evaporated from the heavy residue. The oils in the residues are extracted with propane in the de-asphalting unit and sent to the hydroprocessing unit where the other oils are processed. Then they are treated with hydrogen and fractionated based on the desired base oil features. The re-refined base oil products obtained are of a high quality due to the hydrogenation (Kilmer, 2010).

#### **2.4.5 Studi Technologie Progetti S.p.A(STP) method**

Another advance method that combines vacuum distillation and the hydro-finishing process is the STP method (Pazoki and Hasanidarabadi, 2017). This process produces less harmful pollutants; therefore, its environmentally-friendly (Stan *et al.*, 2018). The method involves dehydration, vacuum distillation, separation of the lubricating fraction and the hydro-finishing of base oil separation from the residue.

#### **2.4.6 Interline process**

The interline process is based on propane de-asphalting at ambient temperature and under a pressure that facilitates separation in the liquid phase. The lubricating oil yield obtained from the Interline process is 79 % (Botas *et al.*, 2017). The extraction process removes the majority of additives. The process is exciting from the economics costs. Because it eliminates thin film distillation and the urgent need for hydrogenation, both investment and maintenance costs are relatively low compared to others.

However, the drawbacks of the Interline process are that the feed should not contain polychlorinated biphenyls (PCBs), and its chlorine content should be below 1000 ppm since this process has no final hydrofinishing step(Kupareva *et al.*, 2013b).

#### **2.4.7 Propak thermal cracking process**

The Propak process involves the following, screening and dewatering sections, a thermal cracking section, a separation or distillation depending on the product state desired and finally purification and stabilisation stages. In some plant configurations, a substantial boiling fraction is recycled back to the fired process heater. Gasoil in the liquid state is led to the stabilisation section from distillation.

This technology is characterised by immense operational and product flexibility. Process operating conditions (temperature, pressure, residence time) can be varied to produce the desired outcome such as heavy fuel oil, gasoil or base oil (Kupareva *et al.*, 2013). The main disadvantage of this technology is that it requires highly skilled human resources due to the multiplex unit operations involved (Boadu *et al.*, 2019).

#### **2.4.8 Hylube process**

The Hylube process leads to the production of mainly base oils. This process is a proprietary process developed by Universal Oil Products (UOP) for the catalytic processing of used lube oils into re-refined lube base stocks for blending into saleable lube base oils (Geyer *et al.*, 2013). The method is among the first re-refining process in which raw used oil (as received used oil) is processed, without any pre-treatment, in a pressurised hydrogen environment. A typical HyLube process feedstock consists of a blend of used lube oils containing high concentrations of particulate matter such as iron and spent additive contaminants such as zinc, phosphorus, and calcium (Epelle *et al.*, 2016).

The Hylube unit operates with reactor section pressures of 60–80 bar and reactor temperatures in the range 300–350°C (Kapustina *et al.*, 2014). As the feed is processed in hydrofinishing reactors, contaminants are removed, and the quality of the lube base oil is rejuvenated and enhanced. In addition to converting hetero-atoms such as sulphur and nitrogen, the catalyst can increase the viscosity index via saturation of multi-ring aromatic compounds. The processed feedstock is transformed into a comprehensive boiling range hydrocarbon product, which is subsequently fractionated into neutral oil products of different viscosity to be used for lube oil blending. Due to hydrogenation, the properties of three different base oil products are a quite high quality of produced based oil (AP II grade) (Azeem and Hassanpour, 2017). The Hylube process is sufficient for dechlorination, including

PCB's destruction and desulphurization (content in fuel is less than 0.03wt. %). The method achieves more than 85% lube oil recovery from the lube boiling range hydrocarbon in the feedstock.

Although, the process can accept raw used oils (as received used oils) from different sources for treatment, but requires skilled personnel due to high temperature and pressure involved. It is also capital intensive process and demands high operating costs. The capital investment and operating costs can only be minimized by eliminating redundant equipment. The hylube process generates heavy residue, which is very stable and can only be accepted for asphalt blending (Boadu *et al.*, 2019).

#### **2.4.9 Snamprogetti process/ IFP technology**

The Snamprogetti process combines vacuum distillation and hydrogenation, including a propane extraction step before and after vacuum distillation. The extraction technology is similar to the one carried out in crude oil refineries to separate asphaltenes. In the first stage of the Snamprogetti technology, the light hydrocarbons and water are removed by atmospheric distillation. In the second stage, all the impurities picked up by the engine oil, including the additives and partly degraded polymers, are removed by extraction with propane in the temperature range 75–95<sup>0</sup>C in a propane-de-asphalting section (PDA I). After stripping the propane, the oil is heated again and vacuum distilled at a temperature of 300<sup>0</sup>C. In this stage, lubricating bases having lower viscosity and free of impurities are separated. The vacuum residue is then heated to 300–450<sup>0</sup>C under adiabatic conditions and sent to the second extraction stage (PDA II) in which metal content and asphaltic components are further reduced. After extraction, propane is stripped and recycled in the process. The base oil cuts from the vacuum residue (bright stock) are finally hydrogenated to improve the colour and to increase the oxidation stability of the base oils.

However, this process accepts all used motor oil feedstocks, but it is relatively expensive due to the two different propane deasphalting (PDA) units and hydrofinishing process involved. Also, the quality of the products is comparable to virgin base oils with the possibility to achieve API group II requirements. Further to that, the PDA bottoms can be used in asphalt production, yet this leads to losses of propane in the process of about 5-10% (Boadu *et al.*, 2019).

#### **2.4.10 Revivoil process**

Revivoil process is made up of three key sections: preflash, thermal de-asphalting and hydrofinishing (Kannan *et al.*, 2014). The filtered used oil from storage tanks is heated to 140°C and then distilled in a preflash column where the water and light hydrocarbons are separated. The dehydrated oil is extracted at 360°C in a vacuum thermal deasphalting unit (TDA), where the oil is separated from substances that can enhance fouling in an intermediate tank. The asphaltic and bituminous products remain at the bottom, and three side cuts of different viscosities are obtained at the same time. Intermediate gas oil is collected from the top of the column. For improvement of the product quality, oil cuts after TDA are treated with hydrogen over the catalyst. The hydrofinishing process starts in a fired heater where the oil and hydrogen are heated to 300°C. They are then sent to a reactor containing a catalyst favouring hydrogenation of the unsaturated compounds, as well as sulphur and nitrogen-containing compounds. The reactor effluent is then separated into two phases, the vapour phase and the liquid phase; the first one is washed with water to remove the chlorine and sulphur compounds, the second one is stripped with steam to eliminate the most volatile compounds and restore the flashpoint. The water contained in the oil after stripping is then removed in a vacuum dryer. The yield of base oils from the Revivoil process is about 72% (Durrani, 2014) and (European Commission, 2015).

Though this process accepts all used motor oils as feedstock, the operating parameters of hydrofinishing do not make it yield quality final base oil. However, the quality of the base oil obtained can be upgraded until the amounts of sulphur, and saturated compounds fulfil the API group II requirements (Boadu *et al.*, 2019). The residue can be used as asphalt extender and in bituminous membranes but requires expensive hydrotreatment catalyst regenerated unit.

#### **2.4.11 Mineral Oil Raffinerie Dollbergen (MRD) solvent extraction process using N-methyl-2-pyrrolidone**

The applied oil re-refining process is based on a patent held by 'AVISTA OIL' (Dalla *et al.*, 2003). The 'Enhanced Selective Refining' process uses solvent N-methyl-2-pyrrolidone (NMP), which is commonly used in the petroleum refining industry. NMP is a powerful, aprotic solvent with low volatility, which shows a selective affinity for unsaturated hydrocarbons, aromatics, and sulphur compounds. Due to its relative non-reactivity and high selectivity, NMP finds broad applicability as an aromatic extraction solvent in lube oil re-refining. The advantages of NMP over other solvents are the non-toxic nature and high solvent power, absence of azeotropes formation with hydrocarbons, the ease of recovery from solutes and its high selectivity for aromatic hydrocarbons. Being a selective solvent for aromatic hydrocarbons and PAH, NMP can be used for the re-refining of waste oils with lower sludge, carbonaceous particles and polymer contents, such as waste insulating, hydraulic and other similar industrial oils (Mohammed *et al.*, 2013).

The MRD solvent extraction process uses the liquid-liquid extraction principle. Vacuum distillates from the flash distillation are used as feed. These distillates are processed in a production cycle which can be adjusted to the quantity to be processed. Before the distillate enters the extraction column, any residues of dissolved oxygen in the distillate are removed in



an absorber using steam. After that, the distillate is sent to the bottom part of the extraction column. As the distillate rises, undesirable aromatic hydrocarbons and other contaminants are separated by the counter-flowing heavier solvent, N-methyl pyrrolidone, which is fed in at the top of the extraction column. The solvent containing raffinate phase leaves the extraction column at the top and is routed to the downstream raffinate recovery section consisting of a distillation and a stripping column where the solvent is removed. The extract phase is continuously withdrawn from the bottom of the extraction column, cooled down to a defined temperature and separated in a separation drum from the separated secondary raffinate. The latter is returned to the extraction column to optimise the process yield. The extract phase from the secondary separation drum is sent to the extract recovery section where the solvent is removed. The extract recovery section also consists of distillation and a stripping column. The resulting extract is routed to the offplot intermediate storage tank and used within the refinery as an energy carrier or mixing component for heavy oil. The dry solvent separated in the distillation columns of the raffinate and extract recovery sections is returned to the solvent tank. The most solvent separated in the stripping columns of the raffinate and extract recovery sections is returned to the solvent drying column, where excess water is removed. The average base oil yield within the process is about 91% (Kilmer, 2010). This process has relatively low operating and capital costs compared with other technologies. The MRD process yields good quality base oils with the following properties: quantitative elimination of PAH and a high viscosity index and oxidation stability.

Though, the base oils produced have high quality (Boadu *et al.*, 2019). The process is characterised by optimised operating conditions which allow the elimination of toxic polyaromatic compounds from the re-refined base oil and preservation of the synthetic base oils like polyalphaolefin (PAO) or hydrocracked oils, which are increasingly present in used oils. Also, the base oil generated contains high sulphur, and its extracts cannot readily be

used. This, therefore, required highly skilled personnel to eliminate the toxic process from polluting the environment. However, technology guarantees the complete preservation of the synthetic oils (XHVI, PAO). Sometimes, the feedstock can contain 5% of vegetable oils.

## **2.5 Modern Technologies for Used Oil Re-refining**

Used lube oil may cause damage to the environment when dumped into the ground or water streams, including sewers. This lead to groundwater and soil contamination. (Boadu et al., 2019). Hence, the development of the environmentally safe, sustainable and cost-effective solution is paramount for the recycling of used lubricating oil(Bosmans *et al.*, 2013).

Recently, due to different treatment and finishing methods, there are currently many available new technologies,(Bridjanian, and Sattarin,2006) such as pyrolytic distillation method (PDM), pyrolysis process (PP), thin-film evaporation (TFE), including combined TFE and clay finishing, TFE and solvent finishing, TFE and hydrofinishing, thermal de-asphalting (TDA), TDA and clay finishing, TDA and hydrofinishing etc. Also, environmentally friendly and affordable solvent extraction and adsorbents are being developed as a means of removing contaminants in used lubricating oil. Some of the current methods are briefly discussed below;

From the research worked by (Arpa *et al.*, 2010), a fuel named as diesel-like fuel (DLF) was obtained by applying the pyrolytic distillation process. Filtration of the waste engine oil sample was done using a quantitative filter. Three additives known as  $\text{Na}_2\text{CO}_3$ , Zeolite and CaO were blended with the purified oil at different ratios and were exposed to thermal and pyrolytic treatment to convert them into a diesel-like fuel. Conclusively, the effects of DLF on the oil properties shows a closer range to that of diesel fuel (Oladimeji *et al.*, 2018).

Also, Pyrolysis process (PP) has been employed as an alternative means of the effective conversion of used lubricating oil to a refined one (Manasomboonphan and Junyapoon,

2012). Lam *et al.*, 2018 describe pyrolysis as a thermal process that heats and decomposes substance at high temperature (300-1000 °C) in an inert environment without oxygen. Pyrolysis process is not yet widespread but it has been receiving much attention recently due to its potential to produce energy-dense products from materials. Examples of pyrolysis process include Microwave Pyrolysis Process (MPP) and Conventional Pyrolysis Process (CPP). The MPP is a thermo-chemical process applied in waste to wealth process of electrical power input of 7.5kW at a flow rate of 5kg/h (Oladimeji *et al.*, 2018).

Thin-film evaporation technology incorporates a rotating mechanism inside the evaporator vessel which creates high turbulence and thereby reduces the residence time of feedstock oil in the evaporator. This is done to minimise coking, which is caused by the cracking of the hydrocarbons due to impurities in the used oil. Cracking starts to occur when the temperature of the feedstock oil rises above 300°C.

However, any coking which does occur will foul the rotating mechanism and other mechanisms such as tube-type heat exchangers are often found in thin-film evaporators. Solvent extraction processes are widely applied to remove asphaltic and resinous components (Kupareva *et al.*, 2013b).

Liquid propane is by far the most preferred solvent for de-asphalting residues to make bright lubricant stock, whereas liquid butane or pentane produces lower grade de-asphalted oils more suitable for feeding to fuel-upgrading units. The liquid propane is kept close to its critical point and, under these conditions, raising the temperature to increases selectivity. A temperature gradient is set up in the extraction tower to facilitate separation. Solvent-to-oil ratios are kept high because this enhances rejection of asphalt from the propane/oil phase. Counter-current extraction takes place in a tall extraction tower. Typical operating conditions can be found in work by (Mortier *et al.*, 2010).

Current studies showed that propane could be replaced by alcohol–ketone mixture, which reduces coking and fouling problems during distillation (Kamal and Khan, 2009a) and (Osman *et al.*, 2017). The solvent selected should meet the following requirements: maximum solubility for the oils and minimum solubility for additives and carbonaceous matter; ability to be recovered by distillation. New plant units increasingly use N-methylpyrrolidone because it has the lowest toxicity and can be used at lower solvent/oil ratios, saving energy. Irrespective of the contacting method used, the result is two product streams. The raffinate stream is mainly extracted oil containing a limited amount of solvent, while the extract stream is a mixture of solvent and aromatic components. The streams are handled independently during solvent recovery and the recovered solvent streams are recombined and recycled within the plant.

Besides, solvent recovery is an energy-intensive part of the solvent extraction process. For several years, catalytic hydrotreatment stood out as the modern and successful refining treatment from the point of view of the yield and quality of the finished products. Hydroprocessing is more often applied as a final step in the re-refining process to correct problems such as poor colour, oxidation or thermal stability, demulsification and electrical insulating properties (Boadu *et al.*, 2019).

In the hydrofinishing process, used oil and hydrogen are pre-heated and then oil allowed to trickle downwards through a reactor filled with catalyst particles where hydrogenation reactions take place. The oil product is separated from the gaseous phase and then stripped to remove traces of dissolved gases or water. Typical reactor operating conditions for hydrofinishing process can be found (Mortier *et al.*, 2010).

The following reactions can be operative: hydrorefining reactions with the objective of removing heteroelements and to hydrogenate olefinic and aromatic compounds, and

hydroconversion reactions aiming at modifying the structure of hydrocarbons by cracking and isomerisation (Ani *et al.*, 2015).

Hydrotreatment catalysts are made of an active phase constituted by molybdenum or tungsten sulphides as well as by cobalt or nickel on oxide carriers. Generally applied combinations are Co-Mo, Ni-Mo, and Ni-W for the active phase and high surface area  $\gamma$ -alumina (transitional alumina) carrier. The metal content, expressed as oxides can reach 12–15 wt. % for Mo and 3–5 wt. % for Co or Ni. Co-Mo catalysts are preferentially used for hydrodesulphurization and Ni-Mo for hydrogenation and hydrodenitrogenation. Ni-W catalysts are applied for low-sulphur feeds. The most-used carriers are alumina and alumina-silica, the latter being characterised by a higher cracking activity\* (Boadu *et al.*, 2019).

The currently applied catalysts in re-refining are modified to improve the product base oil quality and to decrease the coke formation; however, their composition is typically not disclosed in the open literature. The technologies applying hydroprocesses require relatively high costs of investments compared with others. However, depending on the technology adopted, the total costs might be lower than in the solvent extraction process due to the high operating costs to make up for the solvent losses. On the other hand, solvent extraction and chemical treatment processes do not require catalyst regeneration. Moreover, it is not necessary to establish a hydrogen gas supply facility in these methods, which also reduces a risk concerning operation safety. (Boadu *et al.*, 2019)

In this research work, a thorough review on various removal of heavy metals and pollutants in used lubricating oil were considered beginning from conventional methods to the most recent advance methods as well as their limitations; further developments of these areas were also touched.

**Table 2.2. Previous studies conducted on the preparation of activated carbon from coconut and palm shells and their applications in removal of pollutants from wastewater and used lubricating oil.**

Raw Materials	Preparation Method	Application	References
Coconut shell and palm kernel shell	ZnCl <sub>2</sub> and CO <sub>2</sub>	Phenol, Methylene blue	(Hu and Srinivasan, 2001)
Palm kernel shell and coconut shell	Physical activation (N <sub>2</sub> gas)	Nitrogen adsorption	(Daud and Ali, 2004)
Palm kernel shell and coconut shell	Physical activation	Coarse aggregates in building materials	(Olanipekun <i>et al.</i> , 2006)
Palm kernel shell and coconut shell	H <sub>3</sub> PO <sub>4</sub> and ZnCl <sub>2</sub>	Cyanide removal	Jabit (2007)
Palm kernel shell and coconut shell	Physical (Heating and steam in the absence of oxygen)	Purification of polluted water for drinking	(Inegbenebor <i>et al.</i> , 2012)
Palm kernel shell and coconut shell	Physical (Heating and steam in the absence of oxygen) and Chemical (ZnCl <sub>2</sub> )	For CO <sub>2</sub> capture	(Hidayu and Muda, 2016b)
Coconut shell and palm kernel shell	K <sub>2</sub> CO <sub>3</sub> and NaHCO <sub>3</sub>	Adsorbents	(Boadu <i>et al.</i> , 2018)
Coconut shell and palm kernel shell	Physical and chemical	Review methods for treatment of used lubricating oils	Boadu <i>et al.</i> , 2019
Coconut shell and palm kernel shell	KOH and ZnCl <sub>2</sub>	Adsorption of Heavy Metals from Cement Waste Water	(Odisu <i>et al.</i> , 2019)
Coconut shell and palm kernel shell	K <sub>2</sub> CO <sub>3</sub> and NaHCO <sub>3</sub>	Removal of heavy metals and other contaminants in used lubricating oil	Boadu <i>et al.</i> , 2019

## **2.6 Knowledge Gap**

Gaps were identified after detailed discussions of the existing methods as reported in earlier works of literature. As a result of the advantages and disadvantages of each technique, percentage yield, waste disposal and management systems, processing costs, skilled personnel requirements, environmental compliance etc. Hence, there is the need to develop environmentally friendly and affordable adsorption process that can remove heavy metals and other pollutants in used lubricating oil.

In this research work, palm kernel and coconut shells were used to produce activated carbons. The effectiveness of palm kernel and coconut shells activated carbons for the removal of pollutants from used lubricating were investigated. Before, the palm kernel and coconut shells activated carbon samples were characterised by the following; Brunauer, Emmett and Teller (BET), Scanning Electron Microscopy (SEM) and Fourier Transform Infra-Red (FTIR) analysis techniques

## **CHAPTER THREE**

### **MATERIALS AND METHODS**

#### **3.1 Activated Carbon Samples Collection, Preparation and Characterization**

The oil palm kernel and coconut shells were collected from a traditional folks industry at Aluu and Choba Obio-Akpor local government area, Rivers State, Nigeria. The oil palm kernel and coconut shells were washed severally with tap water and finally with distilled water to remove specks of dirt and clouds of dust. The samples were further sun-dried for four days and finally dried thoroughly with a spray drier. The dried samples were pulverised based on ASTM-D2862-(2016) (Standard Test Method for Particle Size Distribution of Granular Activated Carbon). The powdered samples werethen sieved with 500 $\mu$ m mesh and then kept in an air-tight container for further analyses.





**Plate 3.1 Carbolite HT F17/5 High-Temperature Laboratory Chamber Furnace  
(5 litres 1700°C)**

### **3.1.1 Chemical Activation and Carbonization**

Activated carbons were prepared from the palm kernel and coconut shells using chemical activation method by (ASTM-D2862-(2016) and Boadu *et al.*, 2018). 30g of the powdered samples each that is palm kernel and coconut shells were impregnated with 1M solution of  $K_2CO_3$  and  $NaHCO_3$  and left in the room temperature for 3 hours. The samples were activated for 40mins at carbonization temperatures of  $800^\circ C$  using Carbolite Muffle Furnace. The activated carbons produced were washed with 0.5 M acetic acid solution (to neutralise it), rinsed thoroughly with distilled water until the pH's were within 6-7. The samples were sundried and sieved with 500  $\mu m$  mesh. Portions of the activated carbons retained on the mesh were oven-dried for one h, removed and stored in an airtight container. According to the literature, the surface area of chemically activated carbons can range from 250 to 2500  $m^2 g^{-1}$ , depending on the precursor and the type of treatment used for the production of the activated charcoal. However, the most common values are around 600 to 1000  $m^2 g^{-1}$  (Cabal *et al.*, 2009); (Magriotis *et al.*, 2010) and (Olivares-Marín *et al.*, 2009).

### **3.2 Determination of the Physiochemical Properties of the Activated Carbon Samples.**

#### **3.2.1 pH Measurement**

1 g of the samples each (palm kernel and coconut shells) were weighed and dissolved in 3 ml of de-ionised water. Each mixture was heated and stirred for 3 minutes to ensure proper dilution of the sample. The various solutions were filtered out, and their pH's were determined using a digital pH meter as found in the works (Evbuomwan *et al.*, 2013) and (Boadu *et al.*, 2018).

### 3.2.2 Determination of Moisture Content

The hygroscopic moisture content was determined using the method ASTM D2974 –(2014). Clean empty nickel porcelain was oven-dried at 110°C, cooled in a desiccator and then weighed. 1g of the samples each (palm kernel and coconut shells activated carbon) was measured into the porcelain separately, and the weights were recorded. The porcelain and its content were then oven-dried at 110°C to constant weight for 3 hours. The percentage moisture content was calculated using the formula(Boadu *et al.*, 2018).

$$X_o = \frac{W_1 - W_2}{W_1} \times 100\% \quad (3.1)$$

Where:  $X_o$ = Moisture content on wet basis;  $W_1$ = Initial weight of sample (g);  $W_2$ = Final weight of sample after drying (g).

### 3.2.3 Ash content Determination

Ash content determination was done according to the ASTM D2974 –(2014) method and (Verla *et al.*, 2012). Dry activated carbon samples each (palm kernel and coconut shells) 1.0g were placed into a porcelain crucible and transferred into a preheated muffle furnace set at a temperature of 1000°C and was left on for one hour. After which the crucibles and its content were transferred to a desiccator and allowed to cool. The crucibles and content were reweighed, and the weight loss was recorded as the ash content of the activated carbon samples ( $W_{ash}$ ). Then the % ash content (dry basis) for each sample was calculated from the equation below

$$Ash(\%) = \frac{W_{c\&s} - W_c}{W_o} \times 100\% \quad (3.2)$$

Where:  $W_c$  = Weight of crucible (g);  $W_{c\&s}$  = Weight of crucible and sample after ashing (g);  $W_o$ = Dry weight of carbon sample before ashing.

### 3.2.4 Pore Volume Measurement.

1 g each of the samples (palm kernel and coconut shells) were collected and transferred into a 10 ml measuring cylinder to get the total volume of the samples. Each sample was then poured into a beaker containing 20 ml of de-ionised water and boiled for 5 minutes (to ensure uniform distribution of the samples). The content in the beakers was then filtered, dried, and weighed. The pore volume of the samples was determined by dividing the increase in weight of the sample by the density of water (Evbuomwan *et al.*, 2013).

### 3.2.5 Bulk Density and Porosity Determination

The Bulk density and Porosity determined by the method of (Verla *et al.*, 2012). A cylinder and an aluminium plate were each weighed. Samples of activated carbon (palm kernel and coconut shells) were placed into the separate cylinder each, reweighed and transferred into the aluminium plate and then oven-dried to a constant weight at a temperature of 105<sup>0</sup>C for 60 minutes to remove all the trace amount of water present. The weights of the dry sample were recorded after the drying. A clean, dried well-corked density bottle was weighed. A small number of samples of activated carbon were taken and pulverised; sieved using 110 µm mesh size to obtain fine particles with the high surface area. The crushed samples were gradually placed inside the density bottle. 5 ml of distilled water added and weighed. The volume of the void ( $V_v$ ) was obtained by first determining the total volume of the cylinder each ( $V_t = \pi r^2 h$ ) used for the experiment. Also, the volumes of the activated carbons used were determined by the formula

$$V_s = \frac{M_s}{G_s P_w} \quad (3.3)$$

Where  $r$  = radius of cylinder,  $h$  = height of cylinder,  $M_s$  = mass of cylinder,  $G_s$  = specific gravity,  $P_w$  = density of water. The volume of the void ( $V_v$ ) was obtained as:  $V_v = V_t - V_s$ . The bulk density and porosity were calculated as:

$$\text{Bulk density}(B. d) = \frac{\text{Mass of Carbon Sample}}{\text{Volume}} \quad (3.4)$$

$$\text{porosity}(\eta) = \frac{\text{Volume of Void}}{\text{Total Volume}} \quad (3.5)$$

### 3.2.6 Surface Area Determination by Brunauer, Emmett and Teller (BET)

(2015 Model ASAP 2020 Micromeritics Analyzer)

The specific surface area of the chemical activated carbons from the palm kernel and coconut shells were determined including the pore size distribution by means of adsorption and desorption of nitrogen at 77 K using the method of Brunauer, Emmett and Teller (BET) with a 2015 Model ASAP 2020 Micromeritics Analyzer (Norcross, Ga 300093, U.S.A ) and (Odisu *et al.*, 2019).

### 3.2.7 Fourier transform infrared spectra (FTIR)

The Fourier transform infrared spectra (FTIR) of the chemical activated carbons from the palm kernel, and coconut shells (in the form of KBr pellets) were measured using a Digilab Excalibur FTS 3000 series spectrometer in the range 400-4000  $\text{cm}^{-1}$  at a resolution of 4  $\text{cm}^{-1}$ . FTIR spectroscopy was used to analyse and identify the key functional groups present in the structures of the chemically activated carbons from the palm kernel and coconut shells.

### **3.2.8 Scanning Electron Microscopy (SEM)**

The morphology of the samples (chemically activated carbons from the palm kernel and coconut shells) were obtained by scanning electron microscopy (SEM) using a JSM-7610F (Tokyo, Japan). The equipment is an ultra-high resolution Schottky Field Emission Scanning Electron Microscope which has a semi-in-lens objective lens and high power optics that can provide high throughput as well as high-performance analyses. Analyses by scanning electron microscopy were performed to investigate the morphology of the adsorbents (chemically activated carbons from the palm kernel and coconut shells).

### **3.2.9 Determination of Heavy Metals Present**

Perkin Elmer Atomic Absorption Spectrophotometer model number buck Scietchic 210 were used to determine the heavy metals that were present in oil samples before and after filtration processes with the activated carbon samples (palm kernel and coconut shells) (Bentum *et al.*, 2011).

### **3.3 Samples Collection, Preparation and Characterization**

Five litres of used lubricating oil samples (total quartz 20 W 50) that have been used for 3&6 months were collected from Total Service Stations, Port Harcourt, Rivers State, Nigeria. The 3 & 6-month-old used lubricating oils were labelled as sample A &B, respectively. Also, 5 litres of fresh sealed lubricating oil (total quartz 20 W 50) were purchased from the same source and labelled as control sample C. Used lubricating oil samples A&B were stored for seven (7) days to allow large suspended particles and small particles to settle under gravity.

### **3.3.1 Preparation of Samples**

Filtration of the used lubricating oil samples A & B were carried out under gravity using Buchner funnel and filter paper to remove impurities such as sand, metal chips, micro impurities that contaminated the lube oil. Five litres of the used oil was filtered for the sample. The used lubricating oils were allowed to settle for 24 hours (to ensure that all contaminants settle at the bottom) and samples were further filtered.

### **3.3.2 Characterization of Samples**

#### **3.3.2. 1 pH Measurement**

The oil samples pH were measured with the use of pH indicator meter as described by ASTM D 7946 (2014) and(Boadu *et al.*, 2018). 30 ml of the oil samples were measured into 50 ml beakers and vigorously stirred. The pH was obtained using a pH indicator and read after 5 seconds. The pH achieved were cross-matched with the colour scale.

#### **3.3.2.2 Specific gravity**

The specific gravity of both the virgin and used lubricating oil samples was determined using ASTM D 1298 (2004), standard test method for density, relative density, or API gravity of crude petroleum and liquid petroleum products with a hydrometer.

#### **3.3.2.3 Dynamic viscosity**

The dynamic viscosity for the virgin and used lubricating oil samples was ascertained based on ASTM D 1298 (2004), standard test method for density, relative density, or API gravity of crude petroleum and liquid petroleum products with a hydrometer.

#### **3.3.2.4 Kinematic viscosity**

Kinematic viscosities of the virgin and used lubricating oil samples were measured at 37<sup>0</sup>C with Canon-Fenske Routine viscometers or Canon-Fenske Opaque viscometers according to ASTM D 445 (2012), standard test method for transparent and opaque liquids respectively.

#### **3.3.2.5 Water content**

The water content of the virgin and used lubricating oil samples were determined to assess the amount of water contaminant resulting from condensation and combustion chamber blow-by gases into the crankcase. ASTM D6304 (2016), standard test method for determination of Water in Petroleum Products, Lubricating Oils, and Additives by Coulometric Karl Fischer Titration.

#### **3.3.2.6 Sediment content**

Sediments content of the virgin and used lubricating oil samples were determined to ascertain the level of contamination using ASTM D 2273 (2005), standard test methods for trace sediments in lubricating oils determination.

#### **3.3.2.7 Digestion and Elemental Analysis**

According to the acid digestion method used by (Boadu *et al.*, 2018) and ASTM D7455 (2019). 0.5 g each of the excellent oil samples were weighed into a Kjeldahl digestion flask, and 5 mL concentrated H<sub>2</sub>SO<sub>4</sub> was added to each of the oil samples and heated in a fume hood until the oil samples started to char. Then, 10ml of H<sub>2</sub>O<sub>2</sub> were added to the charred mixture and were heated for 5 min, and the mixture turned colourless when the digestion was



completed. The used and virgin lubricating oil (control) samples were digested using the same procedure. The each digested samples were transferred into a 100 ml volumetric flask and made up to the mark. The samples were then transferred into a cleaned plastic container for AAS analyses. The digested samples were analysed using Perkin Elmer Atomic Absorption Spectrophotometer model number Buck Scietiphic 210 at the Pollution Control and Environmental Management Limited, Port Harcourt, Nigeria.

### **3.5 Methods for Data Analysis and Presentation**

XLSTAT-2018-01.01 and SPSS version 23 statistical analysis software's were used to analyse the data generated in the experiments. The results obtained were analysed statistically using the following tables, histogram graphs, isotherm plots, straight-line graphs, contour plots, ANOVA, Linear model, co-efficient of determination, regression model ( $R^2$ ), F-test etc.

## **CHAPTER FOUR**

### **RESULTS AND DISCUSSION**

#### **4.0 Introduction**

In this chapter, all the results obtained from the experiments conducted are presented in the form of tables, graphs, plates, figures and follows up with insightful scientific discussions. The observation of the adsorption process based on the removal of contaminants in used lubricating oil with the chemically activated carbons from palm kernel and coconut shells were thoroughly discussed. Also, models were generated based on the removal of contaminants in used lubricating oil using each of the chemically activated carbons with response variables during the adsorption processes are presented in this chapter.

#### **4.1 Presentation of Results**

This section has an orderly arrangement of all the data obtained throughout the various experiments conducted, and they are shown in the form of Plates, Figures, Tables and Graphs.

Table 4.1 shows the results of the physicochemical parameters of the virgin and used lubricating oil samples. Also, Tables 4.2 shows the results of the concentration levels of various elements present in virgin and used lubricating oil samples

**Table 4.1: Physicochemical parameters of the virgin and used lubricating oil samples.**

Parameters	Units	Sample A	Sample B	Control (Virgin)
pH @ 29 <sup>0</sup> C		5.0	5.0	6.0
Specific gravity @ 29 <sup>0</sup> C		0.89	0.89	0.88
Dynamic viscosity @ 27 <sup>0</sup> C	cP	300+	300+	300+
Kinematic viscosity @ 27 <sup>0</sup> C	cSt	337+	337+	341+
Basic Sediment & Water				
Oil	%	100.0	99.9	100.0
Water	%	0.0	0.1	0.0
Sediments	%	0.0	0.0	0.0

**Table 4.2: Concentration levels of various elements present in virgin and used lubricating oil samples.**

Parameters		Units	Sample A	Sample B	Control (Virgin)
Copper	(Cu)	ppm	0.24	0.21	<0.001
Iron	(Fe)	ppm	4.61	3.33	1.49
Zinc	(Zn)	ppm	19.5	14.8	2.83
Cadmium	(Cd)	ppm	0.02	0.03	0.03
Lead	(Pb)	ppm	0.53	1.45	0.97
Chromium	(Cr)	ppm	0.39	0.45	0.39
Magnesium	(Mg)	ppm	5.10	20.06	37.4

Table 4.3 shows the results obtained for the physico-chemical characteristics of chemical activated carbons from coconut and palm kernel shells respectively while Table 4.4 shows the results of the Concentrations of heavy metals present in Coconut and Palm Kernel Shells. Also, the One-way ANOVA in SPSS Statistics of the activated carbons from coconut and palm kernel shells are presented in Table 4.5.

**Table 4.3: Physico-Chemical Characteristics of Chemical Activated Carbons from Coconut and Palm Kernel Shells.**

<b>Physico-chemical Properties</b>	<b>Coconut Shell</b>	<b>Palm Kernel shell</b>
pH	7.5	8.7
Moisture (%)	19.7	20.4
Ash content (%)	12.3	14.2
Pore Diameter (nm)	2.840e+00	3.000e+00
Bulk density (g/cm <sup>3</sup> )	1.21	1.25
Porosity (%)	70	65
Specific gravity	1.42	1.61
BET Surface area (m <sup>2</sup> /g)	1177.52	717.142

e : exponential

**Table 4. 4: Concentrations of heavy metals present in Coconut and Palm Kernel Shells.**

<b>N/S</b>	<b>Parameters</b>	<b>Unit</b>	<b>Coconut shell</b>	<b>Palm Kernel shell</b>
<b>1</b>	Cadmium, Cd	Ppm	0.01±0.02	0.01±0.01
<b>2</b>	Chromium, Cr	Ppm	0.81±0.45	1.01±0.37
<b>3</b>	Lead, Pb	Ppm	0.57±0.26	0.58±0.26
<b>4</b>	Nickel, Ni	Ppm	0.37±0.16	0.39±0.18
<b>5</b>	Zinc, Zn	Ppm	0.66±0.15	1.52±0.2
<b>6</b>	Calcium, Ca	Ppm	0.55±0.18	2.95±0.35
<b>7</b>	Potassium, K	Ppm	179.33±5.51	128.00±3.00
<b>8</b>	Copper, Cu	Ppm	1.54±0.15	0.91±0.36
<b>9</b>	Magnesium, Mg	Ppm	7.33±0.58	18.00±2.0
<b>10</b>	Iron, Fe	Ppm	132.02±0.50	81.79±0.20

ppm: part per million

**Table 4.5: One-way ANOVA in SPSS Statistics of the activated carbons from coconut and palm kernel shells**

		Sum of Squares	df	Mean Square	F	Sig.
Copper	Between Groups	2.115	2	1.057	17.55	<b>0.003<sup>a</sup></b>
	Within Groups	0.362	6	0.06		
	Total	2.476	8			
Iron	Between Groups	8633.889	2	4316.944	33464.69	<b>0.000<sup>a</sup></b>
	Within Groups	0.774	6	0.129		
	Total	8634.663	8			
Zinc	Between Groups	1.929	2	0.964	27.551	<b>0.001<sup>a</sup></b>
	Within Groups	0.21	6	0.035		
	Total	2.139	8			
Cadmium	Between Groups	0	2	0	0.176	<b>0.842<sup>b</sup></b>
	Within Groups	0.001	6	0		
	Total	0.001	8			
Lead	Between Groups	19.014	2	9.507	35.256	<b>0.000<sup>a</sup></b>
	Within Groups	1.618	6	0.27		
	Total	20.632	8			
Chromium	Between Groups	0.059	2	0.029	0.181	<b>0.839<sup>b</sup></b>
	Within Groups	0.977	6	0.163		
	Total	1.036	8			
Magnesium	Between Groups	2010.889	2	1005.444	129.271	<b>0.000<sup>a</sup></b>
	Within Groups	46.667	6	7.778		
	Total	2057.556	8			
Nickel	Between Groups	0.003	2	0.001	0.047	<b>0.955<sup>b</sup></b>
	Within Groups	0.19	6	0.032		
	Total	0.193	8			
Calcium	Between Groups	9.075	2	4.538	78.702	<b>0.000<sup>a</sup></b>
	Within Groups	0.346	6	0.058		
	Total	9.421	8			
Potassium	Between Groups	4326.222	2	2163.111	111.246	<b>0.000<sup>a</sup></b>
	Within Groups	116.667	6	19.444		
	Total	4442.889	8			

Key: **a**-significant; **b**-non-significant.



Table 4.6 shows the functional groups and the classification of compounds identified in chemically activated carbon from palm kernel shell by FTIR analysis. Also, Table 4.7 shows the functional groups and the classification of compounds identified in chemically activated carbon from Coconut shell by FTIR analysis while Table 4.8 shows the surface area data summary for the palm kernel and coconut shells.

**Table 4.6 Functional groups and the classification of compounds identified in chemically activated carbon from palmkernel shell by FTIR analysis.**

Transmittance peaks indicated by the range of wavenumber ( $\text{cm}^{-1}$ )	Wavenumber of Samples ( $\text{cm}^{-1}$ )	Functional groups	Classification of compounds
3800-4000	3753	O-H stretching	Alcohol, Phenol and Hydroxyl group
3600-3800	3678	O-H stretching	Alcohol, Phenol and Hydroxyl group
3000-3600	3593	O-H stretching	Alcohol, Phenol and Hydroxyl group
2300-2800	2322	-COOH stretching	Carboxylic acid group
2000-2300	2087	C=N stretching	Nitriles
1700-2000	1994	$\text{CH}_2\equiv\text{CH}_2$	Alkynes
1300-1600	1543	$\text{CH}_2$ and $\text{CH}_3$ twisting	Alkanes
1000-1200	1017	C-O Bending	Alcohol; Ether; Carboxylic acid

**Table 4.7 Functional groups and the classification of compounds identified in chemically activated carbon from Coconut shell by FTIR analysis.**

Transmittance peaks indicated by the range of wavenumber ( $\text{cm}^{-1}$ )	Wavenumber of Samples ( $\text{cm}^{-1}$ )	Functional groups	Classification of compounds
3800-4000	3753	O-H stretch	Hydroxyl group
3500-3700	3652	O-H stretch	Hydroxyl group
3100-3400	3190	$\equiv$ C-H stretch	Alkyne
2200-2400	2325	C $\equiv$ C stretching	Aldehyde
2100-2300	2109	C=C=C band	Allene group
1900-2000	1990	C=C=C band	Allene group
1700-1800	1736	C=C Stretching	Pyrone
1600-1700	1621	C=O axial deformation	Aldehyde; Ketones; Carboxylic acid
1500-1600	1543	C=C stretching	Aromatics
1300-1500	1397	C-H Bending ( $\text{CH}_2$ and $\text{CH}_3$ )	Alkanes

**Table 4.8 Surface Area Data Summary.**

<b>Parameters</b>		<b>Palm Kernel shell</b>	<b>Coconut shells</b>
Single Point BET	(m <sup>2</sup> /g)	3.896e+02	7.258e+02
Multi-Point BET	(m <sup>2</sup> /g)	7.171e+02	1.178e+03
Langmuir surface area	(m <sup>2</sup> /g)	2.304e+04	6.642e+03
BJH method cumulative adsorption surface area	(m <sup>2</sup> /g)	7.322e+02	1.340e+03
DH method cumulative adsorption surface area	(m <sup>2</sup> /g)	7.769e+02	1.427e+03
t-method external surface area	(m <sup>2</sup> /g)	7.171e+02	1.178e+03
DR method micropore area	(m <sup>2</sup> /g)	7.114e+02	1.268e+03
DFT cumulative surface area	(m <sup>2</sup> /g)	1.494e+02	2.837e+02

e: exponential

In this Table 4.9, properties of the filter beds for the activated carbons from palm kernel and coconut shells are shown. Table 4.10 shows the results of the volume of samples adsorbed by various filter beds after filtration process and adsorption capacity.

**Table 4.9 Properties of the filter beds for the activated carbons from palm kernel and coconut shells.**

Parameters		Palm kernel shell	Coconut shell
Mass of filter bed	(g)	155.10	155.10
The volume of filter bed	(cm <sup>3</sup> )	200.04	428.65
The density of filter bed	(g/cm <sup>3</sup> )	0.7753	0.3618
Volume of liquid before filtration	(ml)	600	600
Breakthrough time	(hr)	1.15	1.37
Time for the entire filtration process	(hr)	480	120

**Table 4.10 Volume of samples adsorbed by various filter beds, after filtration process and adsorption capacity**

S/N	Volume adsorbed by filter bed (m <sup>3</sup> )	Volume after filtration process (m <sup>3</sup> )	Adsorption capacity (kg/m <sup>3</sup> )
Control sample coconut shell	310	290	$5.00 \times 10^{-4}$
Sample A coconut shell	305	295	$5.09 \times 10^{-4}$
Sample B coconut shell	350	250	$4.43 \times 10^{-4}$
Control sample palm kernel shell	408	192	$3.80 \times 10^{-4}$
Sample A palm kernel shell	420	180	$3.70 \times 10^{-4}$
Sample B palm kernel shell	370	230	$4.19 \times 10^{-4}$

The statistical analysis of virgin and used lubricating oil samples before filtration with palm kernel and coconut shells activated carbons are presented in Tables 4.11. Also the statistical analysis carried out after filtration with palm kernel and coconut shell samples are presented in Tables 4.12 and 4.13 respectively. Furthermore, the Summary (LS means) results obtained from the filtration process for both palm kernel and coconut shells have been presented in Table.4.14 while the Table 4.15 shows the analysis of variance of variables and summary for all Y's for the various heavy metals.



**Table 4.11: Mean,  $\pm$ SD, of virgin and used lubricating oil samples before filtration with palm and coconut shells activated carbons.**

Samples/Parameters	Control	Sample A	Sample B
Cu (ppm)	0.001 $\pm$ 0.000	0.150 $\pm$ 0.008	0.220 $\pm$ 0.096
Fe (ppm)	1.502 $\pm$ 0.092	4.650 $\pm$ 0.159	3.350 $\pm$ 0.289
Zn (ppm)	2.833 $\pm$ 0.034	16.475 $\pm$ 0.950	14.575 $\pm$ 0.272
Cd (ppm)	0.020 $\pm$ 0.008	0.020 $\pm$ 0.008	0.030 $\pm$ 0.008
Pb (ppm)	1.000 $\pm$ 0.093	1.045 $\pm$ 0.478	1.525 $\pm$ 0.222
Cr (ppm)	0.410 $\pm$ 0.051	0.400 $\pm$ 0.065	0.445 $\pm$ 0.039
Mg (ppm)	41.900 $\pm$ 0.258	5.450 $\pm$ 0.265	21.475 $\pm$ 0.650
Specific Gravity @ 29°C	0.880	0.890	0.890
Dynamic Viscosity @ 27°C (Cp)	300+	300+	300+
Kinematic Viscosity @ 27°C (cSt)	341+	337+	337+
pH@ 29°C	6.0	5.0	5.0
<b>Basic Sediment &amp; Water</b>			
Oil (%)	100	100	99.9
Water (%)	0	0	0.1
Sediment (%)	0	0	0

Refer to appendix for isotherms /graphs

**Table 4.12: Mean,  $\pm$ SD of virgin and used lubricating oil samples after filtration with Palm Kernel Shell Sample**

Samples/Parameters	Control	Sample A	Sample B
Cu (ppm)	0.075 $\pm$ 0.013	0.400 $\pm$ 0.018	0.230 $\pm$ 0.008
Fe (ppm)	1.150 $\pm$ 0.129	8.500 $\pm$ 0.258	3.400 $\pm$ 0.183
Zn (ppm)	8.325 $\pm$ 0.275	10.375 $\pm$ 0.171	5.450 $\pm$ 0.300
Cd (ppm)	0.000 $\pm$ 0.000	0.018 $\pm$ 0.009	0.000 $\pm$ 0.000
Pb (ppm)	1.650 $\pm$ 0.039	1.648 $\pm$ 0.097	2.388 $\pm$ 0.070
Cr (ppm)	0.065 $\pm$ 0.013	0.210 $\pm$ 0.026	0.135 $\pm$ 0.013
Mg (ppm)	0.350 $\pm$ 0.026	0.900 $\pm$ 0.025	0.505 $\pm$ 0.013
Specific Gravity @ 29°C	0.885	0.892	0.890
Dynamic Viscosity @ 27°C (Cp)	300+	300+	300+
Kinematic Viscosity @ 27°C (cSt)	>338.980	>336.323	>337.079
pH@ 29°C	6.5	6.0	5.5
<b>Basic Sediment &amp; Water</b>			
Oil (%)	100	99.99	99.99
Water (%)	0	<0.01	<0.01
Sediment (%)	0	0	0

Refer to appendix for isotherms /graphs

**Table 4.13: Mean,  $\pm$ SD of virgin and used lubricating oil samples after filtration with Coconut Shell Sample**

Samples/Parameters	Control	Sample A	Sample B
Cu (ppm)	0.001 $\pm$ 0.000	0.780 $\pm$ 0.014	0.790 $\pm$ 0.026
Fe (ppm)	3.650 $\pm$ 0.625	13.500 $\pm$ 0.942	14.125 $\pm$ 0.618
Zn (ppm)	0.6700 $\pm$ 0.071	5.838 $\pm$ 0.344	5.400 $\pm$ 0.280
Cd (ppm)	0.001 $\pm$ 0.000	0.001 $\pm$ 0.000	0.001 $\pm$ 0.000
Pb (ppm)	0.563 $\pm$ 0.172	0.410 $\pm$ 0.037	0.438 $\pm$ 0.222
Cr (ppm)	0.348 $\pm$ 0.049	0.388 $\pm$ 0.046	0.528 $\pm$ 0.055
Mg (ppm)	1.475 $\pm$ 0.171	3.625 $\pm$ 0.222	0.645 $\pm$ 0.037
Specific Gravity @ 29°C	1.640	1.800	1.740
Dynamic Viscosity @ 27°C (Cp)	300 <sup>+</sup>	300 <sup>+</sup>	300 <sup>+</sup>
Kinematic Viscosity @ 27°C (cSt)	>182.93	>166.60	>106.32
pH@ 29°C	5.5	5.0	5.0
Basic Sediment & Water			
Oil (%)	100	100	100
Water (%)	0	0	0
Sediment (%)	0	0	0

Refer to appendix for isotherms /graphs

**Table.4.14:Summary (LS means) - Filtration process**

N/S	Copper (Cu)	Iron (Fe)	Zinc (Zn)	Cadmium (Cd)	Lead (Pb)	Chromium (Cr)	Magnesium (Mg)
Before filtration	0.1236c	3.1675c	11.2942a	0.0233a	1.1900b	0.4183a	22.9417a
Filtration with Coconut Shell	0.5236a	10.4250a	3.9692c	0.0009b	0.4700c	0.4208a	1.9150b
Filtration with Palm Kernel	0.3625c	4.3500b	8.0500b	0.0058b	1.8950a	0.1367b	0.5850c

Key: **a,b** and **c** shows significance difference

**Table 4.15: Analysis of Variance of Variables and Summary for all Y's for the various Heavy Metals**

S/N	(Cu)	(Fe)	(Zn)	(Cd)	(Pb)	(Cr)	(Mg)
R <sup>2</sup>	0.8185	0.9927	0.9953	0.8347	0.9349	0.9378	0.9997
F	15.2181	459.5948	715.9685	17.0436	48.4738	50.8595	11356.9041
Pr > F	< 0.0001	< 0.0001	< 0.0001	< 0.0001	< 0.0001	< 0.0001	< 0.0001
Filtration process	20.9543	864.8179	1058.5040	51.4600	164.4045	171.7839	26526.6506
	< 0.0001	< 0.0001	< 0.0001	< 0.0001	< 0.0001	< 0.0001	< 0.0001
Samples	13.1799	696.8264	978.8792	3.1714	17.1650	14.7779	5447.8007
	0.0001	< 0.0001	< 0.0001	0.0579	< 0.0001	< 0.0001	< 0.0001
Filtration process* Samples	13.3691	138.3674	413.2453	6.7714	6.1629	8.4382	6726.5826
	< 0.0001	< 0.0001	< 0.0001	0.0007	0.0012	0.0001	< 0.0001

Refer to appendix for isotherms /graphs

In this Figure 4.1, the concentration of various heavy metals present in virgin and used lubricating oil samples are shown. Also, Plates 4.1 and 4.2 SEM micrographs of palm kernel and coconut shells are shown, while Plates 4.3 and 4.4 shows the FT-IR spectra for Palm Kernel and coconut shells respectively used in this study.

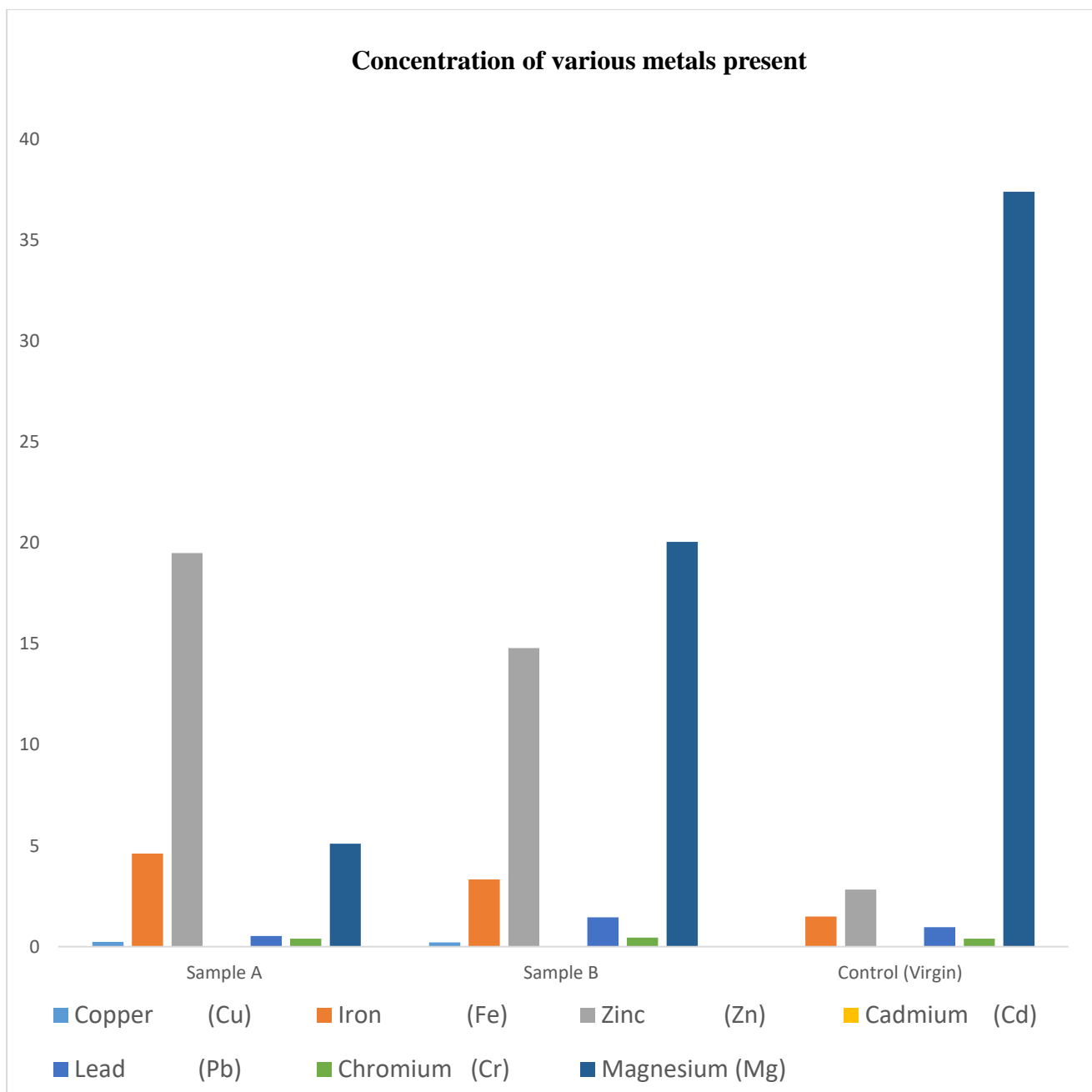


**Figure 4.1 Concentration of various heavy metals present in virgin and used lubricating oil samples.**

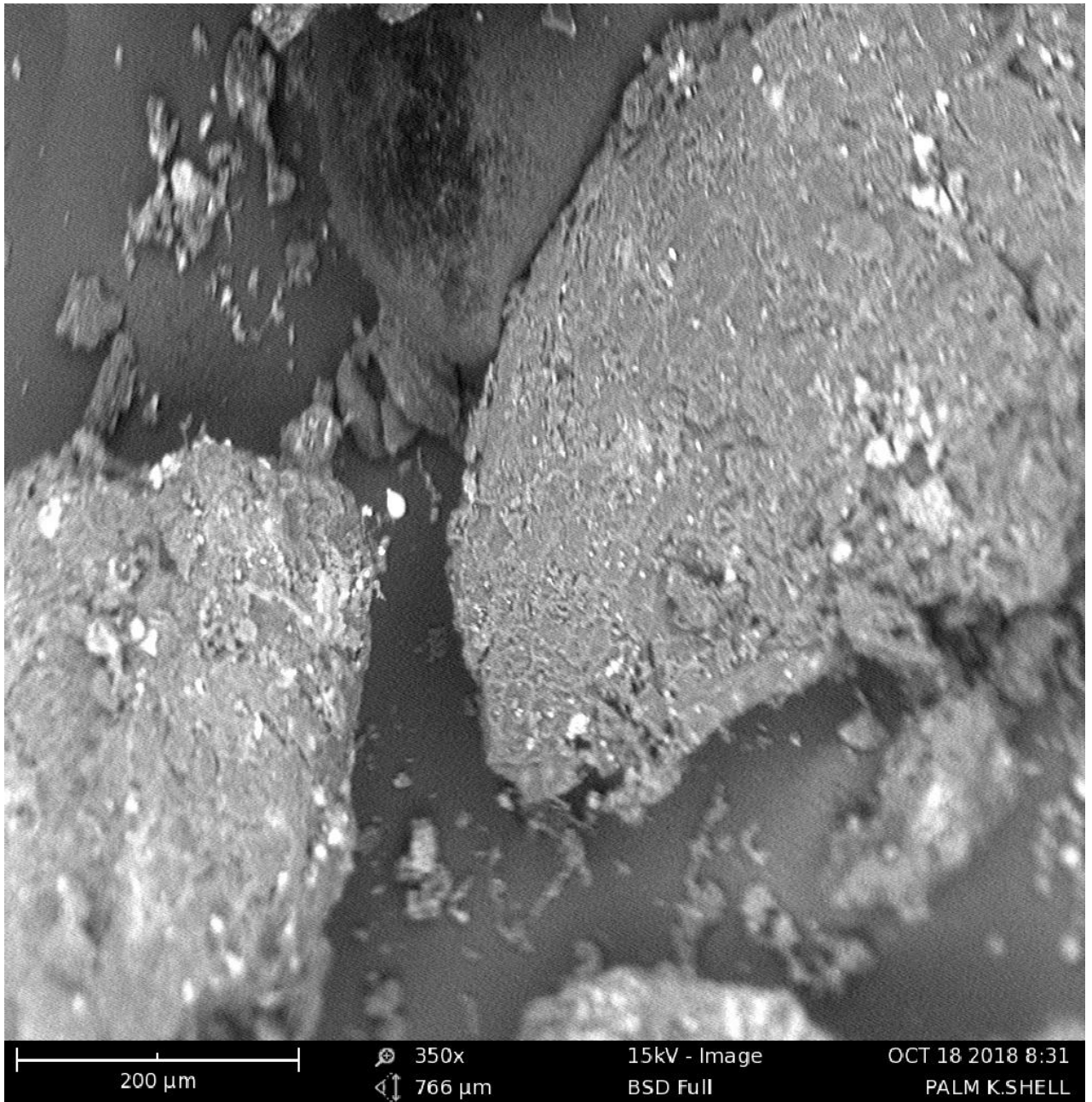


**Plate 4.1 SEM micrograph of Palm Kernel Shell**



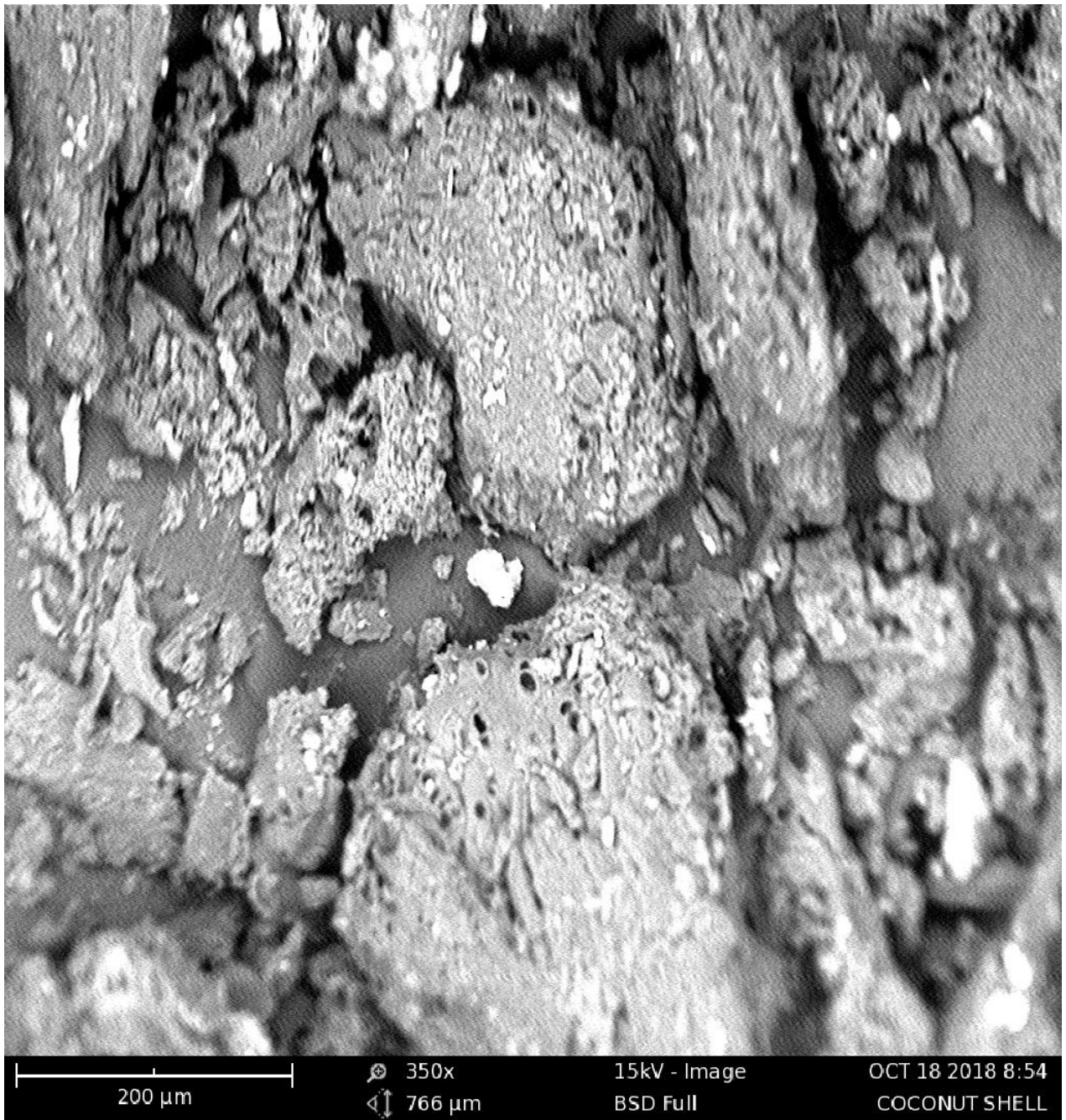


**Plate4.2 SEM micrograph of Coconut Shells**

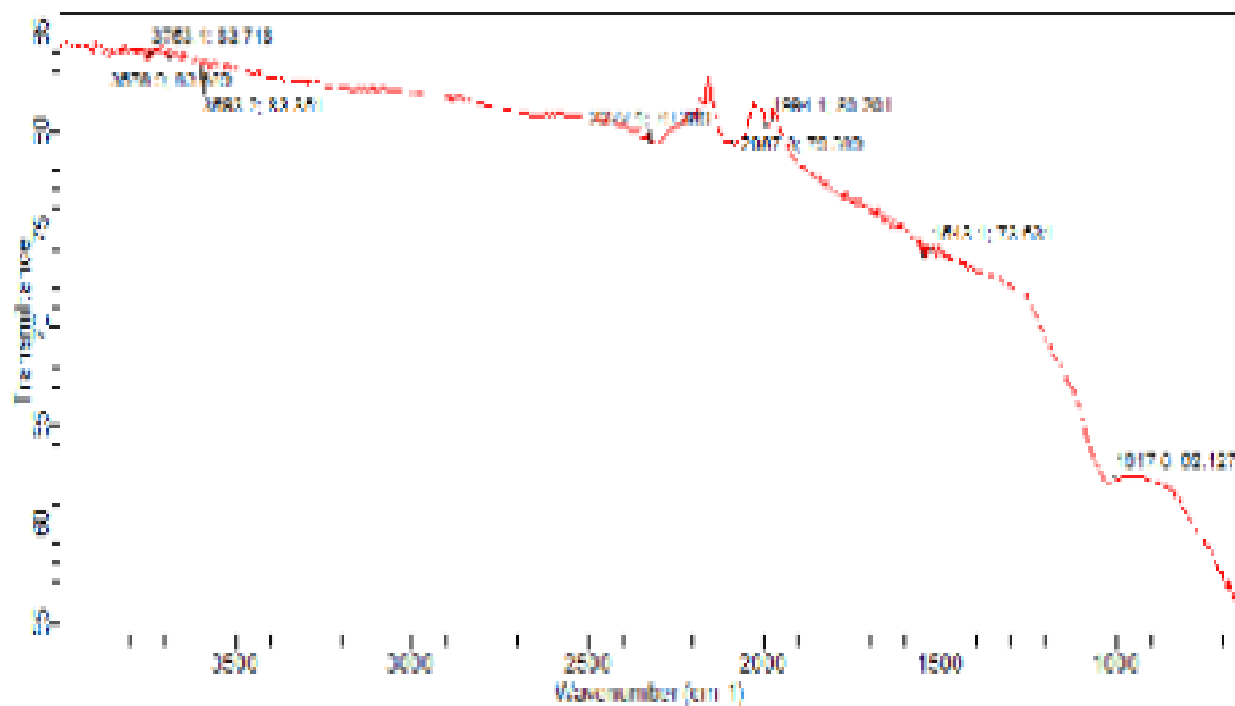


**Plate 4.3** Picture of FTIR spectra of Palm Kernel Shells

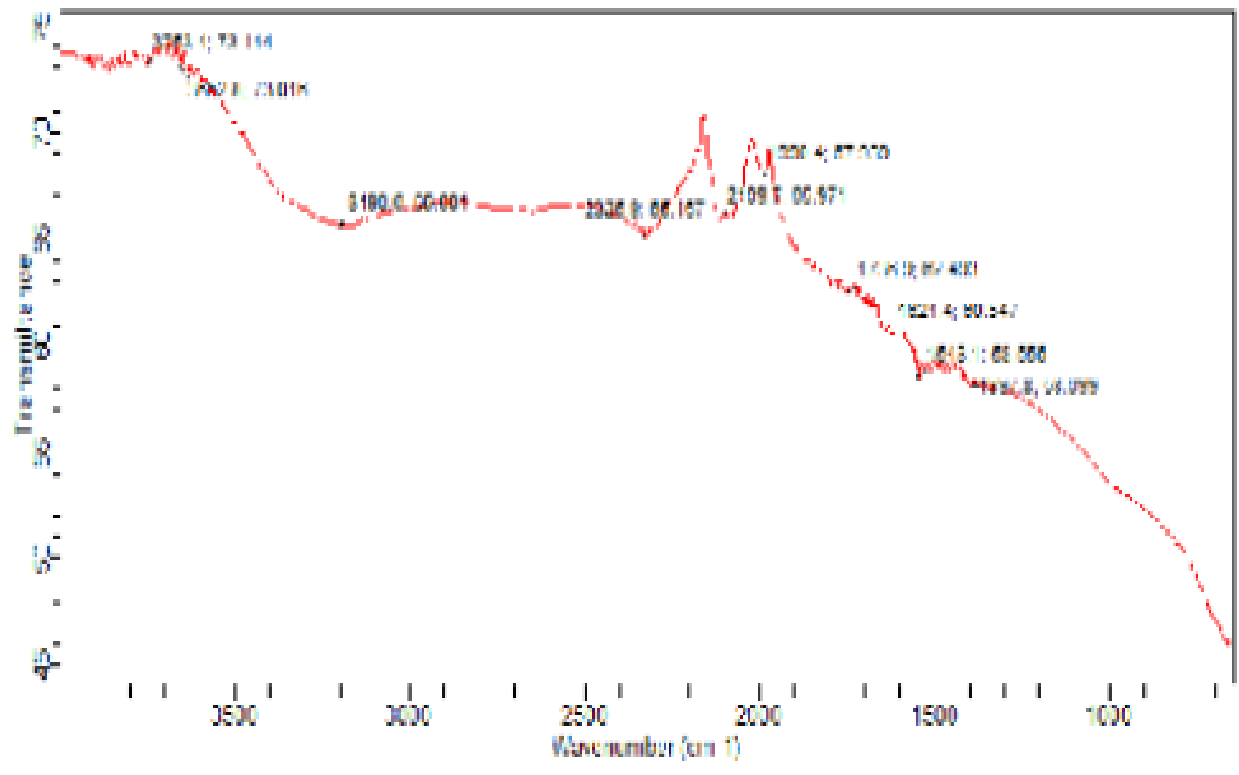


Plate 4.4 Picture of FTIR spectra of Coconut Shells

## **4.2. Discussions of Results**

A detailed description of the different parameters and their effects on the corresponding responses to variables was analysed to explain the parameters evaluated and observed throughout this research work. These analyses were done using the state of the art technology and current best practices available. The various parameters studied include heavy metals and other contaminants present in virgin and used lubricating oil samples; preparation and characterisation of chemically activated carbons from palm kernel and coconut shells; removal and treatment of pollutants in used lubricating oil using palm kernel and coconut shells as adsorbents and finally modelling of the results obtained.

### **4.2.1. The physicochemical and concentration of heavy metals analyses in virgin and used lubricating oils: a spectroscopy study**

The physicochemical and level of heavy metals analyses in virgin and used lubricating oils: a spectroscopy study was carried out. The results are shown in Tables 4.1, 4.2 and Figure 4.1. The results are then discussed under the following properties of lubricants.

**4.2.1.1 pH:** From Table 4.1, it can be observed that the acidic pH values were found in the used lubricating oil compared to that of the virgin lubricating oil. The acid corrosion is caused by hydrogen ions ( $H^+$ ); the measurement of their concentration gives a good indication of how corrosive an oil is becoming. Usually, base (virgin) oil has a pH range 7-8, which decreases steadily over time into the acidic region when it is being used. This account for the reason why high acidic values were found in the used lubricating oil samples (Boadu *et al.*, 2018)

However, the pH 6.0 recorded on the virgin oil samples might be due to the presence of synthetic additives present in the lubricating oil to improve its performance. At a certain

point, the pH begins to decrease more rapidly, and it's at this point when the oil needs to be changed (Boadu *et al.*, 2018).

#### **4.2.1.2 Specific Gravity:**

From the results obtained in Table 4.1, the specific gravity of the used lubricating oil samples was 0.89 while that of the virgin oil was 0.88. Specific gravity is influenced by the chemical composition of the oil. An increase in the number of aromatic compounds in the oil results in an increase in the specific gravity, while an increase in the saturated compounds results in a decrease in specific gravity (Hamawand *et al.*, 2013b). Used lubricating oil samples specific gravity increases with the presence of increasing amounts of solids in the used oil. One percent of the weight of solids in the sample can raise the specific gravity by 0.007 (Forsthoffer, 2011).

#### **4.2.1.3 Dynamic viscosity:**

From the results obtained in Table 4.1 after the analyses of both the virgin oil and used oil samples, the dynamic viscosity at 27<sup>0</sup>C remains the same. This indicates the dynamic viscosity has no positive correlation on both virgins and used lubricating oil samples (Boadu *et al.*, 2018).

#### **4.2.1.4 Kinematic Viscosity:**

Kinematic viscosity at 27<sup>0</sup>C for all the samples were determined. From the results in Table 4.1, it shows that samples A&B have values of 337+ while that of control (virgin) oil was 341+. The lower values obtained in the used lubricating oil samples indicates the destructive effects of sulphuric acid on the oil. Kinematic viscosity and viscosity, in general, are the essential consideration in choosing lubricating oils. The strength of the oil firm is

approximately proportional to its viscosity which determines the thickness of the layer of oil between the metallic surfaces in reciprocal movement(Shoaib, 2013) and (Emam and Shoaib, 2012). From Table.4.1, it was observed that the used lubricating oil samples had lost their kinematic viscosity values. This can be attributed to contamination resulting from thermal degradation effect of molecular constituents of the base oil (Hamawand *et al.*, 2013b) and (Boadu, *et al.*, 2018).

#### **4.2.1.5 Water and sediment contents:**

After the analyses shown in the Table. 4.1, it was observed that there were no sediments materials in all the samples analysed. However, a trace amount of water content in sample B was found. The water content found in sample B can lead to corrosion of the crankcase and other problems in the engine.

For example, lubricating oil's water and sediment content when significant can cause equipment corrosion and processing problems (Ahmed *et al.*, 2009).

#### **4.2.1.6 Elemental Metals:**

Almost all lubricating oils constituents contains metallic elements that have been added to it to improve efficiency. Generally, the presence of heavy metals in lubricating oils is considered as contaminants that should be removed entirely to produce suitable base oil for producing new virgin oil (Al-wesabi *et al.*, 2015). From the analyses, the concentration of seven (7) heavy metals such as copper, (Cu), Iron, (Fe), zinc, (Zn), cadmium, (Cd), lead, (Pb), chromium, (Cr) and magnesium, (Mg) in the two used lubricating oil samples A&B and virgin oil sample are presented in Table.4.2.

From Table. 4.2,the concentration of Mg in the virgin decrease from 37.4 ppm to 20.06 ppm for sample B and 5.10 ppm for sample A respectively. The high concentration of Mg in virgin

oil makes it better. The oil is more viscous by the high concentration of Mg and thus prevents wear or corrosion. The decrease in Mg concentration also indicates that Mg is consumed as suggested in the literature (Zajac *et al.*, 2015) and (Onyekwere *et al.*, 2008).

The presence of wear heavy metals in both virgin and used lubricating oil samples were observed in Table 4.2, though varying in concentrations. The highest value of Pb (1.45ppm) and Cr (0.45ppm) were found in used lubricating oil sample B. Pb (0.53ppm) and Cr (0.39 ppm) were ascertain for used lubricating oil sample A. The value for lead in virgin lubricating oil sample was (0.97ppm) which is in line with that reported by (Cassap, 2008); (Muhammad *et al.*, 2016) and (Buses *et al.*, 2019).

However, the Cr content of 0.45 ppm of used oil sample B was a bit higher than the virgin oil sample and used oil sample A respectively, as suggested by literature (Cassap, 2008).

Also, from Table 4.2, the concentration of Zn increases significantly from virgin to the used lubricating oil samples respectively as follows: Zn in virgin oil was (2.83 ppm) while in used lubricating oil samples B and A are (14.8 ppm) and (19.5 ppm). A similar pattern had been reported in the literature by (Jodeh, Sawalha *et al.*, 2015); (Muhammad *et al.*, 2016) and (Buses *et al.*, 2019).

Also, from the results obtained in Table 4.2, there were increased in wear heavy metal Fe in the used lubricating oils samples B (3.33 ppm) and A (4.61 ppm) compared to that of virgin oil sample (1.49 ppm). This was attributed to wear of the metal Fe from the cylinder liners, piston, and rings, ball roller bearings of gear etc. (Onyekwere *et al.*, 2008); (Lara *et al.*, 2015) and (Abdul *et al.*, 2015). It was not surprising as the cars from where the used lubricating oil samples were obtained were more than ten years old since the date of manufacture.

Finally, from the results obtained in Table 4.2, there was no significant difference in the values of Cd recorded in both the virgin (0.03 ppm) and used lubricating oil samples A (0.02

ppm) and B (0.03 ppm) respectively. Cd is introduced in the lubricating oil as a contaminant during use. Based (virgin) oils usually are free from cadmium (Kwakye-Awuah *et al.*, 2018). However, the trace amount detected might be coming from the additives introduced into the lubricating oils to enhance its performance (Boadu *et al.*, 2018).

#### **4.3.2. Comparative Studies of the Physicochemical Properties and Heavy Metals adsorption Capacity of Chemical Activated Carbon from Palm Kernel and Coconut shells**

From the results of the research carried out on the comparative studies of the physicochemical properties and metals present in chemically activated carbon from palm kernel and coconut shells have been carefully explained in detail in the Tables 4.3 – 4.5 and Figure 4.1. Tables 4.3- 4.5 show the physicochemical parameters, concentration of metals present and one-way ANOVA in SPSS Statistics. Figure 2 shows the graph of the level of heavy metals obtained.

##### **4.3.2.1 pH.**

pH is one of the most important environmental factors influencing not only site dissociation, but also the solution chemistry of heavy metal: hydrolysis, complexation by organic and/or inorganic ligands, redox reactions, and precipitation are strongly influenced by pH, and on the other hand, it strongly affects the speciation and adsorption availability of heavy metals (Largitte and Pasquier, 2016). From Table 4.3, the pH of the samples were found to be 7.5 and 8.7 for coconut and palm kernel shells respectively. The adsorption of the adsorbent (chemically activated carbon) increased with increasing pH, as observed in the literature. For example, a similar result was found by (Singh *et al.*, 2017). The value of pH obtained in these analyses was ideal for adsorption purposes as maximum adsorption of metals by most



activated carbon occur at this pH(Nwabanne and Igbokwe, 2012) and (Babayemi, 2017). Activated Carbons of pH range 6-9 are useful for most applications in adsorption processes(Verla *et al.*, 2012).

#### **4.3.2.2 Moisture (%):**

Moisture is the presence of a liquid, especially water,often in trace amounts. Moisture has different effects on different products, influencing the final quality of the product under study.From table 4.3,the moisture content of the chemically activated carbons were 19.7% and 20.4% respectively forcoconut and palm kernel shells.Moisture content for coconut shells was lower whiles slightly higher for palm kernel shell showing that these carbons were prepared correctly and handheld tightly. It should be noted that when exposed to air the chemically activated carbons are capable of absorbing moisture from the atmosphere. This typically could lead to high moisture content(Verla *et al.*, 2012).

#### **4.3.2.3 Ash content (%):**

The ash content is a measure of the total amount of minerals present within a material, whereas the mineral content is a measure of the amount of specific inorganic components presentwithin a material, such as Ca, Na, K and Cl.From the results obtained in Table 4.3, the ash content of the samples is12.3% and 14.2% for coconut and palm kernel shells respectively. The presence of a considerable amount of ash contents in all the samples indicates that there are a lot of inorganic and organic metals present in them. According to literature, this can serve as a potential source of raw materials for fertiliser. However, higher levels of ash contents reduce the overall activity of activated carbon, and it reduces the

efficiency of reactivation. Also, the presence of ash has been shown to inhibit surface development (Valix *et al.*, 2004) and (Akpen *et al.*, 2018).

#### **4.3.2.4 Pore Diameter (nm):**

From the results obtained in Table 4.3, the pore diameters were 2.840 e+00 nm, and 3.000e+00 for coconut and palm kernel shells, respectively. If the pore diameters are smaller than 2 nm, these are called micropores. If their sizes are between 2 and 50 nm, these are called mesopores. Also, the material is named macropores if their sizes are more significant than 50 nm. The adsorption capacity of the macropores materials is at a negligible level compared to that for the micro- and mesoporous adsorbents (Ajemba and Onukwuli, 2013) and (Salem *et al.*, 2015). From literature values, it was found out the value obtained falls within the acceptable range for mesoporous adsorbents (Boadu *et al.*, 2018).

#### **4.3.2.5 Bulk density (g/cm<sup>3</sup>):**

Bulk density is the weight of soil or powder substance in a given volume. Soils or powder substance with a bulk density higher than 1.6 g/cm<sup>3</sup> tend to restrict root growth. It increases with compaction and tends to increase with depth. The bulk density (g/cm<sup>3</sup>) obtained were 1.21 (g/cm<sup>3</sup>) and 1.25 respectively for coconut and palm kernel shells as shown in Table 4.3. These results are within those found in the literature (Nwabanne and Igbokwe, 2012). These results show that the samples studied were within the recommended values for bulk density making it ideal for adsorbents (Boadu *et al.*, 2018).

#### **4.3.2.6 Porosity (%):**

Pore size distribution has been used to describe the internal structures and adsorption capacities of activated carbons (Daley *et al.*, 1996) and (Odisu *et al.*, 2019). The pore characteristics of the activated charcoal are a determining factor in its rate and ability to adsorb toxins (Ilomuanya *et al.*, 2017). From Table 4.3, the porosity of the samples was 70% and 65% for coconut and palm kernel shells, respectively. The high microporosity in the activated carbon samples suggests their potential applications in gas-phase and liquid adsorption for air as well as liquid pollution control (Kalderis *et al.*, 2008) and (Nwabanne and Igbokwe, 2012).

#### **4.3.2.7 Specific gravity:**

Specific gravity is the ratio of the mass of the volume of the substance to the mass of the same volume of water and depends on two temperatures, at which the mass of the sample and the water were measured. Specific gravity is influenced by the chemical composition of the oil (Hamawand *et al.*, 2013a) and (Gedik and Uzun, 2015). The specific gravity values obtained from Table 4.3 are 1.42 and 1.61 for coconut and palm kernel shells, respectively. The values obtained are within the specific gravity range of 0.8 – 2.1 for chemically activated carbons found in material safety data sheets (Egelhofer *et al.*, 2010); (CAS Number: 7440-44-0; EC Number: 231-153-3); (García *et al.*, 2017) and (Hock and Zaini, 2018).

#### **4.3.2.8 BET Surface area (m<sup>2</sup>/g):**

Specific surface area is a scale-dependent property, with no single actual value of specific surface area definable, and thus quantities of particular surface area determine through BET theory may depend on the adsorbate molecule utilized and its adsorption cross-section (Hanaor *et al.*, 2014) and (Hanaor *et al.*, 2015). The BET surface area values obtained are 1177.520 (m<sup>2</sup>/g) and 717.142 (m<sup>2</sup>/g) respectively for coconut and palm kernel shells as shown in Table 4.3. The high BET surface area values obtained indicates the presence of many adsorption sites and thus showing desirable characteristics for their potential application as pollutant adsorbent in used lubricating oils (Keey *et al.*, 2017a).

#### **4.3.2.9 Heavy Metals (ppm):**

Heavy metals are naturally found in the earth's crust through anthropogenic activities. They cannot be degraded or destroyed entirely by living organisms. To some extent, they enter our living organisms via food, drinking water, air, adsorption, absorption etc. As trace elements, some heavy metals (e.g. copper, selenium, zinc) are essential to maintain the metabolism of the human body. However, at higher concentrations, they can poison the human body (Evbuomwan *et al.*, 2013). Heavy metal poisoning could result from drinking-water contaminated with lead (e.g. lead pipes), high ambient air concentrations near emission sources, or intake via the food chain (Kpan *et al.*, 2014). Results from the heavy metal analyses of the activated carbon samples from Table 4.4 above, the results showed that the toxic metals such as: Cadmium (Cd) and Nickel (Ni) were below the detected limits, whereas, Chromium (Cr), Lead (Pb), Copper (Cu), Zinc (Zn), Calcium (Ca), Potassium (K), Iron (Fe) and Magnesium (Mg) were above the detected limits. Potassium is oxidized easily, thus reducing the available oxidizing agents (Udoetok, 2012). The high concentration of

Potassium in these samples and the presence of other metals like Zinc, Iron, Calcium and Magnesium make it suitable for use in conditions reactions where reduction is paramount (Udoetok, 2012). The toxic metals detected and not detected in the chemically activated carbons from coconut and palm kernel shells, can be used to reduce high toxic metals concentration found in wastewater and used lubricating oil. This was achieved by the principle of ions and metals affinity. From Figure 4.1, above: It can be observed that the concentration of potassium in the samples are higher than other metals in the samples, with the concentration of potassium in coconut shells higher than that in the palm kernel shells. The high concentration of potassium in the chemically activated carbon samples from coconut and palm kernel shells justifies its usage as potential raw material sources for fertilizer. Because potassium is needed by plants in large quantities for growth and support (Udoetok, 2012).

Finally, a One-way ANOVA in SPSS Statistics of the activated carbons from coconut and palm kernel shells were shown in Table 4.5. From the results obtained, statistically significant difference were observed in between groups as determined by one-way ANOVA for the various metals are Copper ( $F(2,6) = 17.550$ ,  $p = .003$ ), Iron ( $F(2,6) = 33464.685$ ,  $p = .000$ ), Zinc ( $F(2,6) = 27.551$ ,  $p = .001$ ), Lead ( $F(2,6) = 35.256$ ,  $p = .000$ ), Magnesium ( $F(2,6) = 129.271$ ,  $p = .000$ ), Calcium ( $F(2,6) = 78.702$ ,  $p = .000$ ) and Potassium ( $F(2,6) = 111.246$ ,  $p = .000$ ).

#### **4.4 Surface morphology of chemically activated carbons produced from palm kernel and coconut shells**

Plate 4.1 shows the 200 $\mu$ m magnification of the surface morphology of chemically activated carbons produced from palm kernel shell using the Carbolite Muffle Furnace set at 1000<sup>0</sup>C.

Pores were observed on the surface of the chemically activated carbon after the carbonization process. This indicates that the carbonization process had led to the production and release of volatile organic matter from the palm kernel shell; the remaining non-volatile components were then transformed into activated carbon with pores of different shapes and sizes found on the surface. There were more pores observed from the activated carbons obtained at a higher temperature (1000<sup>0</sup>C) suggesting temperature is an influential process parameter in the development of surface porosity of activated carbons. When the more elevated temperature was applied, more heat energy was generated within the PKS which then promoted the decomposition of lignocellulosic components into the more volatile matter. Consequently, more pores were obtained that resulted from the volatile organic matter released after the carbonization performed at a higher temperature.

Also, the pores on the surface of chemically activated carbons from palm kernel shells at high temperature were observed with fewer impurities as shown in the Plate. 4.1 with 200 $\mu$ m magnification. This could be attributed to the use of vacuum environment instead of a continuous flow of nitrogen gas by the carbolite muffle furnace pyrolysis approach in this study. In vacuum condition, the pressure inside the reactor was lower. Hence, the volatile matter generated during the pyrolysis was removed immediately from the reactor, reducing the residence time of the volatile matter inside the reactor. As a result, the possible re-condensation reaction of the volatile matter on the surface of activated carbon from palm kernel shell that would have led to the clogging of the pore can be prevented, leading to the formation of 'cleaner' pores on the surface of activated carbon (Tripathi *et al.*, 2016) and (Saleh *et al.*, 2017).

In contrast, the pores that are present on the surface of activated carbon could have clogged or blocked with the condensed volatile matter when nitrogen gas is used during the pyrolysis reaction. This could be due to the cooling effect of the nitrogen gas that can re-condense the

volatile matter released on the surface of activated carbon and clogged the pores, resulting in the lower internal surface area obtained from the activated carbon.

In contrast to the above, Plate 4.2 shows the surface image or morphology of chemically activated carbons produced from coconut shells using the Carbolite Muffle Furnace set at 1000<sup>0</sup>C. The rank of the activated carbon is known to be important for determining the extent of carbon-richness during carbonization process (Jain *et al.*, 2015). The combined effect of the carbonization process of carbon materials leads to hierarchically porous features (Promdee *et al.*, 2017). This result is further confirmed by the SEM image. A transparent mesopore and micropore with a rough surface imply that micropores exist in the exterior and the interior of activated carbons. According to the previous studies, activated carbon with an adequate grainy surface is characterized by a wider range of pores sizes, availability of more active sites and larger BET surface area. These features explain the adsorption mechanism, and also improve the capacity of the adsorbate removal per unit of the sorbent (Jalani *et al.*, 2016). Jalani *et al.*, 2016 reported that rapid adsorption mechanism is usually observed at the beginning of the adsorption treatment due to the availability of more bare pores and active sites. This process could lead to the formation of hazy appearance due to the deposited adsorbate (Pathania *et al.*, 2017) and (Gupta, 2013).

Also, the image of the SEM shows that the activation stage produced a sizeable external surface with quite, pores and very high porosity. SEM patterns revealed the amorphous nature of the carbons, smooth feature and the existence of carbon-rich large molecules. As a result, with the discovery of micro and nanoscale, many researchers (Kumar *et al.*, 2016) now visualise activated carbon as a structure made up of fragments. The micrograph of the activated carbon further demonstrates the transformation of the matrix of the shell as a result of continued heating during the activation. The magnified SEM cross image reveals the composite coal materials between activated carbon and binder composite material. Activated

carbons surface images show a carbon surface more apparent as magnification increases, which has a rough and stacked feature and also arrange a disorder characterized as amorphous. SEM morphology shows that visible pores were seen in the samples of chemical activated carbons from the coconut shells, apparent pores indicating activated carbon processes were successful.

#### **4.4.1 Fourier transform infrared (FTIR) analyses on the chemically activated carbon samples from coconut and palm kernel shells**

The chemically activated carbons produced from the coconut and palm kernel shells were analysed using the FTIR. Because FTIR is a well-known state of the art method for analysing surface area chemistry. Surface functional groups in the various activated carbons were characterized by FTIR spectroscopy, Plate. 4.3 and 4.4 showing palm kernel and coconut shell FTIR spectra respectively. Surface area functional groups containing oxygen plays a major role in activated carbon properties such as surface hydrophobicity and charges (Fletcher *et al.*, 2007) and (García *et al.*, 2017).

Plates 4.3 and 4.4 as well as Tables 4.6 and 4.7 show the results and compares the FTIR spectra of chemically activated carbons from palm kernel (PKS) and coconut shells (CS) produced from Carbolite Muffle Furnace at a temperature of 1000<sup>0</sup>C for 1 hour. The resulted wavenumbers and the classification of functional groups present in chemically activated carbons from palm kernel and coconut shells were almost similar. Majority of the peaks of the activated carbons were divided into different ranges of wavenumber which include the C-H stretching, C-C stretching, O-H stretch, C=C Stretching, C-H bending, C-O bending etc. It was found that some of the peaks (i.e. O-H stretching, C-H stretch, C-H bending and C-O



bending) that originally present in the PKS and CS were also observed from the spectra of activated carbons.

The broad peak of PKS and CS are detected at 3000–3800  $\text{cm}^{-1}$  (i.e. peak (a) in Plates.4.3 and 4.4) attributes to the O-H stretching that indicates the presence of chemical compounds with hydroxyl functional groups such as phenolic or aliphatic alcohol and carboxylic acid in both the activated carbons from PKS and CS. It was found that this hydroxyl group upon further carbonization process may not be detected from the activated carbons spectra, suggesting the hydroxyl-containing compounds were released as volatile matter (e.g.  $\text{CH}_3\text{OH}$  and  $\text{CH}_3\text{COOH}$ ) probably via the fragmentation reaction of hemicellulose (Shen *et al.*, 2011); (Fan *et al.*, 2018) and (Ghalibaf and Pyrolytic, 2019) and cracking of alkyl-hydroxyl chain that present in the lignin (Cao *et al.*, 2013).

However, at 3000–3200  $\text{cm}^{-1}$  (i.e. peak (b) in Plate. 4.4), the peak present in this range was derived from chemical compounds with  $\equiv\text{C-H}$  stretching functional group in CS only and not in PKS as shown in the tables.

Also, at 2300-2800  $\text{cm}^{-1}$  (i.e peak (b) in Plates.4.3 and 4.4), the peak presence in this range was derived from chemical compounds with  $-\text{COOH}$  stretching and  $\text{C}\equiv\text{C}$  stretching functional groups in PKS and CS respectively. At 2000-2300  $\text{cm}^{-1}$  (i.e peak (c) in Plates.4.3 and 4.4), the peak present in this range was derived from chemical compounds with  $\text{C}=\text{C}=\text{C}$  band for CS while  $\text{C}=\text{N}$  was stretching for PKS respectively. A similar pattern of peaks was observed at peak ranges 1900-2000  $\text{cm}^{-1}$  for chemical compounds with  $\text{C}=\text{C}=\text{C}$  band for CS and  $\text{CH}_2=\text{CH}_2$  stretch for PKS respectively. The uniqueness of the activated carbons prepared from coconut and palm kernel shells were observed in the different peaks obtained at these ranges respectively. The difference in the peaks recorded in both CS and PKS shows a clear indication that each activated carbon have peculiar characteristics and adsorption pattern.

The transmittance peaks are shown at 1700–1800  $\text{cm}^{-1}$  and 1600–1700  $\text{cm}^{-1}$  (i.e. peak (d) in Plate.4.4) indicates the presence of compounds with C=C stretching and C=O axial deformation. However, these peaks were only found in CS spectra. However, both CS and PKS recorded a peak each at the ranges of 1500–1600  $\text{cm}^{-1}$  from chemical compounds with C=C stretching and  $\text{CH}_2$  and  $\text{CH}_2$  twisting respectively. Besides, a high transmittance peak (~30%) of PKS spectrum for C-O bending (peak (f) in Plate. 4.3) at the ranges 1000–1200  $\text{cm}^{-1}$  was detected, indicating that alcohols, carboxylic acids, esters or ethers were abundantly present within the PKS. On the other hand, at the ranges 1300–1500  $\text{cm}^{-1}$  a peak from chemical compounds with C-H bending was observed for CS only indicating the presence of alkanes.

Furthermore, the absence of C-O stretching and lower peak intensity of C-O bending detected from activated carbon spectra could have resulted from the elimination of oxygenated compounds during the carbonization conversion of PKS into activated carbon (Nb *et al.*, 2016) and (Osman *et al.*, 2017). During carbonization, these oxygenated compounds were released from the decomposition of lignocellulosic components in the form of volatile matter and released, thus leaving the residual carbon as the activated carbon with low oxygen content. Hence, there was evidence that both the PKS and CS were transformed into activated carbons that have higher aromaticity after the carbonization process. This transformation could be occurred via a few proposed chemical reactions such as dehydrogenation by releasing  $\text{H}_2$  to form the unsaturated compound, demethylation of short substituents (e.g. – $\text{OCH}_3$  and – $\text{CH}_3$ ) to form polycyclic aromatic compound and dehydration by releasing  $\text{H}_2\text{O}$  to form alkene and aromatic compounds.

Finally, the sample from palm kernel shells showed six well-defined signals (i.e. spectra). The broad-bands at 3593  $\text{cm}^{-1}$ , 3678  $\text{cm}^{-1}$  and 3753  $\text{cm}^{-1}$  were due to the O–H stretching mode of hydroxyl, alcohol and phenol groups as well as adsorbed water (Das *et al.*, 2015) and

(Mahamad *et al.*, 2015). The band at  $2322\text{ cm}^{-1}$  can be assigned to  $-\text{COOH}$  stretching mode of carboxylic acid groups (Hamza *et al.*, 2015). A band with  $2087\text{ cm}^{-1}$  can be attributed to  $-\text{C}=\text{N}$  stretching mode of nitriles (Yashim *et al.*, 2016). The band at  $1994\text{ cm}^{-1}$  can be attributed to the  $\text{CH}_2=\text{CH}_2$  stretching mode of alkynes (Yashim *et al.*, 2016). A band with  $1543\text{ cm}^{-1}$  can be assigned  $-\text{CH}_2$  and  $\text{CH}_2$  twisting mode of alkanes (García *et al.*, 2017) while a band with the lower definition at  $1017\text{ cm}^{-1}$  can be attributed to  $-\text{C}-\text{O}$  bending mode of alcohol, ether and carboxylic acid (Keey *et al.*, 2017b).

Also, the presence of the various chemical compounds and their functional groups such as hydroxyl groups, carbonyl groups, ethers, alkanes, alkenes and aromatic groups is an evidence of the lignocellulose structure of coconut shells as was observed in other materials found in Brazilian coconut shells (Cazetta *et al.*, 2011). However, the sample from the coconut shells showed nine well-defined signals (i.e. spectra). The broad-bands at  $3652\text{ cm}^{-1}$  and  $3753\text{ cm}^{-1}$  were due to the  $\text{O}-\text{H}$  stretching mode of hydroxyl, alcohol and phenol groups (Din *et al.*, 2009) and (Angalaeeswari and Kamaludeen, 2017). The band at  $3190\text{ cm}^{-1}$  can be assigned to  $\equiv\text{C}-\text{H}$  stretch mode of the alkyne (Das *et al.*, 2015). A band with  $2325\text{ cm}^{-1}$  can be attributed to  $\text{C}\equiv\text{C}$  stretching mode of aldehyde (Din *et al.*, 2009). The bands at  $2109\text{ cm}^{-1}$  and  $1990\text{ cm}^{-1}$  were assigned to  $\text{C}=\text{C}=\text{C}$  band mode of allene (Angalaeeswari and Kamaludeen, 2017). A band at  $1736\text{ cm}^{-1}$  can be allotted to  $\text{C}=\text{C}$  stretching mode of pyrone (Cazetta *et al.*, 2011). The band at  $1621\text{ cm}^{-1}$  can be attributed to  $\text{C}=\text{O}$  axial deformation modes of aldehyde, Ketone, Carboxylic acids (Das *et al.*, 2015) and (Mahamad *et al.*, 2015). A band with  $1543\text{ cm}^{-1}$  can be assigned to  $\text{C}=\text{C}$  stretching mode of aromatics (Din *et al.*, 2009) while a band with a lower definition at  $1397\text{ cm}^{-1}$  can be attributed to  $\text{C}-\text{H}$  bending mode of alkanes.

#### 4.4.2 Surface Area Data Summary

From Table 4.8, it was observed that the palm kernel shell activated carbon have the following parameters single-point BET  $3.896 \times 10^2$  ( $\text{m}^2/\text{g}$ ) and multi-point BET  $7.171 \times 10^2$  ( $\text{m}^2/\text{g}$ ) while coconut shell activated carbon has single point BET  $7.258 \times 10^2$  ( $\text{m}^2/\text{g}$ ) and multi-point BET  $1.178 \times 10^3$  ( $\text{m}^2/\text{g}$ ). Comparing the surface area data obtained for both unique and multi-points BET surface areas of all the carbons prepared are suitable as adsorbents. But from SEM micrograph, the chemically activated coconut shells shows well highly defined cavities and pores compared to palm kernel shells. This study also shows that coconut shells area better source of high surface area activated carbons compared to palm kernel shells. It can be concluded that coconut shell with better single and multi-points BET was preferred to palm kernel shell activated carbons (Hock and Zaini, 2018).

Also in Table 4.8, it revealed that palm kernel and coconut shells activated carbons have Langmuir surface areas of  $2.304 \times 10^4$  ( $\text{m}^2/\text{g}$ ) and  $6.642 \times 10^3$  respectively. It was observed that palm kernel shell have large Langmuir surface area compared to coconut shell activated carbon.

In Table 4.8, the following parameters were obtained for palm kernel shell activated carbon BJH method cumulative adsorption surface area  $7.322 \times 10^2$  ( $\text{m}^2/\text{g}$ ), DH method cumulative adsorption surface area  $7.769 \times 10^2$  ( $\text{m}^2/\text{g}$ ), t-method external surface area  $7.171 \times 10^2$  ( $\text{m}^2/\text{g}$ ), DR method micropore area  $7.114 \times 10^2$  ( $\text{m}^2/\text{g}$ ) and DFT cumulative surface area  $1.494 \times 10^2$  ( $\text{m}^2/\text{g}$ ) respectively. But in the case of coconut shell activated carbon BJH method cumulative adsorption surface area  $1.340 \times 10^3$  ( $\text{m}^2/\text{g}$ ), DH method cumulative adsorption surface area  $1.427 \times 10^3$  ( $\text{m}^2/\text{g}$ ), t-method external surface area  $1.178 \times 10^3$  ( $\text{m}^2/\text{g}$ ), DR method micropore area  $1.268 \times 10^3$  ( $\text{m}^2/\text{g}$ ) and DFT cumulative surface area  $2.837 \times 10^2$  ( $\text{m}^2/\text{g}$ ) respectively. Comparing these values obtained, it can be concluded

that coconut shell have better surface area parameters than palm kernel shell activated carbons (Islam *et al.*, 2017).

#### **4.4.3 The properties of the filter beds**

From Table 4.9, the features of the filter bed for the activated carbon from palm kernel were as follows mass 155.10 (g), volume 200.04 (cm<sup>3</sup>), density 0.7753 (g/cm<sup>3</sup>), volume of samples before filtration 600 (ml), breakthrough time 1.15 (hr) and time for the entire filtration process 480 (hr). However, in the case of the properties of the filter bed for the activated carbon from coconut shells the following values were recorded; mass 155.10 (g), volume 428.65 (cm<sup>3</sup>), density 0.3618 (g/cm<sup>3</sup>), volume of samples before filtration 600 (ml), breakthrough time 1.37 (hr) and time for the entire filtration process 120 (hr). From the parameters and the values obtained it was observed that the coconut shells were porous compared to that of palm kernel shell activated carbons. (Boadu *et al.*, 2018) reported that coconut shell with good pore diameter would be more suitable than and palm kernel shell respectively.

#### **4.4.4 Adsorption capacities of the filter beds.**

From Table 4.10 the adsorption capacities of the palm kernel shell activated carbon were as follows control sample  $3.80 \times 10^{-4}$  (kg/m<sup>3</sup>), sample A  $3.70 \times 10^{-4}$  (kg/m<sup>3</sup>) and sample B  $4.19 \times 10^{-4}$  (kg/m<sup>3</sup>). But in the case of the adsorption capacities of the coconut shell activated carbon the following values were recorded control sample  $5.00 \times 10^{-4}$  (kg/m<sup>3</sup>), sample A  $5.09 \times 10^{-4}$  (kg/m<sup>3</sup>) and sample B  $4.43 \times 10^{-4}$  (kg/m<sup>3</sup>). Comparing the values recorded, it was observed that coconut shells have high adsorption capacity than palm kernel shells (Ruiz *et al.*, 2015).

#### **4.5 Adsorption of Heavy Metals in Used Lubricating Oil using Palm Kernel and Coconut Shells as Adsorbents.**

Adsorption mechanism is considered to be one of the most efficient and effective technologies widely used in global environmental protection areas. In this regard, a great deal of interest has been focused on the use of different types of materials as adsorbents for heavy metal removal in used lubricating oils such as chemically activated carbon. However, the zeal for exploiting new adsorbents, improving the removal efficiency and effectiveness of adsorbents as well as developing an ideal adsorption system have never been stopped. In this research work, a comparative study was carried out to ascertain the adsorptive capacity of chemically activated carbons produced from palm kernel and coconut shells in producing adsorbents for the removal of some heavy metals from used lubricating oils. The developed chemically activated carbon adsorbents from raw materials such as palm kernel and coconut shells were used to filter the analysed used lubricating oil samples A and B (i.e. total quartz 20 W 50 that have been used for 3 and 6 months each) and fresh lubricating oil total quartz 20 W 50 obtained from Total Service Station at east-west road Choba, Port Harcourt, Nigeria. The results of the analyses of the used and fresh lubricating oil samples before and after the filtration with the chemically activated carbons produced from palm kernel and coconut shells are presented in Tables 4.11, 4.12, 4.13 and 4.14 respectively.

Normally, adsorption takes place because all molecules use forces to adhere to each other. Extensive research data available in the literature have shown that chemically activated carbons adsorb both organic and inorganic materials. Because the attractive forces between the activated carbon surface and the contaminants are stronger than the forces keeping the contaminants dissolved in used lubricating oil samples. The adsorption ability of an adsorbent largely rests on the number of pores and the size of the surface area. The large surface area of the activated carbon, owing to its particle size and pore formation, allows for the adsorption

to take place. Porosity in carbon is developed through an activation process by creating a more orderly porous structure (Abdelali *et al.*, 2019). There are usually four stages in pore development during the activation process: 1) opening of previously inaccessible pores; 2) creation of new pores by selective activation; 3) widening of existing pores; and 4) merging of existing pores due to pore wall breakage (Islam *et al.*, 2016). The specific properties of an activated carbon depend on the nature of the raw materials used to produce it and the type of activation process employed, which boosts its adsorbent potentials. Tables 4.11; 4.12; 4.13 and 4.14 specifically give a summary of the filtration process carried out with the chemically activated carbons produced from palm kernel and coconut shells.

From the results obtained in Tables 4.11; 4.12; 4.13 and 4.14, it can be seen that for both the palm kernel and coconut shells were not suitable for the removal of copper metal in the fresh and used lubricating oil samples. Because, the initial mean concentrations of copper in virgin (C) and used lubricating oil samples (i.e. A & B) were  $0.001 \pm 0.000$  ppm,  $0.1500 \pm 0.008$  ppm and  $0.220 \pm 0.026$  ppm respectively before filtration processes. But after the filtration process with the palm kernel shell activated carbon, the mean concentration of copper metal increases for virgin (C) to  $0.075 \pm 0.013$  ppm and used lubricating oil samples (A & B) are  $0.400 \pm 0.018$  ppm and  $0.230 \pm 0.008$  ppm respectively. In the case of the coconut shell activated carbon, the mean concentration of copper also in virgin lubricating oil remains the same  $0.001 \pm 0.000$  whereas for used lubricating oils samples (i.e. A & B) it increases to  $0.780 \pm 0.014$  and  $0.790 \pm 0.026$  respectively. The increase in mean concentrations after the filtration processes with both the palm kernel and coconut shells activated carbons can be attributed to leaching of copper ions already present in the filter beds as ascertain in the physio-chemical characterization analysis of the filter beds by (Boadu *et al.*, 2018).

Though, the percentage leached in palm kernel was small compared to that of coconut shells. Hence, there is the need to further search for better and potential raw materials for the

production of activated carbons that can meet industrial needs of removal of copper metals in both fresh and used lubricating oil samples.

However, (Abdel-Jabbar *et al.*, 2010) reported that the date palm kernel could slightly reduce copper metals in used lubricating oils from 7mg/kg to 6mg/kg. But several works of literature have shown that chemical activated carbons from palm kernel and coconut shells are useful in the removal of pollutants in muddy water and colour from wastewater (Akpen and Leton 2014). Also, (Kwakyee-Awuah *et al.*, 2018) reported that laboratory-synthesized zeolite types LTA and LSX successfully removed heavy metals, notably lead, copper and iron that was in the spent oil.

Also, it can be observed from the results obtained in tables 4.11; 4.12; 4.13 and 4.14 that the concentrations of iron metal increases after filtration processes with both the chemically activated carbons produced from coconut and palm kernel shells. The levels of iron metal before the filtration processes were  $1.502 \pm 0.092$  ppm for virgin and  $4.650 \pm 0.159$  ppm and  $3.350 \pm 0.289$  ppm for both used oil samples A&B. However, after filtration processes with chemically activated carbons produced from palm kernel and coconut shells, the concentrations of the iron metal increases. For the palm kernel activated carbon, the values obtained are  $1.150 \pm 0.129$  ppm for virgin,  $8.500 \pm 0.258$  ppm for sample A and  $3.400 \pm 0.183$  ppm for sample B respectively. In the case of the coconut activated carbons, the observed values are  $3.650 \pm 0.625$  ppm for virgin,  $13.500 \pm 0.942$  ppm for sample A and  $14.125 \pm 0.618$  for samples B respectively. The level of increase was not much in palm kernel as compared to coconut shells. The concentration increase in iron metal after the filtration process with both the coconut and palm kernel shells might be due to leaching of the iron metal concentration already present in the filter beds by (Boadu *et al.*, 2018). According to their research works reported, chemically activated carbons produced from coconut and palm kernels contain a high amount of iron metal concentration. Though, the analyses of iron



revealed that palm kernel shell activated carbon performed better followed by coconut shell activated carbon respectively. Because of this reason, activated carbons produced from palm kernel and coconut shells as adsorbents are not recommended for the removal of iron metals present in used lubricating oil samples. However, (Kwakye-Awuah *et al.*, 2018) reported that laboratory-synthesized zeolite types LTA and LSX successfully removed heavy metals, notably lead, copper and iron that was in the spent oil.

In general, zinc is added to fresh lubricating oil as zinc diethyl dithiophosphate (ZDDP), zinc dithiophosphates, and zinc dialkyl dithiocarbamates. This was added to the base oil as part of multi-functional additives for improving oil's performance (Kwakye-Awuah *et al.*, 2018). From all the tests conducted on the zinc before filtration with activated carbons produced from coconut and palm kernel shells the results were for virgin was  $2.833 \pm 0.275$  ppm and used lubricating oil samples A&B are  $16.475 \pm 0.950$  ppm and  $14.57 \pm 0.272$  ppm respectively. But after the filtration process with palm kernel shell activated carbon the values recorded were for virgin was  $8.325 \pm 0.275$  ppm and used lubricating oil samples A&B are  $10.375 \pm 0.171$  ppm and  $5.450 \pm 0.300$  ppm. For coconut shell activated carbon, the results obtained were for virgin was  $0.670 \pm 0.071$  ppm and used lubricating oil samples A&B are  $5.838 \pm 0.344$  ppm and  $5.400 \pm 0.280$  ppm respectively. Comparing the different outcomes observed in Tables 4.11; 4.12; 4.13 and 4.14, it proved that coconut shell activated carbon has the best adsorption capacity followed by palm kernel shell activated carbon. Inegbenebor *et al.*, (2012), conducted similar research using activated carbons from palm kernel and coconut shells for purification of polluted water for drinking but reported that palm kernel was somewhat effective than coconut shells. The disparity might be due to the used lubricating oils sample instead of the polluted water for drinking. Kwakye-Awuah *et al.*, (2018), reported that the recycling of the used oil with metakaolin and the zeolites as compared to that of the used oil led to a reduction in zinc content by 94.96 %, 96.76 % for zeolite LTA and 93.88 % for

zeolite LSX figure. This shows that coconut shell activated carbon produced can be used effectively and efficiently as an alternative to those prepared by other researchers.

Analysis of the heavy metal such as cadmium from Tables 4.11; 4.12; 4.13 and 4.14 revealed that both coconut and palm kernel shells activated carbons are very efficient and effective in the adsorption processes. Because the concentrations of cadmium metal before the filtration process with palm kernel and coconut shells activated carbons were for virgin  $0.020 \pm 0.008$  ppm and used samples A&B lubricating oils are  $0.0200 \pm 0.008$  ppm and  $0.030 \pm 0.008$  ppm respectively. But after the filtration with palm kernel shell activated carbon the concentrations of cadmium metal reduces, for lubricating oils; virgin  $0.000 \pm 0.000$  ppm and used samples A&B to  $0.018 \pm 0.009$  ppm and  $0.000 \pm 0.000$  ppm lubricating oils respectively. Also, with the coconut shells activated carbon after the filtration processes, they all drop in the concentrations of the cadmium metals, with lubricating oils; virgin  $0.001 \pm 0.000$  ppm and used samples are A&B the recorded values are  $0.001 \pm 0.000$  and  $0.001 \pm 0.000$  respectively. This affirmed what (Abdel-Jabbar *et al.*, 2010) had reported earlier that, date palm kernel powder was a suitable adsorbent for removal of cadmium metal in used lubricating oils.

However, (Okafor *et al.*, 2012) reported that coconut shell adsorbed  $Pb^{2+}$ ,  $Cu^{2+}$ ,  $Cd^{2+}$  and  $As^{3+}$  ions from aqueous solutions and the concentration of the metal ions adsorbed increased with increase in levels, increase in contact time, increase in temperature and increases in pH for each metal. He concludes that coconut shell could serve as a cheap, readily available effective adsorbent for the removal of  $Pb^{2+}$ ,  $Cu^{2+}$ ,  $Cd^{2+}$  and  $As^{3+}$  from wastewater as a way of treatment before discharge into the environment. From the literature findings reported earlier, it can be concluded that chemically activated carbons produced from both coconut and palm kernel shells are suitable adsorbents for removal of heavy metal such as cadmium from used lubricating oils.

From the analysis of chromium metal in Tables 4.11; 4.12; 4.13 and 4.14, it was observed that concentrations of chromium metal before the filtration processes with both palm kernel and coconut shells activated carbons were, for lubricating oils; virgin  $0.410 \pm 0.051$  ppm used samples A&B are  $0.400 \pm 0.065$  ppm and  $0.445 \pm 0.039$  ppm respectively. But after filtration with palm kernel shells activated carbon, the values obtained were  $0.065 \pm 0.013$  ppm for virgin,  $0.210 \pm 0.026$  ppm for used sample A and  $0.135 \pm 0.013$  ppm for used sample B lubricating oils respectively. In the case of after filtration with coconut shell activated carbons, the values recorded are  $0.348 \pm 0.049$  ppm for virgin,  $0.388 \pm 0.046$  ppm for used sample A and  $0.528 \pm 0.055$  ppm for used sample B. From all the results obtained, it revealed that palm kernel shell activated carbon is a suitable adsorbent compared to coconut shell activated carbon. Because the palm kernel shell reduces the concentrations of chromium metal compared to coconut shell activated carbons. Babayemi, (2017), revealed that palm kernel shell being an agricultural waste could be converted to useful and efficient adsorbent through the use of activating chemicals, particularly  $H_2SO_4$ . Also, (Abdel-Jabbar *et al.*, 2010) reported a similar phenomenon with chromium metal.

However, (Hidayu and Muda, 2016b) reported that palm kernel and coconut shells could be used as the perfect raw material to prepare activated carbon with the high surface area for  $CO_2$  adsorption rate. Also, (Mehr *et al.*, 2019) found out that palm kernel shell, an inexpensive and readily available material, was very useful to remove Cr (VI) from aqueous solutions. He reported that the tested activated carbon produced from palm kernel shells showed higher adsorption capacities compared to those of some coconut shell and other activated carbons found in the works of literature. (Ruiz *et al.*, 2015) reported that palm kernel shells could be used as an alternative to available commercial adsorbents for cement wastewater treatment. They also affirmed that the combination of physical and chemical treatment of these

adsorbents could enhance their adsorption capabilities due to their resultant high surface area and increased depth of pore spaces.

From the Tables 4.11;4.12; 4.13 and 4.14, the analysis of heavy metal such as lead (Pb) concentrations before filtration processes with both chemically activated carbons produced from palm kernel and coconut shells gave the following results for the lubricating oil samples; for virgin  $1.000\pm 0.093$  ppm, used sample A  $1.045\pm 0.478$  ppm and used sample B  $1.525\pm 0.222$  ppm respectively. But after the filtration process with the chemically activated carbon prepared from palm kernel shells, the values recorded were as follows, for virgin  $1.650\pm 0.039$  ppm, used sample A  $1.648\pm 0.099$  ppm and used sample B  $2.388\pm 0.070$  ppm lubricating oils in that order. However, with the chemically activated carbon produced from coconut shells, the results obtained after the filtration process were as follows, for virgin  $0.563\pm 0.172$  ppm, used sample A  $0.410\pm 0.037$  ppm and used sample B  $0.438\pm 0.220$  ppm lubricating oils respectively. From all the test results recorded, it shows that coconut shell activated carbon as having the best adsorption capacity of lead metals after the filtration processes with various types of lubricating oil samples compared to palm kernel shells activated carbons. This proofed that coconut shell activated carbon was effective and efficient adsorbent. Therefore, it can be used as a suitable adsorbent for the removal of lead metal concentration in used lubricating oils. However, (Hidayu and Muda, 2016a) reported that palm kernel and coconut shells could be used as the perfect raw material to prepare activated carbon with the high surface area for CO<sub>2</sub> adsorption rate. But usually, coconut shell is preferred to palm kernel shell activated carbons because of its large surface area and other BET parameters.

In the case of palm kernel shell activated carbon, the concentration of lead metals increases. This can be attributed to the high levels of lead concentration already present in the activated

carbon(Jahangar *et al.*, 2015) and the high contact time of the filtration process. (Mehr *et al.*, 2019), also reported an increase in lead metal concentration with activated carbon prepared from date palm kernel. Jodeh *et al.*,(2015), found out that level of heavy metal lead in used lubricating oil is higher than the level of other metals and adsorption of lead increases with increase adsorbent dosage, temperature and time of contact.

Finally, the adsorption results obtained for heavy magnesium metal analysed indicated that activated carbons produced from the coconut and the palm kernel shells can be used as a high-performance adsorbent with higher adsorption capacity. It was worthy of note that from all the analysis performed, the magnesium metal contents of the used lubricating oil samples were generally far below the broad range reported in the literature with both palm kernel and coconut shells activated carbons. From Tables 4.11; 4.12; 4.13and 4.14, the results obtained for the analysis of magnesium concentrations before the filtration process was as follows for the various lubricating oils, for virgin was  $41.900\pm 0.258$  ppm, used sample A was  $5.450\pm 0.265$  ppm and used sample B was  $21.475\pm 0.650$  ppm respectively. But after the filtration process with activated carbon produced from palm kernel shells, the values obtained for the respective lubricating oils were, virgin  $0.350\pm 0.026$  ppm and used samples A&B are  $0.900\pm 0.025$  ppm and  $0.505\pm 0.013$  ppm in that order. In the case of the coconut shell activated carbon, the results recorded for the various types of lubricating oils are as follows, virgin  $1.475 \pm 0.171$  ppm, used sample A  $3.625\pm 0.222$  ppm and used sample B  $0.645\pm 0.645$  ppm respectively. Onundi *et al.*, (2010b), reported a similar trend of a decrease in magnesium metal concentration from fresh to used lubricating oil samples with activated carbons prepared from date palm kernel powder. Also,(Ab. Jabal *et al.*, 2016), found that the increase of chitosan dosage from 0.5 to 1.0 g decrease the metals such as sodium, magnesium, calcium and zinc removal percentage in used lubricating oils. Furthermore, they observed that the

increase of temperature from 30 to 70°C and the rise of contact time from 2 to 10 min resulted in a decrease of metals removal from used lubricating oils.

#### 4.6 Adsorption Isotherms

Adsorption isotherm reveals the relationship between the amount of a solute adsorbed at constant temperature and its concentration in the equilibrium solution. It provides essential physiochemical data for assessing the applicability of the adsorption process as a complete unit operation (Ghazalet *et al.*, 2016). Langmuir isotherm models are widely used to investigate the adsorption process (Adib *et al.*, 2018). The model parameters can be construed further, providing understandings on sorption mechanism, surface properties, and an affinity of the adsorbent (Nayak and Singh, 2007) and (Ghorbanian *et al.*, 2016). The Langmuir isotherm was developed on the assumption that the adsorption process will only take place at specific homogenous sites within the adsorbent surface with uniform distribution of energy level. Once the adsorbate is attached on the site, no further adsorption can take place at that site; which concluded that the adsorption process is monolayer in nature. The Langmuir adsorption model further based on the assumption that all the adsorption sites are energetically identical and adsorption occurs on a structurally homogeneous adsorbent. Linearized form of the Langmuir equation based on those assumptions is given as (Langmuir, 1917); (Chen, 2015) and (Patiha *et al.*, 2016).

$$\frac{1}{q_e} = \frac{1}{Q^o} + \frac{1}{bQ^o C_e}$$

Where  $q_e$  is the amount of solute adsorbed on the surface of the adsorbent ( $\text{mmol g}^{-1}$ ),  $C_e$  is the equilibrium ion concentration in the solution ( $\text{mmol L}^{-1}$ ),  $Q^o$  is the maximum surface density at monolayer coverage and  $b$  is the Langmuir adsorption constant ( $\text{L mmol}^{-1}$ ). The plots of  $1/q_e$  versus  $1/C_e$  give a straight line and the values of  $Q^o$  and  $b$  can be calculated from

the intercept and slope of the plots, respectively. So, it can be concluded that the Langmuir model showed a better fit due to the high coefficient of determinant ( $R^2 \approx 1$ ). Langmuir constants and correlation determinant ( $R^2$ ) are given in Table 4.15.

The constants of all models were obtained by an ordinary coefficient of determinant parameter using the Quantitative Micro Software LLC., EViews 4 User's Guide, 2002 and XLSTAT version.1.(2018), In both Eviews software" version 3.1 and XLSTAT version 2018.1software, several examinations were performed for analysing and fitting of data. The models are developed based on the statistical function such as coefficient of determinationparameter ( $R^2$ ) and Durbin-Watson Test (D. W. T.).  $R^2$  is the most critical parameter to obtain the model ability in the fitting of various conditions provided based on experimental data. In general, the amount of this parameter is between 0.0 and 1.0, and the quality of fitting increases with the nearness of  $R^2$  to 1.0.From a statistics point of view, it can be concluded that the Langmuir model showsa better fit due to the high coefficient of determination ( $R^2 \approx 1$ ). D. W. T. is another parameter considering the difference between the real and model amount in every point knowing as residual. In fact, this parameter determines the relation adsorption on both sizes of activated carbon.

Tables 4.15, shows that copper have the  $R^2$  (0.8185), D.W.T (1.4546) and  $Pr > F (< 0.0001)$ . In this model, the amounts of  $R^2$  are close to 1 for the adsorbate and D. W. T. is more than 1 for the solute, which confirms the definition of modelling basis. Also, in the ANOVA, the lesser the  $Pr > F$  value, the more significant the results. The equilibrium isotherm for the copper metal analysed was determined and plotted separately, as shown in the figure. The copper metal analysed was found to conform to a straight line Langmuir adsorption isotherm(Kamal *et al.*, 2014) and (Teoh *et al.*, 2018). This result obtained for copper indicated that activated carbons produced from the coconut and the palm kernel shells could

be used as a high-performance adsorbent with higher adsorption capacity (Babayemi, 2017) and (Baeten *et al.*, 2019). The adsorption data obtained after the analysis fitted well to the Langmuir model and adsorptive surface area of 717.120 m<sup>2</sup>/g palm kernel and 1177.524 m<sup>2</sup>/g coconut shells were obtained for the activated carbons respectively.

From the results in Table 4.15, iron metal have R<sup>2</sup>(0.9927), D.W.T (2.6443) and Pr > F (< 0.0001) respectively. R<sup>2</sup> is the most important parameter to obtain the model ability in the fitting of various conditions provided based on experimental data. In this model, the amounts of R<sup>2</sup> are close to 1 for the adsorbate and D. W. T. is more than 1 for the solute, which confirms the definition of modelling basis. Also, in the ANOVA, the lesser the Pr > F value, the more significant the results. The iron metal revealed that it conforms to a straight line Langmuir adsorption isotherm (Pinheiro *et al.*, 2018). This result obtained for iron showed that activated carbons produced from the coconut and the palm kernel shells could be used as a high-performance adsorbent with higher adsorption capacity (Abdelali *et al.*, 2019).

The values recorded in Table 4.15 zinc have R<sup>2</sup>(0.9953), D.W.T (2.2315) and Pr > F (< 0.0001) respectively. R<sup>2</sup> is the most important parameter to obtain the model ability in the fitting of various conditions provided based on experimental data. In this model, the amounts of R<sup>2</sup>(0.9953) are close to 1 for the adsorbate, and D. W. T. (2.2315) was more than 1 for the solute which confirms the definition of modelling basis. Also, in the ANOVA, the lesser the Pr > F value, the more significant the results. Hence, the zinc metal was found to conform to a straight line Langmuir adsorption isotherm (Shiva, 2014). This result obtained for iron showed that activated carbons produced from the coconut and the palm kernel shells could be used as a high-performance adsorbent with higher adsorption capacity (Chavan, 2017).

Also from the results obtained in Table 4.15 cadmium have R<sup>2</sup>(0.8347), D.W.T (2.7000) and Pr > F (< 0.0001). From the statistic point of view, R<sup>2</sup> is the most critical parameter to obtain



the model ability in the fitting of various conditions provided based on experimental data. For this model, the amounts of  $R^2$  (0.8347) are relatively close to 1 for the adsorbate, and D. W. T. (2.700) was more than 1 for the solute which confirms the definition of modelling basis. Also, in the ANOVA, the lesser the  $Pr > F$  value, the more significant the results. Therefore, these results showed that cadmium metal conforms to a straight line Langmuir adsorption isotherm (Teoh et al., 2018). The results obtained for cadmium revealed that activated carbons produced from the coconut and the palm kernel shells could be used as an adsorbent with higher adsorption capacity (Thitame and Shukla, 2016).

In Table 4.15, lead recorded values of  $R^2$  (0.9349), D.W.T (2.3732) and  $Pr > F$  ( $< 0.0001$ ) respectively.  $R^2$  is the most important parameter to obtain the model ability in the fitting of various conditions provided based on experimental data. It can be seen from the results obtained in tables that, the Langmuir isotherm best fitted to the experimental data since it had the highest value for the coefficient of determination  $R^2$  (0.9349). This data has revealed that activated carbons produced from palm kernel and coconut which are an agricultural waste, can be used as an adsorbent for lead metal (Ofomaja, 2010) and (Asgari *et al.*, 2014).

From the results obtained in Table 4.15, chromium have  $R^2$  (0.9378), D.W.T (2.1824) and  $Pr > F$  ( $< 0.0001$ ). From the statistic point of view,  $R^2$  is the most critical parameter to obtain the model ability in the fitting of various conditions provided based on experimental data. Hence, the results recorded showed that chromium metal conforms to a straight line Langmuir adsorption isotherm (Rolence *et al.*, 2014). The results obtained for chromium revealed that activated carbons produced from the coconut and the palm kernel shells could be used as a high-performance adsorbent with higher adsorption capacity (Mehr *et al.*, 2019).

Finally, from Table 4.15 magnesium recorded the following results  $R^2$  (0.9997), D.W.T (2.4396) and  $Pr > F$  ( $< 0.0001$ ).  $R^2$  is the most important parameter to ascertain the model

ability in the fitting of various situations provided based on experimental data. In this model, the amounts of  $R^2$  (0.9997) are close to 1 for the adsorbate, and D. W. T. (2.4396) was more than 1 for the solute which confirms the definition of modelling basis. Also, in the ANOVA, the lesser the  $Pr > F$  value, the more significant the results. This revealed that magnesium metal conforms to a straight line Langmuir adsorption isotherm (Akpen *et al.*, 2018). This result obtained for magnesium proved that activated carbons produced from the coconut and the palm kernel shells could be used as a high-performance adsorbent with higher adsorption capacity (Akpen *et al.*, 2018)

## CHAPTER FIVE

### SUMMARY, CONCLUSIONS AND RECOMMENDATION

#### 5.1 Summary

In this study, physicochemical analyses of virgin and two different used lubricating oil samples were conducted to ascertain the concentration of heavy metals present in them. Chemical activated carbons were successfully produced from palm kernel and coconut shells using a 1M solution of potassium carbonate ( $K_2CO_3$ ) and sodium bicarbonate ( $NaHCO_3$ ). Physico-chemical analyses and characterisation with BET, FTIR and SEM were done on the chemical activated carbons produced. A comprehensive study was performed on its adsorption efficiency for the removal of some heavy metals, and other contaminants from used lubricating oil samples were investigated. BET surface analysis revealed that the synthesised samples were made up of both micro and mesoporous solid. FTIR analysis revealed several functional groups present in the activated carbons. Also, the SEM experiment conducted showed a detailed morphology of the activated carbons as a suitable adsorbent. A kinetic study showed that the adsorption behaviour of the activated carbons followed the straight line Langmuir model. Also, the experimental result obtained proof that the chemical activated carbons prepared were able to remove some of the heavy metals present in the two different used lubricating oil samples analysed. From literature findings reported earlier, it can be concluded that chemically activated carbons produced from both coconut and palm kernel shells are suitable adsorbents for removal of heavy metal such as cadmium, magnesium, chromium and zinc from used lubricating oils.

## 5.2 Conclusions

Based on the in-depth research work on the analyses of the virgin and two different used lubricating oil samples; analyses of the physicochemical properties of the chemical activated carbon produced from palm kernel and coconut shells; the removal of heavy metals using chemically activated carbons produced and co-efficient of determination results obtained from the Langmuir model, the following conclusions were made;

1. There was a significant increase in the concentration of heavy metals present in the used lubricating oil compared to that of virgin lubricating oil. This proved that the virgin lubricating oil got deteriorated with time when being used.
2. It was also established that there were high concentration of heavy metals such as copper, (Cu), Iron, (Fe), zinc, (Zn), cadmium, (Cd), lead, (Pb), chromium, (Cr) and magnesium, (Mg) in used lubricating oils analysed.
3. It was found out that the virgin lubricating oil procured as control sample contained the required physio-chemical parameters suitable for lubricating purposes.
4. That the activated carbons prepared from coconut and palm kernel shells have excellent physicochemical properties for adsorption.
5. The chemically activated carbons produced from palm kernel and coconut shells were able to remove heavy metals such as zinc, chromium, cadmium and magnesium contaminants from the used lubricating oil to considerable levels.
6. It was also observed that the coconut shell activated carbons was effective in the removal of lead metals while palm kernel could not.
7. The chemically activated carbons produced from palm kernel and coconut shells were not suitable for the removal of both copper and iron metals.
8. It was observed that the Langmuir model shows a better fit for all the heavy metals analysed due to the high coefficient of determination ( $R^2 \approx 1$ ).

9. The recovered oil could be also re-used.
10. Finally, agriculture waste such as palm kernel and coconut shells can be converted to high-performance adsorbents.

### **5.3 Recommendations**

1. Further research should be conducted using different activation agents or chemicals aside potassium carbonate ( $K_2CO_3$ ) and sodium bicarbonate ( $NaHCO_3$ ) used in this work.
2. The re-refining industries should explore the use of other agricultural waste as an alternative adsorbent, having provided insight that some agricultural waste such as palm kernel and coconut shells could be used in the production of suitable adsorbents.
3. A study should be conducted on what it would cost to set-up a commercial plant for the large scale production of activated carbons from coconut and palm kernel shells.
4. Studies should be carried out on the effect of regeneration (re-use) of the activated carbon adsorbents produced from the palm kernel and coconut shells.

### **5.4 Contributions to Knowledge**

The following contributions to knowledge were achieved after extensive research work:

1. The work was able to generate results and trend of high adsorption performance with the chemical activated carbons produced from the palm kernel and coconut shells that were not previously available with used lubricating oil samples.
2. The experimental set-up, data obtained, and research findings have contributed to the already existing body of literature and would serve as reference material in future related research into this area.

3. The study had proven that activated carbon adsorbents produced from palm kernel and coconut shells can be used as suitable adsorbents for removal of some heavy metals present in used lubricating oil samples.
4. The study had shown that activated carbon adsorbents produced from palm kernel and coconut shells are a good substitute for synthetic adsorbent such as silica gel for removal of contaminants.
5. The correlation determination ( $R^2$ ) data obtained from this study revealed that the Langmuir isotherm model can be employ.
6. New literatures have been published out of this research based on factorial design and analyses in studying the parameters that have an impact on used lubricating oil samples and chemically activated carbons produced from palm kernel and coconut shells.

## REFERENCES

- Ab. Jabal, S. N., Been Seok, Y., and Fwen Hoon, W. (2016). the Potential of Coconut Shell Powder (Csp) and Coconut Shell Activated Carbon (Csac) Composites As Electromagnetic Interference (Emi) Absorbing Material. *Malaysian Journal of Analytical Science*, 20(2), 444–451.
- Abdel-Jabbar, M, N.; Zubaidy,A.H.E.; and Mehrvar,M. (2010). Waste Lubricating Oil Treatment by Adsorption Process Using Different Adsorbents. *International Journal of Chemical and Biological Engineering*, Vol.3 (2), pp.70-73
- Abdelali, G., Abdelmalek, C., Réda, Y. A., Ammar, S., and Boubekour, N. (2019). Removal of methylene blue using activated carbon prepared from date stones activated with NaOH. *Global NEST Journal**Global NEST: The International Journal*, 21(X).
- Abdul, M., Kamaruzaman, W., Ahmad, W., Retnam, A., and Catrina, N. (2015). Concentration of heavy metals in virgin , used , recovered and waste oil : a spectroscopic study. *Procedia Environmental Sciences*, 30, 201–204.
- Abu-Elella, R., Ossman, M. E., Farouq, R., and Abd-Elfatah, M. (2015). Used Motor Oil Treatment: Turning Waste Oil Into Valuable Products. *Ijchs*, 7,pp. 57–67.
- Adib, M., Razi, M., Al-gheethi, A., and Al-qaini, M. (2018). Efficiency of activated carbon from palm kernel shell for treatment of greywater. *Arab Journal of Basic and Applied Sciences*, 0(0), 1–8.
- Ajemba, R. O., and Onukwuli, O. D. (2013). Adsorptive removal of colour pigment from palm oil using acid activated Nteje clay. Kinetics, equilibrium and thermodynamics. *Physicochemical Problems of Mineral Processing*, 49(1), 369–381.
- Akpen, G.D., Aho, M. I., and Mamwan, M. H. (2018). Equilibrium and kinetics of colour adsorption from textile wastewater by a novel adsorbent. *Global Journal of Pure and Applied Sciences*, 24(1), 61.
- Akpen, G D, Okparaku, L. A., and Odoh, F. O. (2017). Removal Of Colour From Wastewater By Raffia Palm Seed Activated Carbon,*Journal of Emerging Trends in Engineering and*

- Akpen, Gabriel Delian, and Leton, T. (2014). Adsorption characteristics of mango ( *magnifera indica* ) seed shell activated carbon for removing phenol from wastewater. *Journal of Applied Science and Technology*, 19(1–2), 37-42–42.
- Al-wesabi, E. O., Zinadah, O. A. A., Zari, T. A., and Al-hasawi, Z. M. (2015). Original Research Article Comparative assessment of some heavy metals in water and sediment from the Red Sea coast , Jeddah , Saudi Arabia,*Int.J.Curr.Microbiol.App.Sci*, Vol.4(8), pp. 840-855.
- Angalaeeswari, K., and Kamaludeen, S. (2017). Production and characterization of coconut shell and mesquite wood biochar. *International Journal of Chemical Studies*, 5(4), 442–446.
- Ani, I., Okafor, J., Olutoye, M., and Akpan, U. (2015). Effects of Process Variables and a Comparative Study of Methods for Transfer Oil Production from Spent Engine Oil. *British Journal of Applied Science and Technology*, 9(1), 65–76.
- Anyika, C., Asilayana, N., Asri, M., and Abdul, Z. (2017). Synthesis and characterization of magnetic activated carbon developed from palm kernel shells. *Nanotechnology for Environmental Engineering*, 2(1), 1–25.
- Arpa, O., Yumrutas, R., and Demirbas, A. (2010). Production of diesel-like fuel from waste engine oil by pyrolytic distillation. *Applied Energy*, 87(1), 122–127.
- Asgari, M., Anisi, H., Mohammadi, H., and Sadighi, S. (2014). Designing a commercial scale pressure swing adsorber for hydrogen purification. *Petroleum and Coal*, 56(5), 552–561.
- ASTM-D2862, (2016): Standard Test Method for Particle Size Distribution of Granular Activated Carbon, ASTM international, West Conshohocken, PA,USA, [www.astm.org](http://www.astm.org)
- ASTM D2273,(2005): Standard Test Method for Trace Sediments in Lubricating Oils, ASTM international, West Conshohocken, PA,USA, [www.astm.org](http://www.astm.org)



ASTM D 1298,(2004): Standard test method for density, relative density, or API gravity of crude petroleum and liquid petroleum products by hydrometer method, ASTM international, West Conshohocken, PA, USA, [www.astm.org](http://www.astm.org)

ASTM D 445,(2012): Standard test method for transparent and opaque liquids, ASTM international, West Conshohocken, PA, USA, [www.astm.org](http://www.astm.org)

ASTM D6304 – (2016):Standard Test Method for Determination of Water in Petroleum Products, Lubricating Oils, and Additives by Coulometric Karl Fischer Titration., ASTM international, West Conshohocken, PA,USA, [www.astm.org](http://www.astm.org)

ASTM D7946,(2014): Standard Test Method for Initial pH (i-pH)-Value of Petroleum Products, ASTM international, West Conshohocken, PA, USA, [www.astm.org](http://www.astm.org)

ASTM D7455, (2019): Standard Practice for Sample Preparation of Petroleum and Lubricant Products for Elemental Analysis, ASTM international, West Conshohocken, PA,USA, [www.astm.org](http://www.astm.org)

ASTM D2974 - (2014), Standard Test Methods for Moisture, Ash, and Organic Matter of Peat and Other Organic Soils,ASTM international, West Conshohocken, PA,USA, [www.astm.org](http://www.astm.org)

Azeem, S., and Hassanpour, M. (2017). Development circumstances of four recycling industries ( used motor oil , acidic sludge , plastic wastes and blown bitumen ) in the world. *Renewable and Sustainable Energy Reviews*, 72, 605–624.

Babayemi,A, K. (2017). Effects of Activating Chemicals on the Adsorption Capacity of Activated Carbons Prepared from Palm Kernel Shells ,*Journal of Environmental Science, Toxicology and Food Technology*, Vol 11(1), pp. 60-64.

Babayemi, A. K. (2017). Performance Evaluation of Palm Kernel Shell Adsorbents for the Removal of Phosphorus from Wastewater, 215–227.

- Baeten, J. E., Batstone, D. J., Schraa, O. J., van Loosdrecht, M. C. M., and Volcke, E. I. P. (2019). Modelling anaerobic, aerobic and partial nitrification-anammox granular sludge reactors - A review. *Water Research*, 149, 322–341.
- Barakat, M. A. (2011). New trends in removing heavy metals from industrial wastewater. *Arabian Journal of Chemistry*, 4(4), 361–377.
- Bentum, J. K., Anang, M., Boadu, K. O., Koranteng-Addo, E. J., and Owusu Antwi, E. (2011). Assessment of heavy metals pollution of sediments from Fosu lagoon in Ghana. *Bulletin of the Chemical Society of Ethiopia*, 25(2), 191–196.
- Boadu, KO; Joel, OF; Essumang, DK; Evbuomwan, B. (2018). Comparative Studies of the Physicochemical Properties and Heavy Metals adsorption Capacity of Chemical Activated Carbon from Palm Kernel , Coconut and Groundnut Shells. *J. Appl. Sci. Environ. Manage.*, Vol. 22 (1),pp.1833–1839.
- Boadu, K. O., Joel, O. F., Essumang, D. K., and Evbuomwan, B. O. (2019). A Review of Methods for Removal of Contaminants in Used Lubricating Oil. *Chemical Science International Journal*, 26(4), 1–11.
- Bosmans, A., Vanderreydt, I., Geysen, D., and Helsen, L. (2013). The crucial role of Waste-to-Energy technologies in enhanced landfill mining: A technology review. *Journal of Cleaner Production*, 55, 10–23.
- Botas, J. A., Moreno, J., Espada, J. J., Serrano, D. P., and Dufour, J. (2017). Resources , Conservation and Recycling Recycling of used lubricating oil : Evaluation of environmental and energy performance by LCA. *Resources, Conservation and Recycling*, 125(January), 315–323.
- Bridjanian, H. ; Sattarin, M. ( 2006). Modern recovery methods in used oil re-refining. *Petroleum and Coal*, 48 (1), 40-43.
- Brunauer, Emmett and Teller (BET), 2015 Model ASAP 2020 Micromeritics Analyzer, All Rights Reserved 2015. Micromeritics Instrument Corporation. Norcross, Ga 30093. 770-662-3636, U.S.A

- Buses, U., Raposo, H., Farinha, T., and Ferreira, L. A. (2019). Condition Monitoring with Prediction Based on Diesel Engine Oil Analysis : A Case Study for. *Actuators*, (8)(14), 1-14.
- Cabal, B., Budinova, T., Ania, C. O., Tsyntsarski, B., Parra, J. B., and Petrova, B. (2009). Adsorption of naphthalene from aqueous solution on activated carbons obtained from bean pods. *Journal of Hazardous Materials*, 161(2–3), pp.1150–1156.
- Cao, J., Xiao, G., Xu, X., Shen, D., and Jin, B. (2013). Study on carbonization of lignin by TG-FTIR and high-temperature carbonization reactor. *Fuel Processing Technology*, 106, 41–47.
- CAS Number: 7440-44-0; EC Number: 231-153-3
- Cassap, M. (2008). The analysis of used lubrication oils by inductively coupled plasma spectrometry for predictive maintenance. *Spectroscopy Europe*, 20, 17–20.
- Cazetta, A. L., Vargas, A. M. M., Nogami, E. M., Kunita, M. H., Guilherme, M. R., Martins, A. C., ... Almeida, V. C. (2011). NaOH-activated carbon of high surface area produced from coconut shell : Kinetics and equilibrium studies from the methylene blue adsorption, *Chemical Engineering Journal*, Vol.174(1), pp.117–125.
- Chavan, P.J. P. (2017). Preparation of Activated Carbon from Coconut Shell, *International Journal of Recent Research in Science, Engineering and Technology*, Vol. 3, (4), pp.598-603
- Chen, X. (2015). Modeling of experimental adsorption isotherm data. *Information (Switzerland)*, 6(1), 14–22.
- Daley, M. A., Tandon, D., Economy, J., and Hippo, E. J. (1996). Elucidating the porous structure of activated carbon fibers using direct and indirect methods. *Carbon*, 34(10), 1191–1200.
- Dalla, G., Khlebinkaia, O., Lodolo, A., and Miertus, S. (2003). Compendium of Used Oil

Regeneration Technologies. *United Nations Industrial Development Organization*, 10–15.

Das, D., Samal, D. P., and BC, M. (2015). Preparation of Activated Carbon from Green Coconut Shell and its Characterization. *Journal of Chemical Engineering and Process Technology*, 06(05).

Daud, W. M. A. W., and Ali, W. S. W. (2004). Comparison on pore development of activated carbon produced from palm shell and coconut shell. *Bioresource Technology*, 93(1), 63–69.

Din, A. T. M., Hameed, B. H., and Ahmad, A. L. (2009). Batch adsorption of phenol onto physiochemical-activated coconut shell, *Journal of Hazardous Materials*, Vol.161, pp. 1522–1529.

Diphare, M. J., Pilusa, J., Muzenda, E., and Mollagee, M. (2013). A Comparison of Waste Lubricating Oil Treatment Techniques, *International Conference on Environment, Agriculture and Food Sciences*, Kuala Lumpur (Malaysia), Vol.2028, pp. 106-109

Durrani, H. A. (2014). Re-Refining Recovery Methods of Used Lubricating Oil. *International Journal of Engineering Sciences and Research Technology*, 3(3), 1216–1220.

Durrani, H. a L. I., Panhwar, M. I., and Kazi, R. A. (2011). Re-Refining of Waste Lubricating Oil by Solvent Extraction. *Mehran University Research Journal of Engineering and Technology*, 30(2), 237–246.

Egelhofer, V., Schomburg, I., and Schomburg, D. (2010). Automatic assignment of EC numbers. *PLoS Computational Biology*, 6(1).

Emam, E. A., and Shoaib, A. (2012). Re-refining of used lube oil, II-by solvent/clay and acid/clay-percolation processes. *ARPJ. Sci. Technol.*, 2, 1034–1041.

Emetere, M. E., Okoro, E. E., Adeyemi, G. A., and Sanni, S. E. (2019). Air pollution assessment: a preliminary study towards citing industry. *Procedia Manufacturing*, 35,

681–688.

Epelle, E., Lukman, Y., and Otaru, A. J. (2016). A comparative study of the solvent powers of phenol, furfural and NMP in improving the viscosity index of spent lubricating oil. *International Research Journal on Engineering*, 3(1), 8–24.

European Commission. (2015). *Best Available Techniques (BAT) Reference Document for the Refining of Mineral Oil and Gas*. JRC Science and Policy Reports, pages.754.

Evbuomwan, B. O., Agbede, A. M., and Atuka, M. M. (2013). A Comparative Study of the Physico-Chemical Properties of Activated Carbon from Oil Palm Waste ( Kernel Shell and Fibre ), 2(19), 75–79.

EViews 4 Users Guide (2002), EViews Software Version 3.1, U.S.A

Examiner, P., and Fortuna, A. (2000).Refining of Used Oils using Membrane- and Adsorption-Based Processes United States Patent (19), (19).

Fan, F., Li, H., Xu, Y., Liu, Y., Zheng, Z., and Kan, H. (2018). Thermal behaviour of walnut shells by thermogravimetry with gas chromatography-mass spectrometry analysis. *Royal Society Open Science*, 5(9).

Fletcher AJ, Uygur Y, Thomas KM (2007) Role of surface functional groups in the adsorption kinetics of water vapor on microporous activated carbons. *J Phys Chem*, Vol. 111, pp.8349–8359.

Foo, K., B. Hameed. Insights into the modelling of adsorption isotherm systems. *Chemical Engineering Journal*, 2010, 156: 2–10

Forsthoffer, W.E. Lube, seal and control oil system best practices. In *Forsthoffer's Best Practice Handbook for Rotating Machinery*, 1st ed.; Elsevier: Oxford, UK, 2011; pp. 347–468.

Fu, F., and Wang, Q. (2011). Removal of heavy metal ions from wastewaters: A review. *Journal of Environmental Management*, 92(3), 407–418.

- García, J. R., Sedran, U., Abbas, M., Zaini, A., and García, J. R. (2017). Preparation , characterization , and dye removal study of activated carbon prepared from palm kernel shell. *Environ Sci Pollut Res*, pp.1-10
- Gedik, K., and Uzun, Y. (2015). Characterization of the properties of diesel-base oil-solvent-waste oil blends used as generic fuel in diesel engines. *Fuel Processing Technology*, 139(x), 135–141.
- Geyer, R., Kuczynski, B., Henderson, A., and Zink, T. (2013). Life Cycle Assessment of Used Oil Management in California Pursuant to Senate Bill 546 (Lowenthal), *California Department of Resources Recycling and Recovery*, Vol. 546.
- Ghalibaf, A., C, T. R. K., and Pyrolytic, R. (2019). This is a self-archived version of an original article . This version may differ from the original in pagination and typographic details . Copyright : Rights : Rights url : Please cite the original version : Pyrolytic behavior of lignocellulosic-based pol. *Journal of Thermal Analysis and Calorimetry*, 137(1), 121–131.
- Ghazal, F. M., Battah, M. G., El-Aal, A. A. A., Eladel, H. M., and Adly, S. E. (2016). Studies on the efficiency of cyanobacteria on textile wastewater treatment. *Research Journal of Pharmaceutical, Biological and Chemical Sciences*, 7(4), 2925–2931.
- Ghorbanian, A., Naghdi, B., Jafari, H., and Sadeghi, A. (2018). The Effect of Organizational Culture and Individual Motivation Resources on Staff Burnout : Structural Equation Modeling Approach, 2(3), 181–192.
- Ghorbanian, S. A., Bagheri, N., and Khakpay, A. (2016). Investigation of Adsorption Isotherms of Aniline on Activated Carbon Investigation of Adsorption Isotherms of Aniline on Activated Carbon, 1st National Conference on Industrial Water and Wastewater Treatment, Tehran, Iran.
- Giovanna FD, European Landscape. 4th European Rerefining Congress, Brussels (2009).
- Gopalswami, P. M., Ponnusamy, S., Sivakumar, N., and Ilamparithi, A. (2010). Methylene blue adsorption onto low cost powdered activated carbon from agricultural waste - Morus plant. *Nature Environment and Pollution Technology*, 9(2), 317–322.

- Guerin, T. F. (2008). Environmental liability and life-cycle management of used lubricating oils. *Journal of Hazardous Materials*, 160(2–3), 256–264.
- Gupta, V. K. (2013). Adsorptive remediation of Cu ( II ) and Ni ( II ) by microwave assisted H 3 PO 4 activated carbon. *Arabian Journal of Chemistry*. 10, S2836–S2844,
- Hamawand, I., Yusaf, T., and Rafat, S. (2013a). Recycling of waste engine oils using a new washing agent. *Energies*, 6(2), pp.1023–1049.
- Hamawand, I., Yusaf, T., and Rafat, S. (2013b). Recycling of Waste Engine Oils Using a New Washing Agent, *Energies*, 6(2), pp.1023–1049.
- Hamza, U. D., Nasri, N. S., Amin, N. S., Mohammed, J., and Zain, H. M. (2015). Characteristics of oil palm shell biochar and activated carbon prepared at different carbonization times. *Desalination and Water Treatment*, Vol.57(17). pp. 7999-8006'
- Hanaor, D. A. H., Gan, Y., and Einav, I. (2015). International Journal of Solids and Structures Contact mechanics of fractal surfaces by spline assisted discretisation. *International Journal of Solids and Structures*, Vol.59, 121–131.
- Hanaor, D.A.H; Ghadiri, M; Chrzanowski, W; Gan, Y (2014). "Scalable Surface Area Characterization, *Electrokinetic Analysis of Complex Anion Adsorption*" (PDF). *Langmuir*. Vol.30 (50):pp.15143- 15152
- Hani, F. B., and Al-Wedyan, H. (2011). Regeneration of base-oil from waste-oil under different conditions and variables. *African Journal of Biotechnology*, 10(7), 1150–1153.
- Hidayu, A. R., and Muda, N. (2016a). Preparation and characterization of impregnated activated carbon from palm kernel shell and coconut shell for CO 2 capture. *Procedia Engineering*, Vol.148, 106–113.
- Hidayu, A. R., and Muda, N. (2016b). Preparation and Characterization of Impregnated Activated Carbon from Palm Kernel Shell and Coconut Shell for CO2 Capture. In *Procedia Engineering*, Vol.148, pp.106–113

- Hock, P. E., and Zaini, M. A. A. (2018). Activated carbons by zinc chloride activation for dye removal – a commentary. *Acta Chimica Slovaca*, 11(2), 99–106.
- Hu, Z., and Srinivasan, M. P. (2001). Mesoporous high-surface-area activated carbon. *Microporous and Mesoporous Materials*, 43(3), 267–275.
- Hussein, M., Amer, A. A., and Gaberah, A. S. (2014). Used lubricating oils re-refining by solvent extraction. *American Journal of Environmental Engineering and Science*, 1(3), 44–50.
- Ilomuanya, M. O., Ohere, A. F., Zubair, S. A., and Ubani-Ukoma, U. (2017). Evaluation of adsorption capacity of acetaminophen on activated charcoal dosage forms available in Nigeria by in vitro adsorption studies and scanning electron microscopy. *Tropical Journal of Pharmaceutical Research*, 16(5), 1105–1112.
- Inegbenebor, A. I., Inegbenebor, A. O., and Boyo, H. I. (2012). Comparison of the Adsorptive Capacity of Raw Materials in Making Activated Carbon Filter for Purification of Polluted Water for Drinking. *ARPN Journal of Science and Technology*, 2(9), 754–760.
- Islam, A., Ahmed, M. J., Khanday, W. A., Asif, M., and Hameed, B. H. (2017). Mesoporous activated carbon prepared from NaOH activation of rattan (*Lacosperma secundiflorum*) hydrochar for methylene blue removal. *Ecotoxicology and Environmental Safety*, 138, 279–285.
- Islam, B. (2015). Petroleum sludge, its treatment and disposal: A review. *International Journal of Chemical Sciences*, 13(4), 1584–1602.
- Islam, S., Ang, B. C., Gharekhani, S., Binti, A., and Afifi, M. (2016). Adsorption capability of activated carbon synthesized from coconut shell, 20, 1–9.
- Jabit, N. B. (2007). The Production and Characterization of Activated Carbon Using Local Agricultural Waste through Chemical Activation Process. Master of Science Thesis, School of Material and Mineral Engineering, Universiti Sains Malaysia, Pp. 1-24.



- Jafari, A. J., and Hassanpour, M. (2014). Analysis and comparison of used lubricants, regenerative technologies in the world. *Resources, Conservation and Recycling*, 103, 179–191.
- Jahangard, A., Sohrabi, M., and Beigmohammadi, Z. (2016). Sorption of Lead (II) Ions on Activated Coconut Husk, *Iranian Journal of Toxicology*, 10(6), 23–29.
- Jain, A., Balasubramanian, R., and Srinivasan, M. P. (2015). Production of high surface area mesoporous activated carbons from waste biomass using hydrogen peroxide-mediated hydrothermal treatment for adsorption applications. *Chemical Engineering Journal*, 273, 622–629.
- Jalani, N., Aziz, A., Wahab, N., Hassan, W. W., and Zainal, N. (2016). Application of Palm Kernel Shell Activated Carbon for the Removal of Pollutant and Color in Palm Oil Mill Effluent Treatment. *Journal of Earth, Environment and Health Sciences*, 2(1), 15.
- Jiménez-Castañeda, M. E., and Medina, D. I. (2017). Use of surfactant-modified zeolites and clays for the removal of heavy metals from water. *Water (Switzerland) MDPI AG*, 9(4).
- Jodeh, S., Odeh, R., Sawalha, M., Abu Obeid, A., Salghi, R., Hammouti, B., Warad, I. (2015). Adsorption of lead and zinc from used lubricant oil using agricultural soil: Equilibrium, kinetic and thermodynamic studies. *Journal of Materials and Environmental Science*, 6(2), 580–591.
- Joel, O. F. (2013). “Tapping The Untapped Wealth in our Backyard : Pathway to Local Content Development ” An Inaugural Lecture, (104).
- Josiah, P. N., and Ikiensikimama, S. S. (2010). The Effect of Desludging and Adsorption Ratios on the Recovery of Low Pour Fuel Oil (LPFO) from Spent Engine Oil. *Chemical Engineering Research Bulletin*, 14(1), 25–28.
- Kajdas, C. (2000). Major pathways for used oil disposal and recycling. Part 2. *Tribotest*, 7(2), 137–153.

- Kalderis, D., Bethanis, S., Paraskeva, P., and Diamadopoulos, E. (2008). Production of activated carbon from bagasse and rice husk by a single-stage chemical activation method at low retention times. *Bioresource Technology*, 99(15), 6809–6816.
- Kamal, A., and Khan, F. (2009a). Effect of Extraction and Adsorption on Re-refining of Used Lubricating Oil, *Oil and Gas Science and Technology*, 64(2), 191–197.
- Kamal, A., and Khan, F. (2009b). Effet de l'extraction et de l'adsorption sur le retraitement des huiles usagées. *Oil and Gas Science and Technology*, 64(2), 191–197.
- Kamal, M. A., Naqvi, S. M. D., and Khan, F. (2014). Optimized liquid-liquid extractive re-refining of spent lubricants. *The Scientific World Journal*, Vol.2014, pp.1-10
- Kannan, S., Mohan, K., Hussain, S., Priya, D., and Saravanan, K. (2014). Studies on Reuse of Re-Refined Used Automotive Lubricating Oil. *Research Journal of Engineering Sciences*, 3(6), 8–14.
- Kapustina, V., Havukainen, J., Virkki-Hatakka, T., and Horttanainen, M. (2014). System analysis of waste oil management in Finland. *Waste Management and Research*, 32(4), 297–303.
- Key, R., Lun, W., Yee, M., Yee, X., Huan, M., Nai, P., Shiung, S. (2017a). Oil palm waste : An abundant and promising feedstock for microwave pyrolysis conversion into good quality biochar with potential multi-applications. *Process Safety and Environmental Protection*, 115, 57–69.
- Key, R., Lun, W., Yee, M., Yee, X., Huan, M., Nai, P., Shiung, S. (2017b). Oil palm waste : An abundant and promising feedstock for microwave pyrolysis conversion into good quality biochar with potential multi-applications. *Process Safety and Environmental Protection*, 1–13.
- Kilmer, P. D. (2010). Review Article: Review Article. *Journalism: Theory, Practice and Criticism*, 11(3), 369–373.

- Kpan, J. D. A., Opoku, B. K., and Gloria, A. (2014). Heavy Metal Pollution in Soil and Water in Some Selected Towns in Dunkwa-on-Offin District in the Central Region of Ghana as a Result of Small Scale Gold Mining. *Journal of Agricultural Chemistry and Environment*, 03(02), 40–47.
- Kumar, V. B., Borenstein, A., Markovsky, B., Aurbach, D., Gedanken, A., Talianker, M., and Porat, Z. (2016). Activated Carbon Modified with Carbon Nanodots as Novel Electrode Material for Supercapacitors. *Journal of Physical Chemistry C*, 120(25), 13406–13413.
- Kupareva, A., Mäki-Arvela, P., and Murzin, D. Y. (2013a). Technology for rerefining used lube oils applied in Europe: A review. *Journal of Chemical Technology and Biotechnology*, 88(10), 1780–1793.
- Kupareva, A., Mäki-Arvela, P., and Murzin, D. Y. (2013b). Technology for rerefining used lube oils applied in Europe: A review. *Journal of Chemical Technology and Biotechnology*, 88(10), 1780–1793.
- Kwakye-Awuah, B., Kwakye, R., Sefa-Ntiri, B., Nkrumah, I., Von-Kiti, E., and Williams, C. (2018). Comparison of the Recycling Efficiency of Metakaolin and Laboratory-Synthesized Zeolite Types LTA and LSX on Used Lubricant Engine Oil. *Applied Physics Research*, 10(4), 11.
- Lam, S. S., Liew, R. K., Cheng, C. K., Rasit, N., Ooi, C. K., Ma, N. L., Chase, H. A. (2018). Pyrolysis production of fruit peel biochar for potential use in treatment of palm oil mill effluent. *Journal of Environmental Management*, 213, 400–408.
- Lam, S. S., Liew, R. K., Jusoh, A., Chong, C. T., Ani, F. N., and Chase, H. A. (2016). Progress in waste oil to sustainable energy, with emphasis on pyrolysis techniques. *Renewable and Sustainable Energy Reviews*, 53, 741–753.
- Langmuir, I. (1917). The constitution and fundamental properties of solids and liquids. II. Liquids. *Journal of the American Chemical Society*, 39(9), 1848–1906.

- Lara, R. F., Azcarate, S. M., Cantarelli, M. Á., Orozco, I. M., Caroprese, M. E., Savio, M., and Camiña, J. M. (2015). Lubricant quality control: A chemometric approach to assess wear engine in heavy machines. *Tribology International*, 86, 36–41.
- Largitte, L., and Pasquier, R. (2016). A review of the kinetics adsorption models and their application to the adsorption of lead by an activated carbon. *Chemical Engineering Research and Design*, 109, 495–504.
- Liew, R. K., Nam, W. L., Chong, M. Y., Phang, X. Y., Su, M. H., Yek, P. N. Y., ... Lam, S. S. (2018). Oil palm waste: An abundant and promising feedstock for microwave pyrolysis conversion into good quality biochar with potential multi-applications. *Process Safety and Environmental Protection*, 115, 57–69.
- Ling, O.H.L., Ting, K.H., Shaharuddin, A., Kadaruddin, A., and Yaakob, M.J. (2010). Urban growth and air quality in Kuala Lumpur city, Malaysia. *Environment Asia*, 3(2), 123-128.
- Magriotis, Z. M., Leal, P. V. B., Sales, P. F., Papini, R. M., and Viana, P. R. M. (2010). Adsorption of etheramine on kaolinite: A cheap alternative for the treatment of mining effluents. *Journal of Hazardous Materials*, 184(1–3), 465–471.
- Mahamad, M. N., Zaini, M. A. A., and Zakaria, Z. A. (2015). Preparation and characterization of activated carbon from pineapple waste biomass for dye removal. *International Biodeterioration and Biodegradation*, 102, 274–280.
- Manasomboonphan, W., and Junyapoon, S. (2012). Production of Liquid Fuels from Waste Lube Oils Used by Pyrolysis process. *2012 2nd International Conference on Biomedical Engineering and Technology IPCBEE*, 34, 4–7.
- Manyuchi, M. M., Nengiwa, T., Mbohwa, C., Muzenda, E., and Mpeti, M. (2018). Potential for re-refining of used lubricating oils for re-use using zinc dialkyl dithiosulphate as an additive. In *Proceedings of the International Conference on Industrial Engineering and Operations Management* (Vol. 2018, pp. 1357–1364).
- Mehr, M. R., Fekri, M. H., Omidali, F., Eftekhari, N., and Akbari-Adergani, B. (2019). Removal of chromium (VI) from wastewater by palm kernel shell-based on a green method. *Journal of Chemical Health Risks*, 9(1), 75–86.

- Mekonnen, H. A. (2014). Recycling of Used Lubricating Oil Using Acid-Clay Treatment Process Recycling of Used Lubricating Oil Using Acid-Clay Treatment Process, *A Thesis Submitted in Partial Fulfilment of the Requirements for the Award of a Master's Degree in Chemical Engineering under Environmental Engineering*, School of Chemical and Bio-Engineering, Addis Ababa Institute Of Technology (Aait), Addis Ababa University,
- Mohammed, R. R., Ibrahim, I. A. R., Taha, A. H., and Mckay, G. (2013). Waste lubricating oil treatment by extraction and adsorption. *Chemical Engineering Journal*, 220, 343–351.
- Mortier, R. M., Fox, M. F., and Orszulik, S. T. (2010). Chemistry and technology of lubricants: Third edition. *Chemistry and Technology of Lubricants: Third Edition*, 1–560.
- Muhammad, A. B., Alhassan, B. B. U., Sulaiman, M., and Sahabi, Y. M. (2016). Investigation of the Extent of Wear Metals in Five Different Lubricating Oils Before and After Exposure to Engine Stress, 9(8), 75–78.
- Nayak, P. S., and Singh, B. K. (2007). Removal of phenol from aqueous solutions by sorption on low cost clay. *Desalination*, 207(1–3), 71–79.
- Nb, O., Shamsuddin, N., and Uemura, Y. (2016). Activated Carbon of Oil Palm Empty Fruit Bunch ( EFB ); Core and Shaggy. *Procedia Engineering*, 148, 758–764.
- Nicholas, A. F., Hussein, M. Z., Zainal, Z., and Khadiran, T. (2018). Palm kernel shell activated carbon as an inorganic framework for shape-stabilized phase change material. *Nanomaterials*, 8(9).
- Nwabanne, J. T., and Igbokwe, P. K. (2012). Comparative study of lead ( II ) removal from aqueous solution using different adsorbents. *International Journal of Engineering Research and Applications (IJERA)*, 2(4), 1830–1838.
- Nwachukwu, A. (2012). Review and assessment of mechanic village potentials for small scale used engine oil recycling business. *African Journal of Environmental Science and Technology*, 6(12), 464–475.

- Odisu, T; Edomwonyi-Otu, LC; Anih, E. (2019). Comparative Studies of Adsorption of Heavy Metals from Cement Waste Water Using Activated Carbon from Palm Kernel Husk , Coconut and Groundnut Shells. *J. Appl. Sci. Environ. Manage.*, Vol. 23, 967–975.
- Ofomaja, A. E. (2010). Equilibrium studies of copper ion adsorption onto palm kernel fi bre. *Journal of Environmental Management*, 91(7), 1491–1499.
- Okafor, P. C., Okon, P. U., Daniel, E. F., and Ebenso, E. E. (2012). Adsorption Capacity of Coconut ( *Cocos nucifera* L . ) Shell for Lead , Copper , Cadmium and Arsenic from Aqueous Solutions, *Int. J. Electrochem. Sci.*,7, 12354–12369.
- Oladimeji, T. E., and Sonibare, J. A. (2018). Data on the treatment of used lubricating oil from two different sources using solvent extraction and adsorption Data in Brief Data on the treatment of used lubricating oil from two different sources using solvent extraction and adsorption. *Data in Brief*, 19, 2240–2252.
- Oladimeji, T. E., Sonibare, J. A., Omoleye, J. A., Emetere, M. E., and Elehinafe, F. B. (2018). A review on treatment methods of used lubricating oil. *International Journal of Civil Engineering and Technology*, 9(12), 506–514.
- Olanipekun, E. A., Olusola, K. O., and Ata, O. (2006). A comparative study of concrete properties using coconut shell and palm kernel shell as coarse aggregates. *Building and Environment*, 41(3), 297–301.
- Olivares-Marín, M., Del Prete, V., Garcia-Moruno, E., Fernández-González, C., Macías-García, A., and Gómez-Serrano, V. (2009). The development of an activated carbon from cherry stones and its use in the removal of ochratoxin A from red wine. *Food Control*, 20(3), 298–303.
- Onundi, Y. B., Mamun, A. A., Al Khatib, M. F., and Ahmed, Y. M. (2010a). Adsorption of copper, nickel and lead ions from synthetic semiconductor industrial wastewater by palm shell activated carbon. *International Journal of Environmental Science and Technology*, 7(4), 751–758.

- Onundi, Y. B., Mamun, A. A., Al Khatib, M. F., and Ahmed, Y. M. (2010b). Adsorption of copper, nickel and lead ions from synthetic semiconductor industrial wastewater by palm shell activated carbon. *International Journal of Environmental Science and Technology*, 7(4), 751–758.
- Onyekwere Nwosu, F., Iromidayo Olu-Owolabi, B., Oyeboade Adebawale, K., and Leke, L. (2008). Comparative Investigation of Wear Metals in Virgin and Used Lubricant Oils. *Terrestrial and Aquatic Environmental Toxicology*, 1(2), 38–43
- Osman, D. I., Attia, S. K., and Taman, A. R. (2017). Recycling of used engine oil by different solvent. *Egyptian Journal of Petroleum*, Vol.27(2),pp.221-225
- Ossman, M. E., and Farouq, R. (2015). Used Motor Oil Treatment : Turning Waste Oil Into Valuable Products Used Motor Oil Treatment : Turning Waste Oil Into Valuable Products,*International Journal of Chemical and Biochemical Sciences (ISSN 2226-9614)*, 7,pp:57-67
- Pathania, D., Sharma, S., and Singh, P. (2017). Removal of methylene blue by adsorption onto activated carbon developed from Ficus carica bast. *Arabian Journal of Chemistry*, Vol.10, pp.S1445-S1451
- Patiha, Herald, E., Hidayat, Y., and Firdaus, M. (2016). The langmuir isotherm adsorption equation: The monolayer approach. *IOP Conference Series: Materials Science and Engineering*, 107(1).
- Pazoki, M., and Hasanidarabadi, B. (2017). Management of toxic and hazardous contents of oil sludge in Siri Island. *Global J. Environ. Sci. Manage*, 3(1), 33–42.
- Pelitli, V. Ö. D. and H. J. K. (2017). Waste oil management : Analyses of waste oils from vehicle crankcases and gearboxes. *Global J. Environ. Sci. Manage*, 3(1), 11–20.
- Pinheiro, C T, Pais, R. F., Ferreira, A. G. M., Quina, M. J., and Gando-Ferreira, L. M. (2018). Measurement and correlation of thermophysical properties of waste lubricant oil. *The Journal of Chemical Thermodynamics*, 116, 137–146.  
<https://doi.org/10.1016/J.JCT.2017.08.039>

- Pinheiro, Carolina T, Pais, R. F., Quina, M. J., and Gando-ferreira, L. M. (2018). An overview of waste lubricant oil management system: Physicochemical characterization contribution for its improvement, *Journal of Cleaner Production*. Vol.150, pp. 301-308
- Promdee, K., Chanvidhwatanakit, J., and Satitkune, S. (2017). Characterization of carbon materials and differences from activated carbon particle ( ACP ) and coal briquettes product ( CBP ) derived from coconut shell via rotary kiln. *Renewable and Sustainable Energy Reviews*, 7, 1175–1186.
- Rincón, J., Cañizares, P., and García, M. T. (2007). Regeneration of used lubricant oil by ethane extraction. *Journal of Supercritical Fluids*, 39(3), 315–322.
- Rolence, C., Machunda, R. L., and Njau, K. N. (2014). Water hardness removal by coconut shell activated carbon, *International Journal of Science, Technology and Society*, Vol.2(5), 97–102.
- Ruiz, H., Zambrano, M., Giraldo, L., Sierra, R., and Moreno-pirajan, J. C. (2015). Production and Characterization of Activated Carbon from Oil-palm Shell for Carboxylic Acid Adsorption, *Oriental Journal of Chemistry*, Vol.31(2), pp. 753-762
- Saleh, T. A., Tuzen, M., and Sarı, A. (2017). Polyethylenimine modified activated carbon as novel magnetic adsorbent for the removal of uranium from aqueous solution. *Chemical Engineering Research and Design*. Vol.117, pp. 218-227
- Salem, S., Salem, A., and Agha Babaei, A. (2015). Preparation and characterization of nano porous bentonite for regeneration of semi-treated waste engine oil: Applied aspects for enhanced recovery. *Chemical Engineering Journal*, 260, 368–376.
- Shahbeig, H., Bagheri, N., Ghorbanian, S. A., Hallajisani, A., and Poorkarimi, S. (2013). A new adsorption isotherm model of aqueous solutions on granular activated carbon. *World Journal of Modelling and Simulation*, 9(4), 243–254.
- Shen, D., Xiao, R., and Luo, K. (2011). The pyrolytic behavior of cellulose in lignocellulosic biomass : a review, *RSC Advances*, Vol.1(9), pp.1641–1660.



- Shiva, Q. (2014). Journal of Industrial and Engineering Chemistry Application of Iranian nano-porous Ca-bentonite for recovery of waste lubricant oil by distillation and adsorption techniques. *Journal of Industrial and Engineering Chemistry*, Vol.23,pp. 154-162
- Shoaib, A. (2013). Re-refining of used lube oil , i- by solvent extraction and vacuum distillation followed by hydrotreating, *Petroleum and Coal*, Vol. 55(3), pp. 179-187
- Singh, S., Ramakrishna, S., and Gupta, M. K. (2017). Towards zero waste manufacturing: A multidisciplinary review. *Journal of Cleaner Production*, 168, 1230–1243.
- Sonibare, J. A., and Omoleye, J. A. (2018). A REVIEW ON TREATMENT METHODS OF. *International Journal of Civil Engineering and Technology (IJCIET)*, 9(12), 506–514.
- Stan, C., Andreescu, C., and Toma, M. (2018). Some aspects of the regeneration of used motor oil. *Procedia Manufacturing*, 22, 709–713.
- Sterpu, A.-E., Dumitru, A. I., and Popa, M.-F. (2013). Regeneration of used engine lubricating oil by solvent extraction. *Analele Universitatii "Ovidius" Constanta - Seria Chimie*, 23(2), 149–154.
- Tabassi, D., Harbi, S., Louati, I., and Hamrouni, B. (2017). Response surface methodology for optimization of phenol adsorption by activated carbon: Isotherm and kinetics study. *Indian Journal of Chemical Technology*, 24(3), 239–255.
- Tan, K. L., and Hameed, B. H. (2017). Insight into the adsorption kinetics models for the removal of contaminants from aqueous solutions. *Journal of the Taiwan Institute of Chemical Engineers*, 74, 25–48.
- Taylor, R. T., Examiner, P., and Nguyen, T. M. (2010). ( 12 ),Methods of Removing Contaminants from Used Oil, United States Patent, 2(12).
- Tchounwou, P. B., Yedjou, C. G., Patlolla, A. K., and Sutton, D. J. (2012). *Molecular, clinical and environmental toxicology Volume 3:Vol.101*, pp. 133-164

- Teoh, W. P., Noor, Z. H., Ng, C. A., and Swee, Y. C. (2018). Catalyzed waste engine oil as alternative binder of roofing tiles – Chemical analysis and optimization of parameters. *Journal of Cleaner Production*, 174, 988–999.
- Thitame, P. V., and Shukla, S. R. (2016). Adsorptive removal of reactive dyes from aqueous solution using activated carbon synthesized from waste biomass materials. *International Journal of Environmental Science and Technology*, 13(2), 561–570.
- Tripathi, M., Sahu, J. N., and Ganesan, P. (2016). Effect of process parameters on production of biochar from biomass waste through pyrolysis : A review. *Renewable and Sustainable Energy Reviews*, 55, 467–481.
- Tsai, W. T. (2011). An analysis of used lubricant recycling, energy utilization and its environmental benefit in Taiwan. *Energy*, 36(7), 4333–4339.
- Udoetok, I. A. (2012). Characterization of ash made from oil palm empty fruit bunches, *International Journal of Environmental Sciences*, 3(1), pp.518–524.
- Udonne, J. D., and Bakare, O. A. (2013). Recycling of Used Lubricating Oil Using Three Samples of Acids and Clay as a Method of Treatment. *International Archive of Applied Sciences and Technology*, 4(2), 8–14.
- Valix, M., Cheung, W. H., and McKay, G. (2004). Preparation of activated carbon using low temperature carbonisation and physical activation of high ash raw bagasse for acid dye adsorption. *Chemosphere*, 56(5), 493–501.
- Verla, A., Horsfall(Jnr), M., and Verla, E. (2012). Preparation and Characterization of Activated Carbon From Fluted Pumpkin (*Telfairia Occidentalis* Hook. F) Seed Shell. *Asian Journal of Natural and Applied Sciences*, 1(3), 39–50.

XLSTAT (2018), Quantitative Micro Software LLC, U.S.A

- Yashim, M. M., Razali, N., Saadon, N., and Rahman, N. A. (2016). Effect of activation temperature on properties of activated carbon prepared from oil palm kernel shell (OPKS). *ARPJ Journal of Engineering and Applied Sciences*, 11(10), 6389–6392.
- Zacaroni, L. M., Magriotis, Z. M., Cardoso, M. das G., Santiago, W. D., Mendonça, J. G., Vieira, S. S., and Nelson, D. L. (2015). Natural clay and commercial activated charcoal: Properties and application for the removal of copper from cachaça. *Food Control*, 47, 536–544.
- Zajac, G., Szyszlak-Bargłowicz, J., Słowik, T., Kuranc, A., and Kamińska, A. (2015). Designation of chosen heavy metals in used engine oils using the XRF method. *Polish Journal of Environmental Studies*, 24(5), 2277–2283.

## APPENDICES

### APPENDIX A: EXPERIMENTAL RAW DATA

**Table A.1: Raw data of Heavy metals present in coconut and palm kernel shell sample from AAS**

S/N	Parameters	Coconut shell	Palm kernel shell
<b>1</b>	Copper (Cu)	1.50	1.19
		1.41	1.03
		1.47	1.20
		1.52	1.08
<b>2</b>	Iron, Fe	131.67	81.79
		131.60	80.80
		131.80	81.40
		132.00	81.21
<b>3</b>	Zinc, Zn	0.69	1.67
		0.50	1.64
		0.62	1.60
		0.57	1.58
<b>4</b>	Cadmium, Cd	0.03	0.02
		0.03	0.02
		0.04	0.01
		0.04	0.03
<b>5</b>	Lead (Pb)	0.79	0.33
		0.63	0.55
		0.74	0.48
		0.76	0.42
<b>6</b>	Chromium (Cr)	0.82	0.76
		0.36	0.83
		0.78	0.68
		0.54	0.72
<b>7</b>	Magnesium (Mg)	8.00	18.00
		7.00	16.00
		7.80	17.0
		8.20	17.60
<b>8</b>	Nickel, Ni	0.28	0.53
		0.28	0.45
		0.30	0.40
		0.32	0.50
<b>9</b>	Calcium, Ca	0.36	3.04
		0.56	3.25
		0.48	3.00
		0.54	2.85
<b>10</b>	Potassium, K	179.00	128.00
		176.00	125.00
		178.0	123.00
		174.00	126.00

**Table A.2: Virgin and used lubricating oil samples raw data from AAS**

S/N	PARAMETERS	SAMPLE A	SAMPLE B	CONTROL
<b>1</b>	Copper (Cu)	0.15	0.20	<0.001
		0.14	0.21	<0.001
		0.16	0.23	<0.001
		0.15	0.24	<0.001
<b>2</b>	Iron, Fe	4.43	3.02	1.41
		4.79	3.64	1.56
		4.64	3.20	1.60
		4.74	3.54	1.44
<b>3</b>	Zinc, Zn	17.5	14.75	2.83
		15.4	14.80	2.82
		16.0	14.20	2.88
		17.0	14.55	2.80
<b>4</b>	Cadmium, Cd	0.02	0.03	0.02
		0.02	0.03	0.03
		0.03	0.02	0.01
		0.01	0.04	0.02
<b>5</b>	Lead (Pb)	0.53	1.25	0.87
		1.50	1.65	1.09
		1.40	1.45	1.01
		0.75	1.75	1.03
<b>6</b>	Chromium (Cr)	0.32	0.40	0.36
		0.47	0.49	0.41
		0.43	0.43	0.48
		0.38	0.46	0.39
<b>7</b>	Magnesium (Mg)	5.7	22.1	42.0
		5.1	20.6	41.6
		5.4	21.4	41.8
		5.6	21.80	42.2

**Table A.3: Raw data of heavy metals after filtration with palm kernel sample from AAS**

S/N	Parameters	Sample A	Sample B	Control
<b>1</b>	Iron, Fe	8.40	3.60	1.30
		8.20	3.50	1.00
		8.60	3.20	1.20
		8.80	3.30	1.10
<b>2</b>	Chromium, Cr	0.22	0.14	0.08
		0.18	0.13	0.06
		0.20	0.15	0.07
		0.24	0.12	0.05
<b>3</b>	Lead, Pb	1.51	2.47	1.61
		1.65	2.38	1.66
		1.70	2.30	1.70
		1.73	2.40	1.63
<b>4</b>	Cadmium, Cd	0.01	0.00	0.00
		0.01	0.00	0.00
		0.03	0.00	0.00
		0.02	0.00	0.00
<b>5</b>	Zinc, Zn	10.30	5.20	8.50
		10.40	5.20	8.60
		10.20	5.80	8.20
		10.60	5.60	8.00
<b>6</b>	Magnesium, Mg	0.89	0.51	0.38
		0.87	0.50	0.36
		0.91	0.52	0.34
		0.93	0.49	0.32
<b>7</b>	Copper, Cu	0.42	0.23	0.07
		0.39	0.23	0.06
		0.41	0.24	0.08
		0.38	0.22	0.09

**Table. A.4: Raw data of heavy metals present in Used lubricating oil after filtration with coconut shell sample from AAS**

S/N	Parameters	Sample A	Sample B	Control
<b>1</b>	Iron, Fe	12.10	14.10	4.3
		14.10	15.00	2.9
		13.80	13.60	3.4
		14.00	13.80	4.0
<b>2</b>	Chromium, Cr	0.33	0.49	0.36
		0.38	0.60	0.41
		0.40	0.54	0.32
		0.44	0.48	0.30
<b>3</b>	Lead, Pb	0.45	0.46	0.79
		0.37	0.43	0.44
		0.43	0.45	0.42
		0.39	0.41	0.60
<b>4</b>	Cadmium, Cd	<0.001	<0.001	<0.001
		<0.001	<0.001	<0.001
		<0.001	<0.001	<0.001
		<0.001	<0.001	<0.001
<b>5</b>	Zinc, Zn	5.58	5.66	0.77
		5.57	5.62	0.67
		5.90	5.20	0.63
		6.30	5.12	0.61
<b>6</b>	Magnesium, Mg	3.50	0.69	1.70
		3.40	0.66	1.30
		3.70	0.62	1.50
		3.90	0.61	1.40
<b>7</b>	Copper, Cu	0.77	0.78	<0.001
		0.77	0.76	<0.001
		0.78	0.80	<0.001
		0.80	0.82	<0.001

## APPENDIX B: STATISTICAL ANALYSIS

**Table B.1: Summary for all Y's (Heavy Metals)**

	<b>Copper (Cu)</b>	<b>Iron (Fe)</b>	<b>Zinc(Zn)</b>	<b>Cadmium (Cd)</b>	<b>Lead (Pb)</b>	<b>Chromium (Cr)</b>	<b>Magnesium (Mg)</b>
<b>R<sup>2</sup></b>	0.8185	0.9927	0.9953	0.8347	0.9349	0.9378	0.9997
<b>F</b>	15.2181	459.5948	715.9685	17.0436	48.4738	50.8595	11356.9
<b>Pr &gt; F</b>	< 0.0001	< 0.0001	< 0.0001	< 0.0001	< 0.0001	< 0.0001	< 0.0001
<b>Filtration process</b>	20.9543	864.8179	1058.504	51.46	164.4045	171.7839	26526.65
	< 0.0001	< 0.0001	< 0.0001	< 0.0001	< 0.0001	< 0.0001	< 0.0001
<b>Samples</b>	13.1799	696.8264	978.8792	3.1714	17.165	14.7779	5447.801
	0.0001	< 0.0001	< 0.0001	0.0579	< 0.0001	< 0.0001	< 0.0001
<b>Filtration process*Samples</b>	13.3691	138.3674	413.2453	6.7714	6.1629	8.4382	6726.583
	< 0.0001	< 0.0001	< 0.0001	0.0007	0.0012	0.0001	< 0.0001



**Table B.2: Regression of Variable (Heavy Metals)**

<b>Regression of Variable (Heavy Metals)</b>							
<b>The goodness of fit of Statistics Variable</b>	<b>Copper (Cu)</b>	<b>Iron (Fe)</b>	<b>Zinc (Zn)</b>	<b>Cadmium (Cd)</b>	<b>Lead (Pb)</b>	<b>Chromium(Cr)</b>	<b>Magnesium (Mg)</b>
<b>Observations</b>	36	36	36	36	36	36	36
<b>Sum of weights</b>	36	36	36	36	36	36	36
<b>DF</b>	27	27	27	27	27	27	27
<b>R<sup>2</sup></b>	0.8185	0.9927	0.9953	0.8347	0.9349	0.9378	0.9997
<b>Adjusted R<sup>2</sup></b>	0.7647	0.9906	0.9939	0.7857	0.9156	0.9193	0.9996
<b>MSE</b>	0.0232	0.2104	0.1527	0	0.0371	0.0019	0.0712
<b>RMSE</b>	0.1523	0.4587	0.3908	0.0057	0.1925	0.0432	0.2667
<b>DW</b>	1.4546	2.6443	2.2315	2.7	2.3732	2.1824	2.4396

MSE- Mean Square Error, RMSE-Root Mean Square Error, R<sup>2</sup>Coefficient of determination (Measure of the degree of variability in the dependent variable that is explained or explainable by the independent variables).

**Table B.3: Analysis of Variance of Variables (Heavy Metals)**

<b>N/S</b>	<b>Copper (Cu)</b>	<b>Iron (Fe)</b>	<b>Zinc (Zn)</b>	<b>Cadmium (Cd)</b>	<b>Lead (Pb)</b>	<b>Chromium (Cr)</b>	<b>Magnesium (Mg)</b>
<b>DF</b>	8	8	8	8	8	8	8
<b>Error</b>	27	27	27	27	27	27	27
<b>Corrected Total</b>	35	35	35	35	35	35	35
<b>Sum of squares</b>	2.8239	773.5593	874.8074	0.0044	14.3698	0.7584	6464.5181
<b>Error</b>	±0.6263	±5.6806	±4.1238	±0.0009	±01.0005	±0.0503	±1.9211
<b>Corrected Total</b>	3.4502	779.2399	878.9312	0.0053	15.3703	0.8087	6464.5181
<b>Mean squares</b>	0.3530	96.6949	109.3509	0.0006	1.7962	0.0948	808.0648
<b>Error</b>	±0.0232	±0.2104	±0.1527	±0.0000	±0.0371	±0.0019	±0.0712
<b>F</b>	15.2181	459.5948	715.9685	17.0436	48.4738	50.8595	11356.9041
<b>Pr &gt; F</b>	< 0.0001	< 0.0001	< 0.0001	< 0.0001	< 0.0001	< 0.0001	< 0.0001

**Table B.4:Summary (LS means) - Filtration process:**

<b>N/S</b>	<b>Copper (Cu)</b>	<b>Iron (Fe)</b>	<b>Zinc (Zn)</b>	<b>Cadmium (Cd)</b>	<b>Lead (Pb)</b>	<b>Chromium (Cr)</b>	<b>Magnesium (Mg)</b>
<b>Before filtration</b>	0.1236	3.1675	11.2942	0.0233	1.1900	0.4183	22.9417
<b>Filtration with Coconut Shell</b>	0.5236	10.4250	3.9692	0.0009	0.4700	0.4208	1.9150
<b>Filtration with Palm Kernel</b>	0.3625	4.3500	8.0500	0.0058	1.8950	0.1367	0.5850

**Table B.5:Summary (LS means) - Filtration process\*Samples**

<b>N/S</b>	<b>Copper (Cu)</b>	<b>Iron, Fe</b>	<b>Zinc, Zn</b>	<b>Cadmium, Cd</b>	<b>Lead (Pb)</b>	<b>Chromium (Cr)</b>	<b>Magnesium (Mg)</b>
<b>Before filtration*Sample B</b>	0.2200	3.3500	14.5750	0.0300	1.5250	0.4450	21.4750
<b>Before filtration*Sample A</b>	0.1500	4.6500	16.4750	0.0200	1.0450	0.4000	5.4500
<b>Filtration with Palm Kernel *Sample A</b>	0.4000	8.5000	10.3750	0.0175	1.6475	0.2100	0.9000
<b>Filtration with Coconut Shell*Sample B</b>	0.7900	14.1250	5.4000	0.0009	0.4375	0.5275	0.6450
<b>Filtration with Coconut Shell*Sample A</b>	0.7800	13.5000	5.8375	0.0009	0.4100	0.3875	3.6250
<b>Before filtration*Control</b>	0.0009	1.5025	2.8325	0.0200	1.0000	0.4100	41.9000
<b>Filtration with Palm Kernel *Sample B</b>	0.2300	3.4000	5.4500	0.0000	2.3875	0.1350	0.5050
<b>Filtration with Palm Kernel *Control</b>	0.4575	1.1500	8.3250	0.0000	1.6500	0.0650	0.3500
<b>Filtration with Coconut Shell*Control</b>	0.0009	3.6500	0.6700	0.0009	0.5625	0.3475	1.4750

## APPENDIX C: GRAPHS / ISOTHERMS (HEAVY METALS)

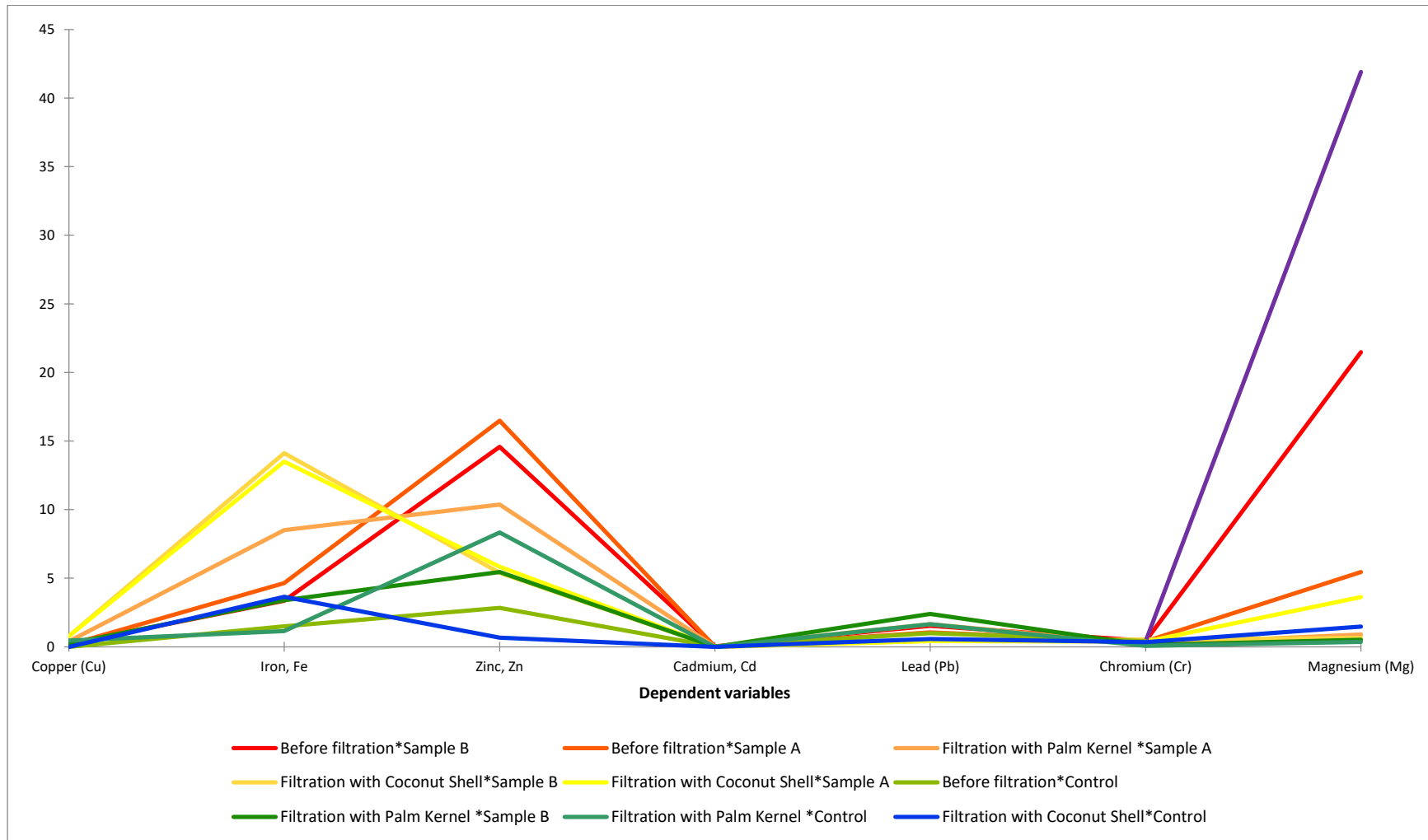
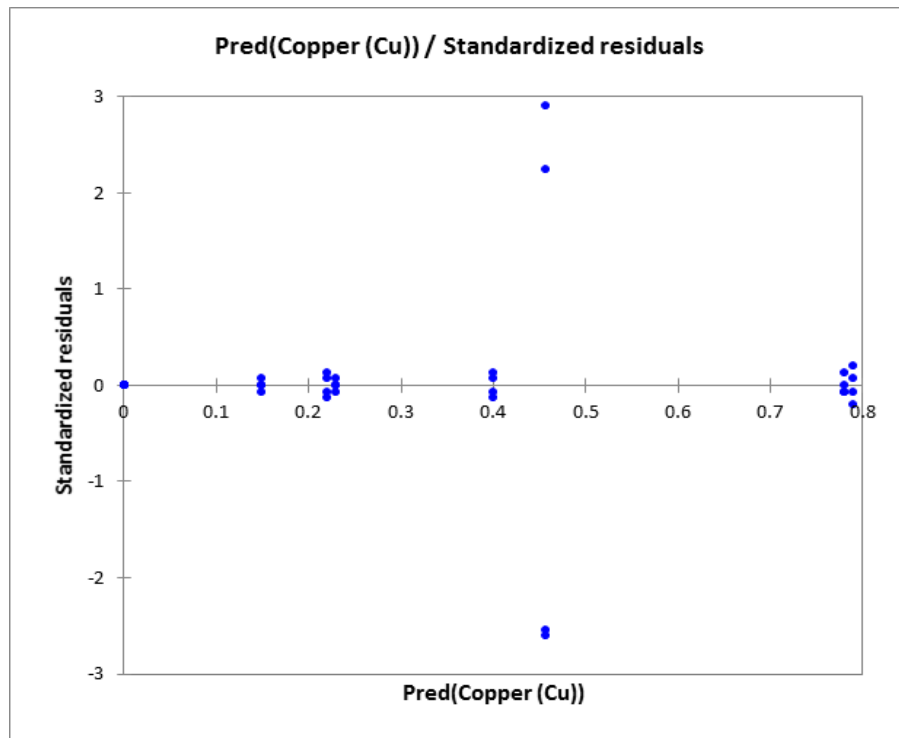
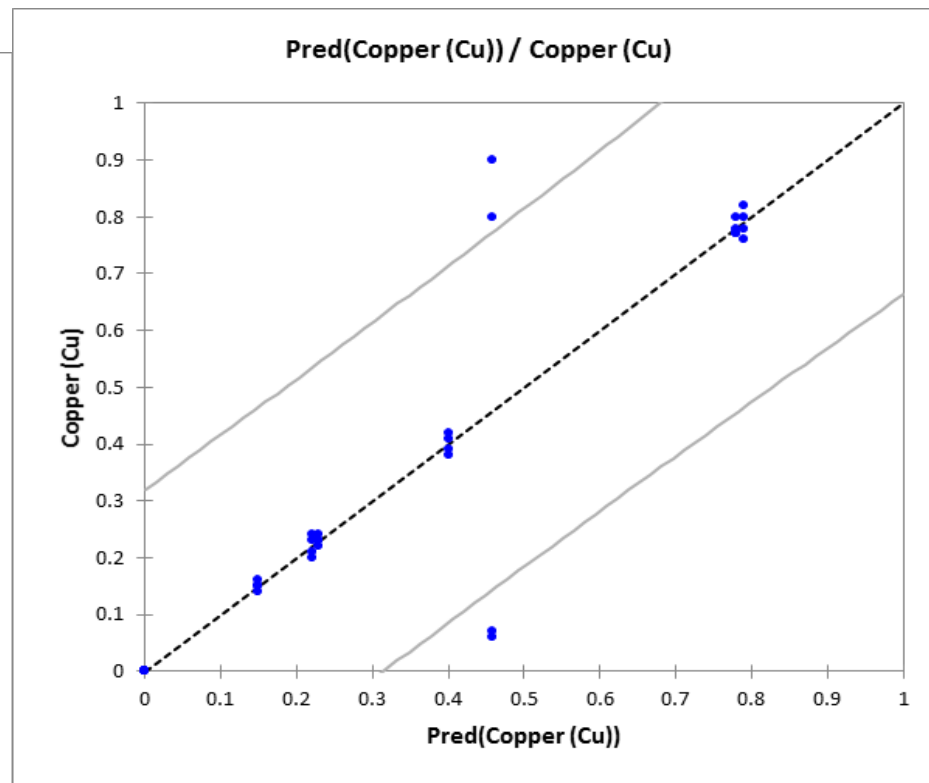


Figure C.1: Summary (LS means) - Filtration process\*Samples



**Figure C.2a: Pred(Copper (Cu))/Standardized residuals**



**Figure C.2b: Pred(Copper (Cu))/copper**

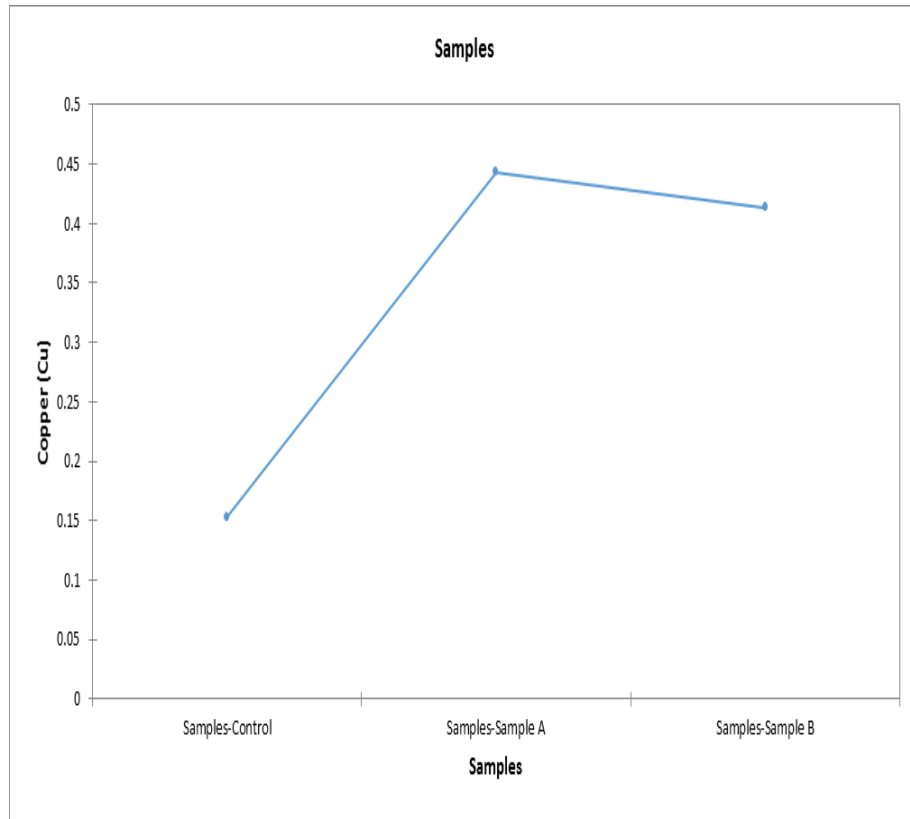


**Figure C.3a: Copper Samples**

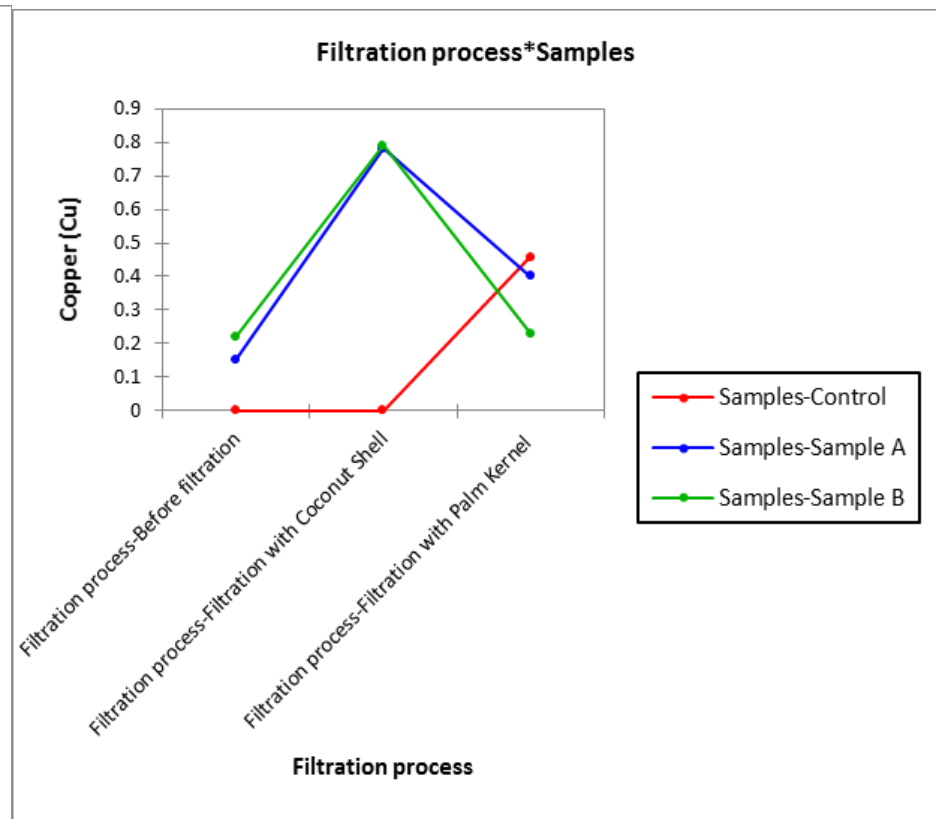


**Figure C.3b: Filtration process\* Copper Samples**

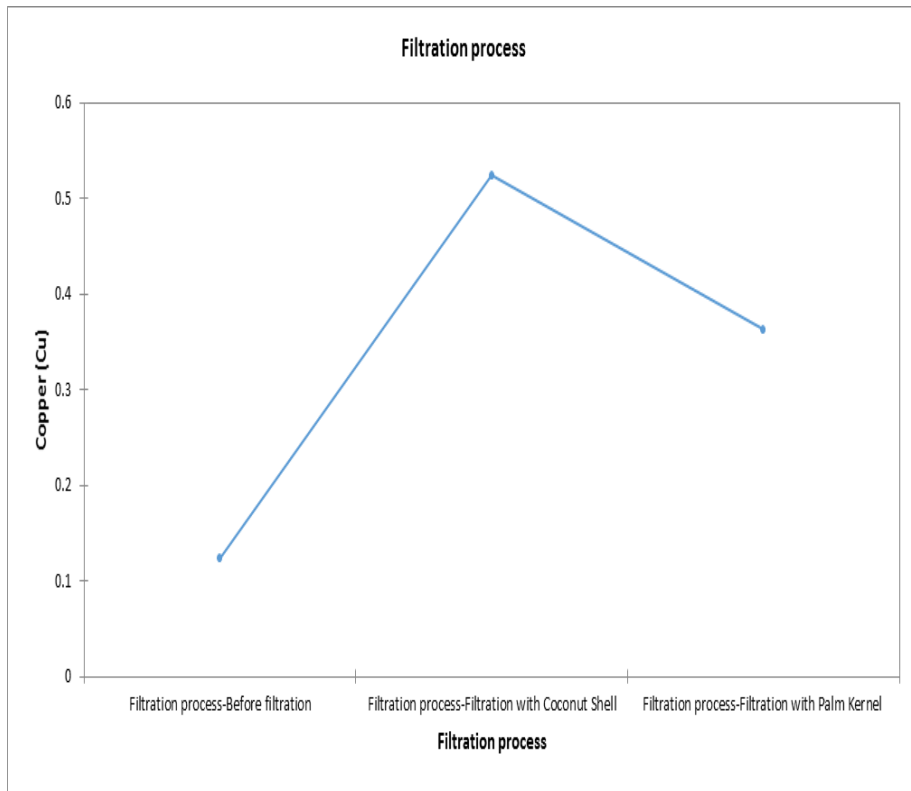


Figure C.4a: Filtration process

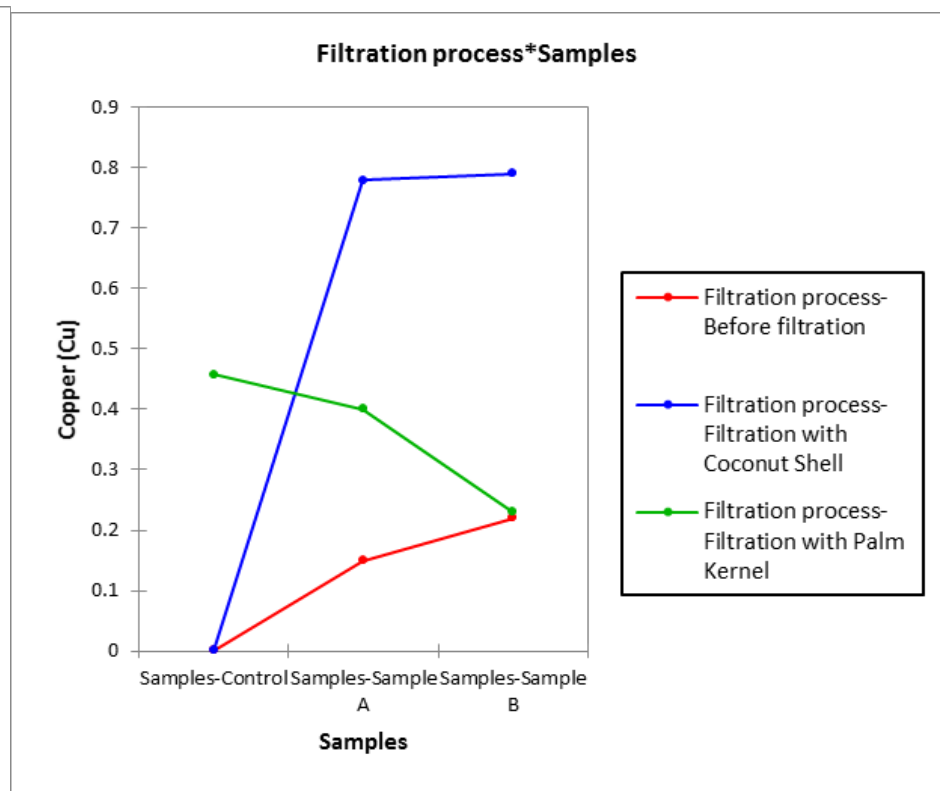
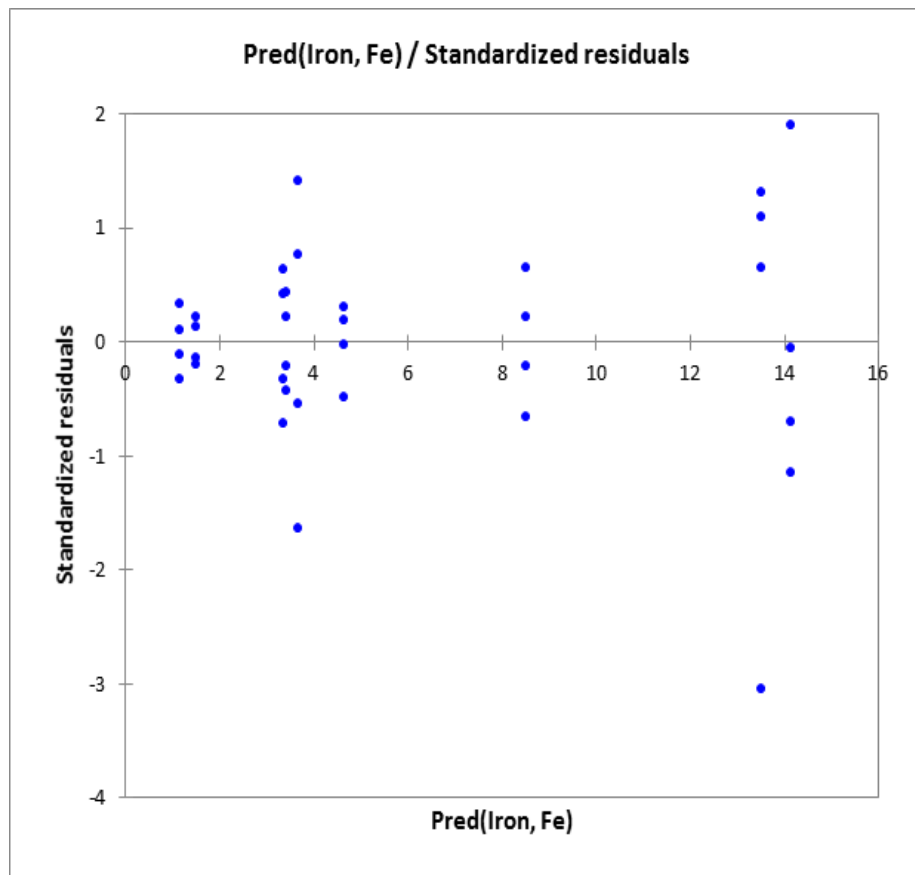
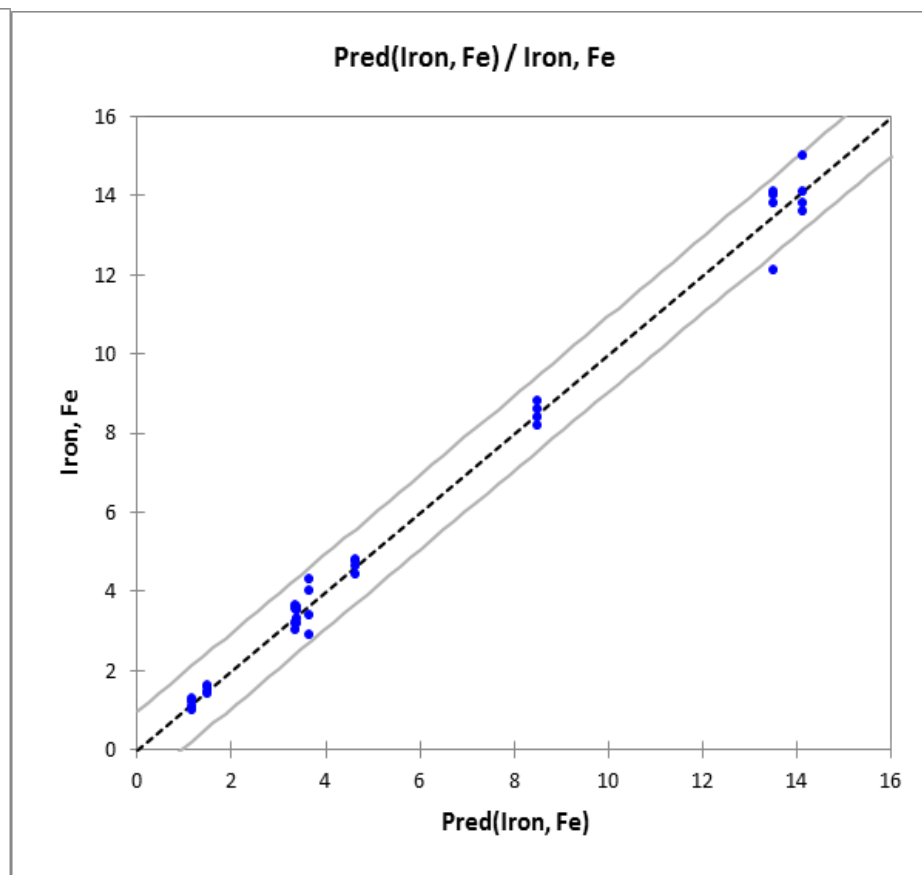


Figure C.4b: Filtration process\* Copper Samples





**Figure C.5a: Pred(Iron (Fe))/Standardized residuals**



**Figure C.5b: Pred(Iron (Fe))/ iron**

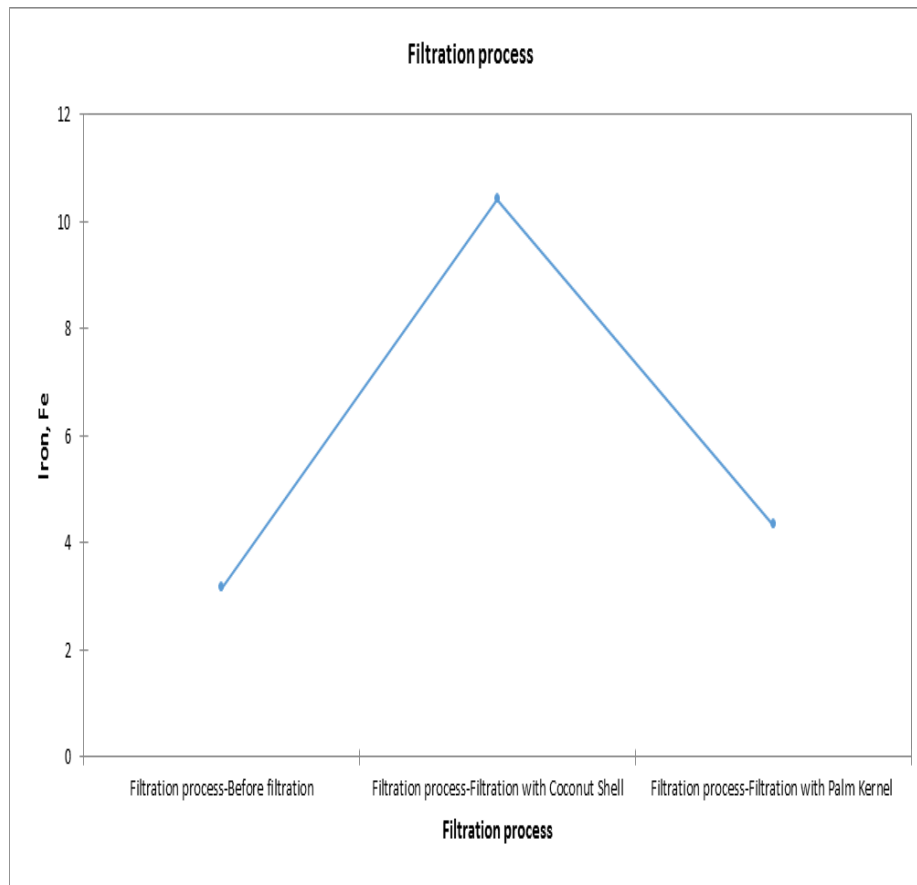


**Figure C.6a: Iron Samples**

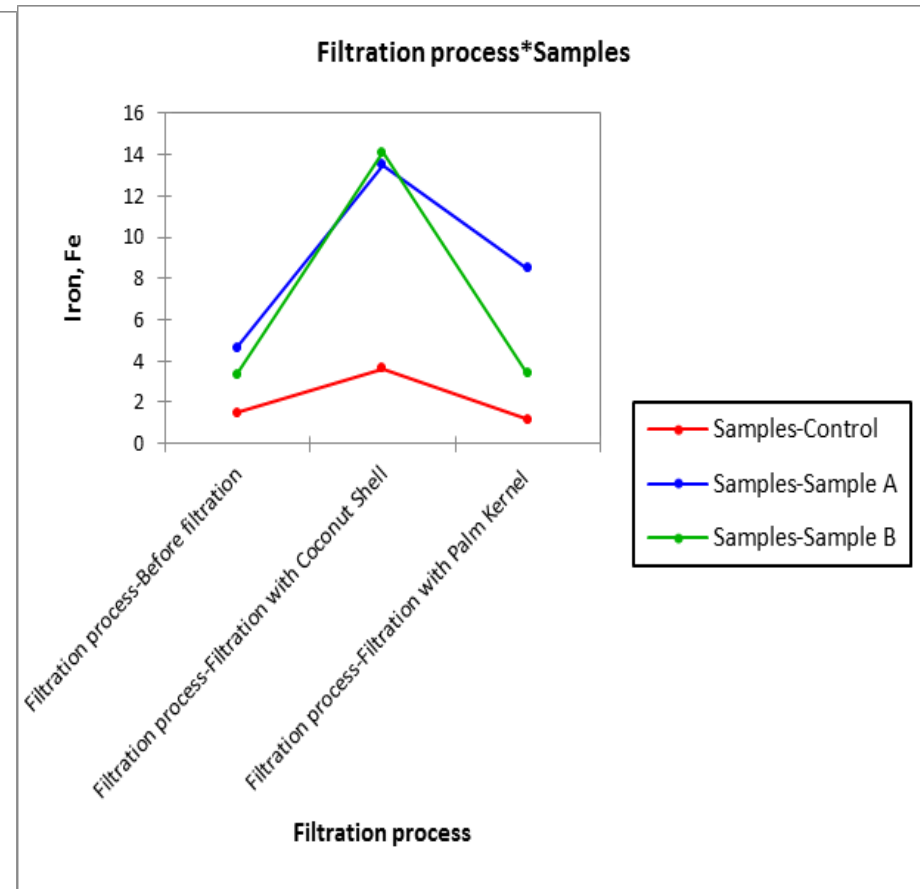


**Figure C.6b: Filtration process\* Iron Samples**

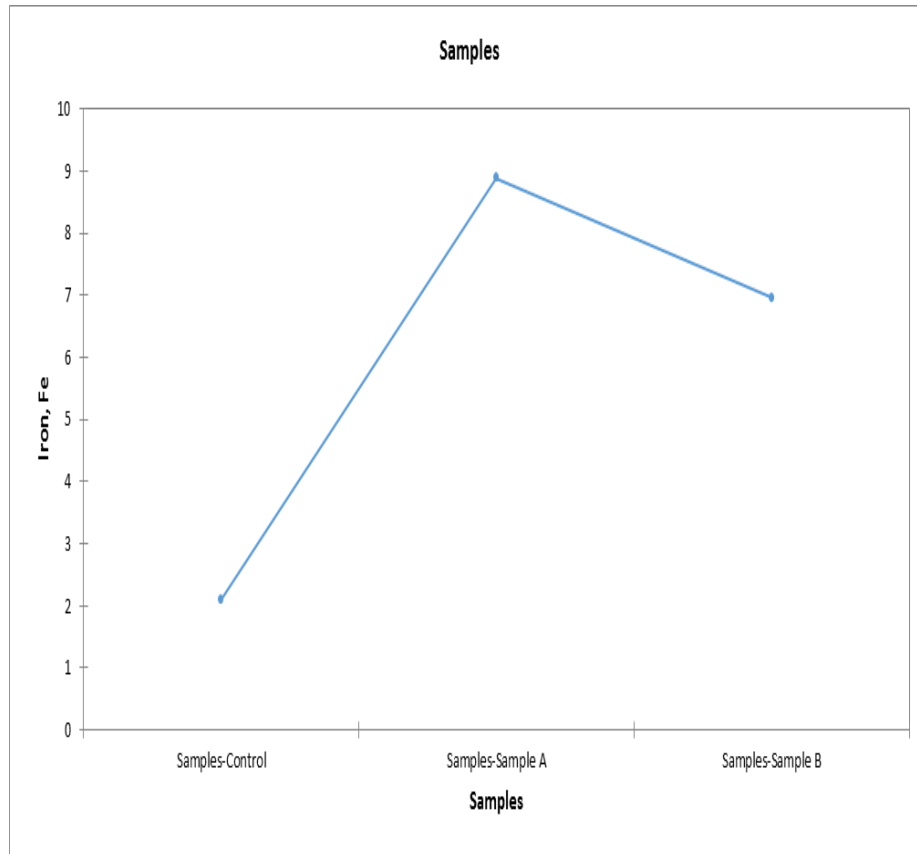


**Figure C.7a: Filtration process**

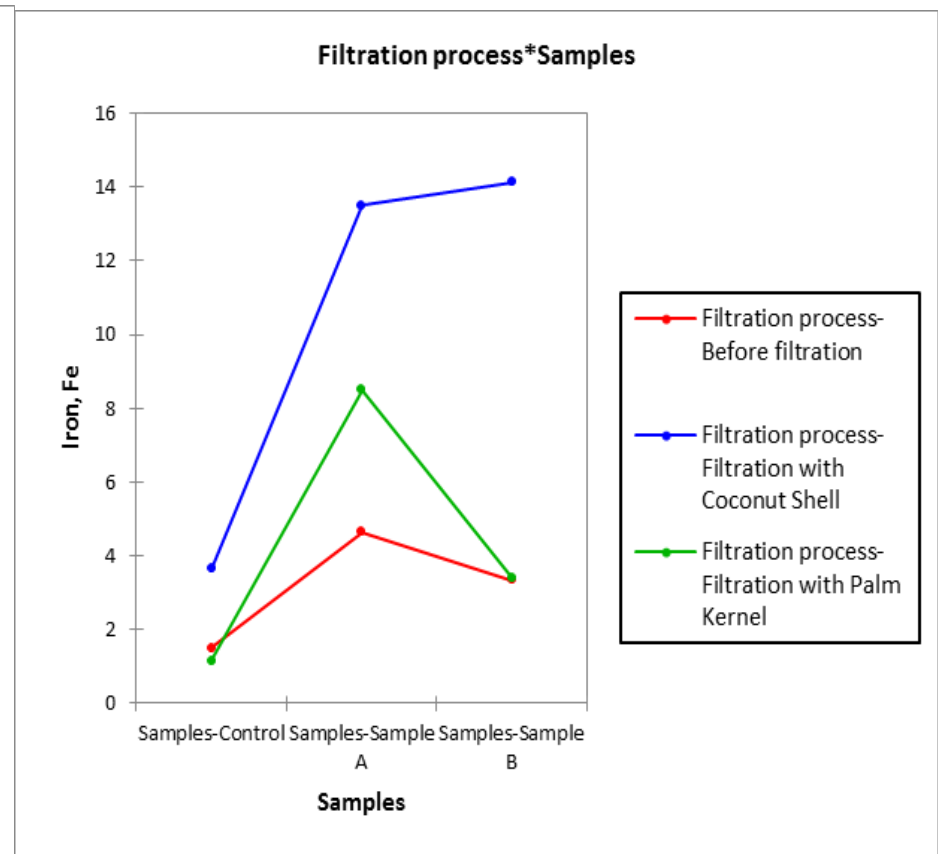


**Figure C.7b: Filtration process\* Iron Samples**

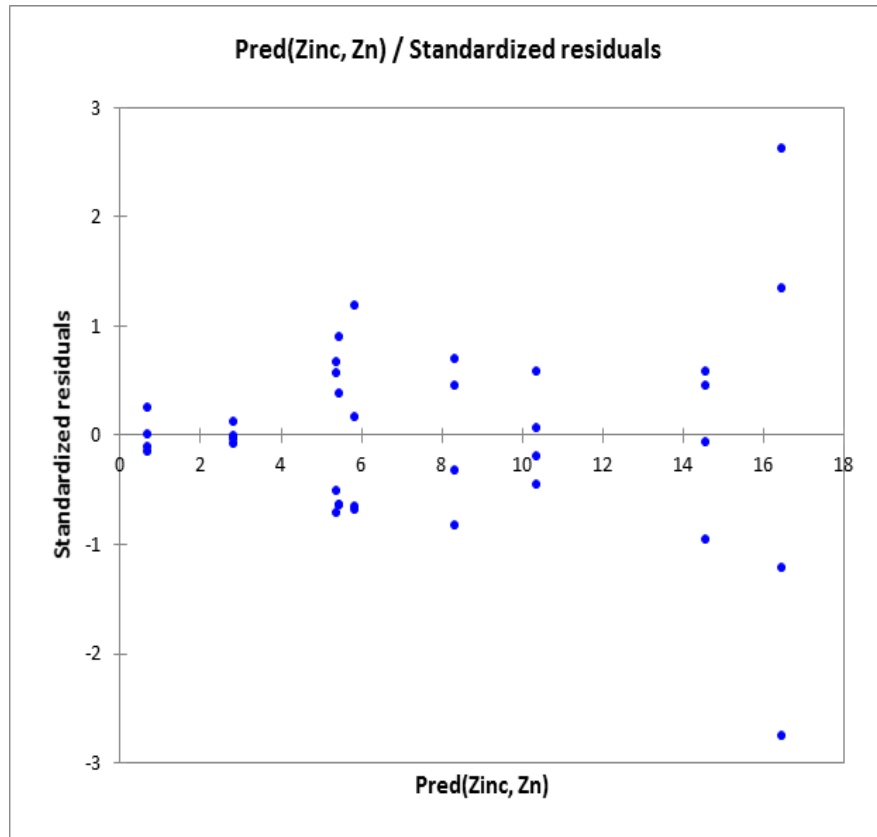


**Figure C.8a: Pred(Zinc (Zn))/Standardized residuals**

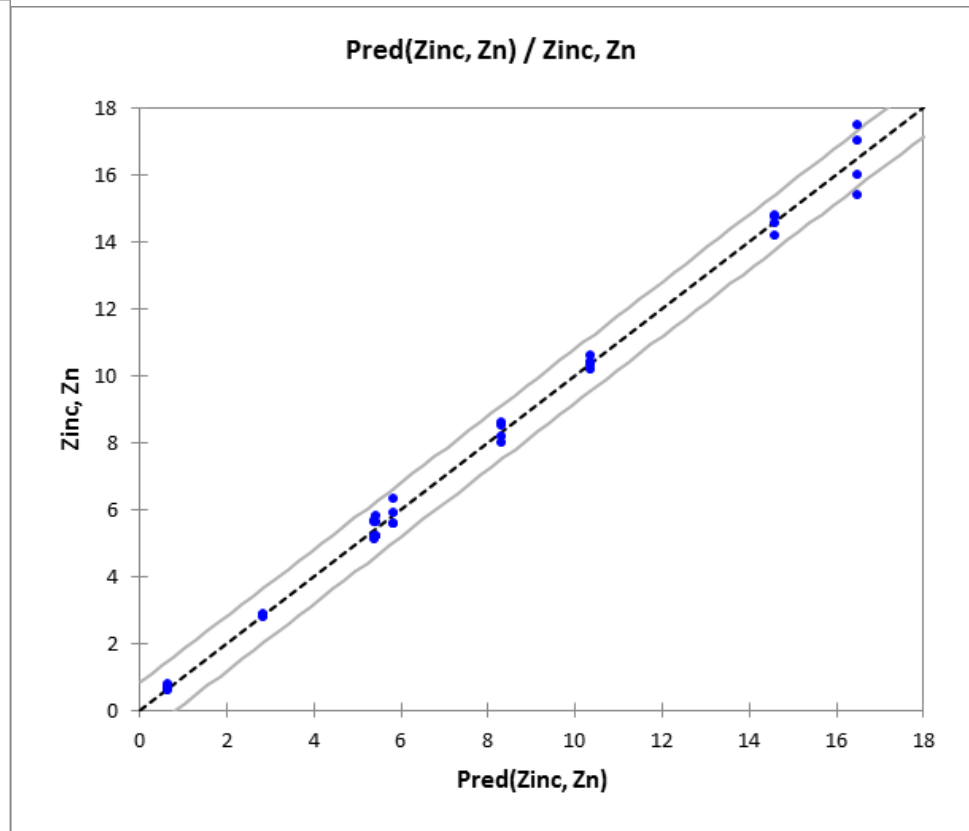


**Figure C.8b: Pred(Zinc (Zn))/ zinc**

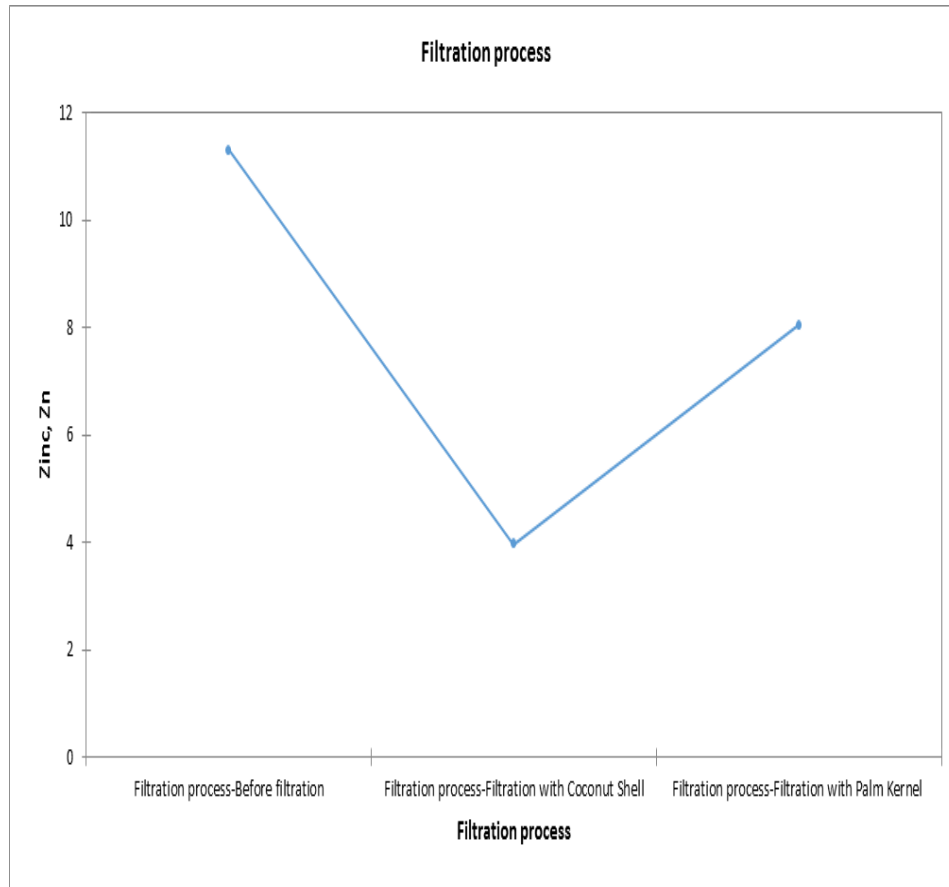


Figure C.9a: Zinc Samples

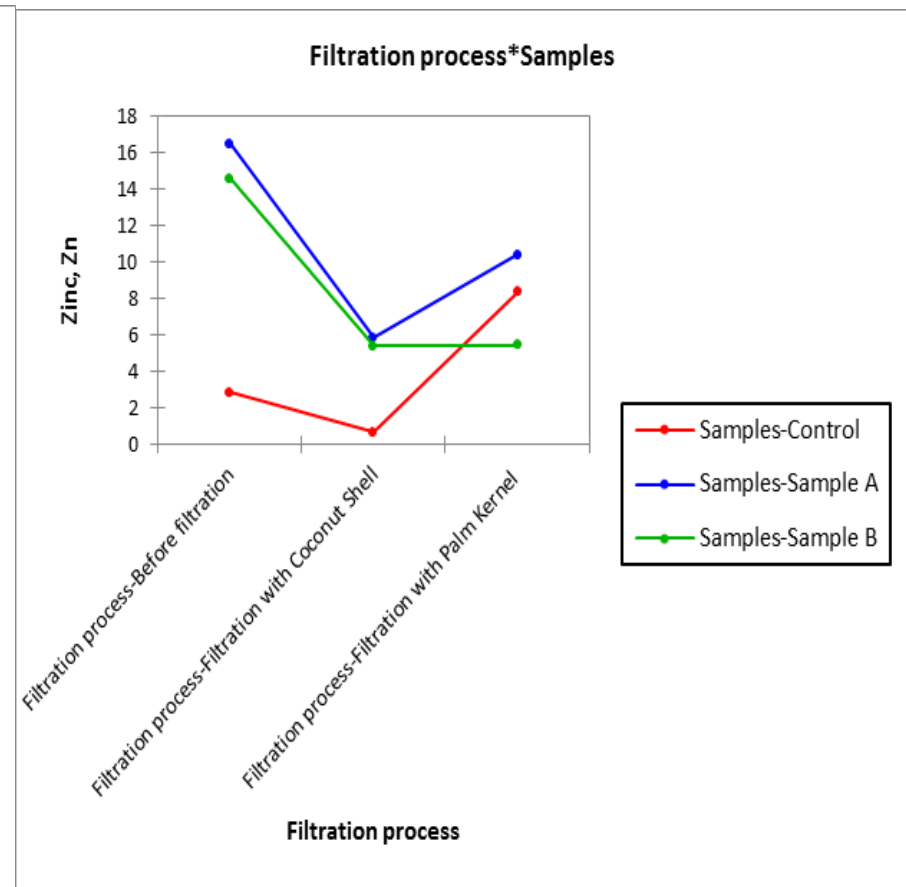
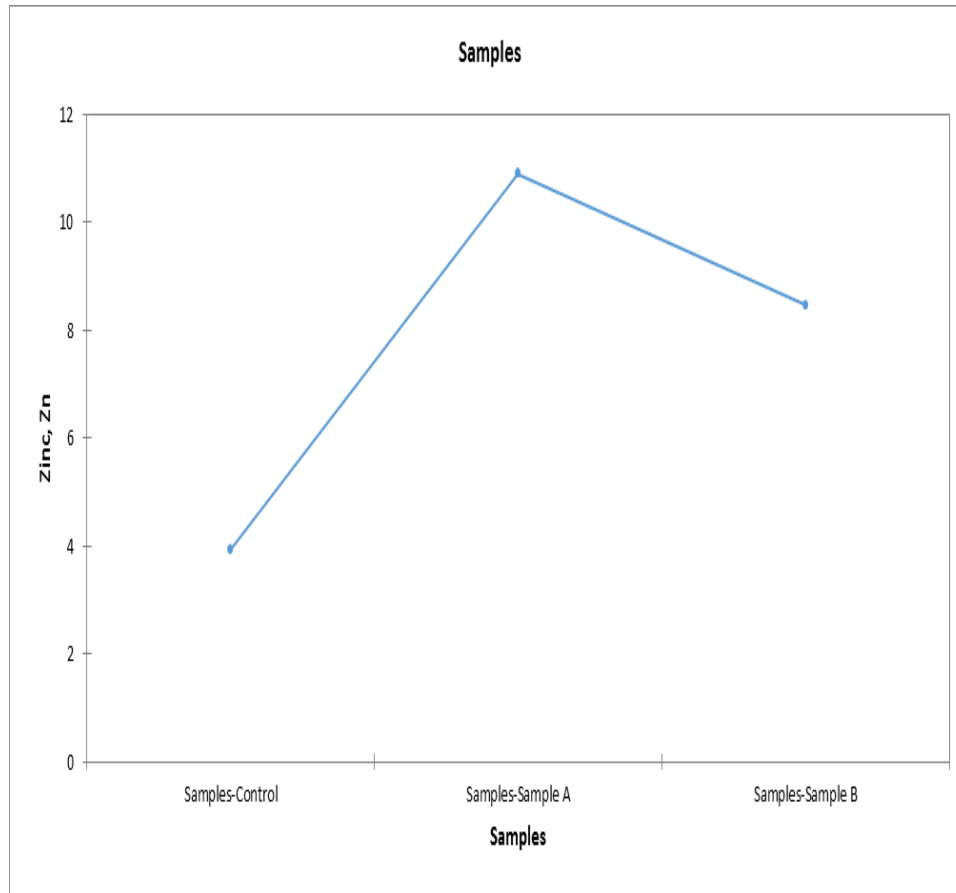
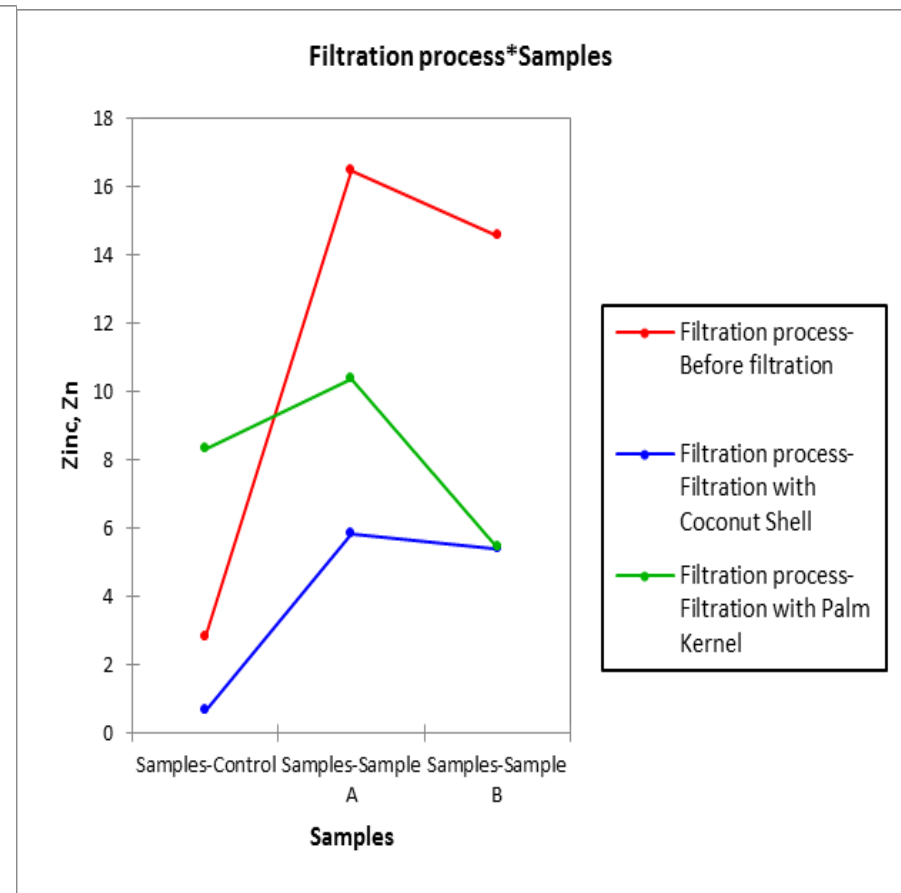


Figure C.9b: Filtration process\* Zinc Samples



**Figure C.10a: Filtration process**



**Figure C.10b: Filtration process\* Zinc Samples**

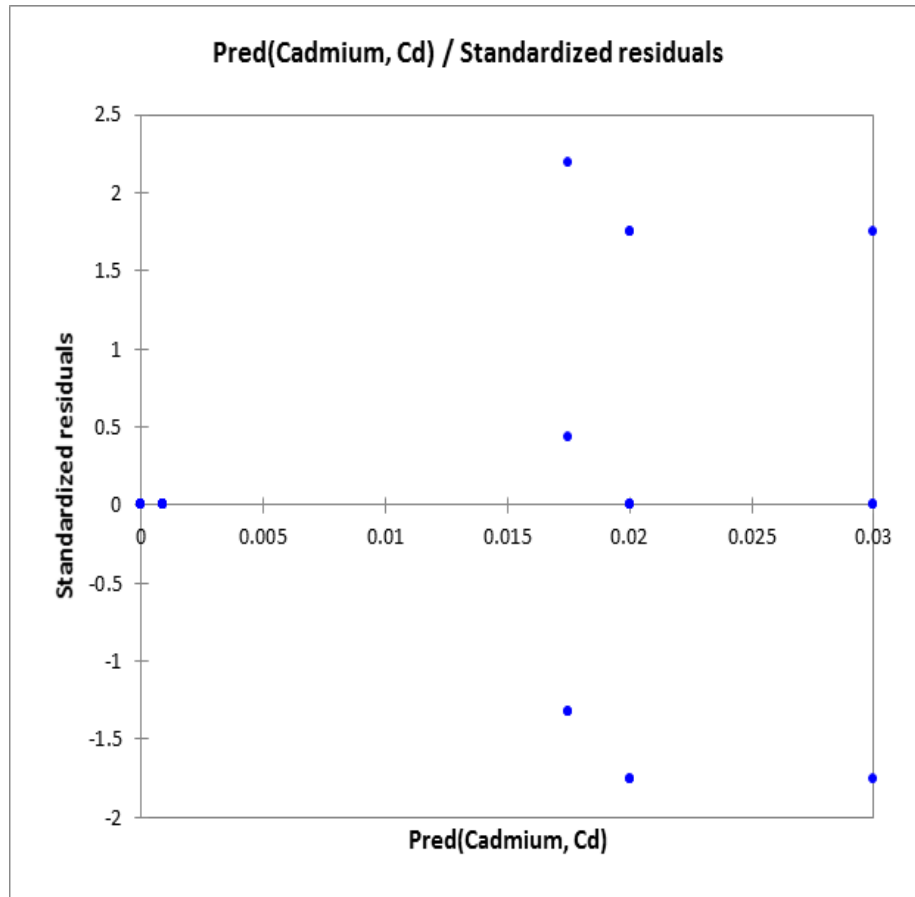


**Figure C.11a: Pred(Cadmium (Cd))/Standardized residuals**

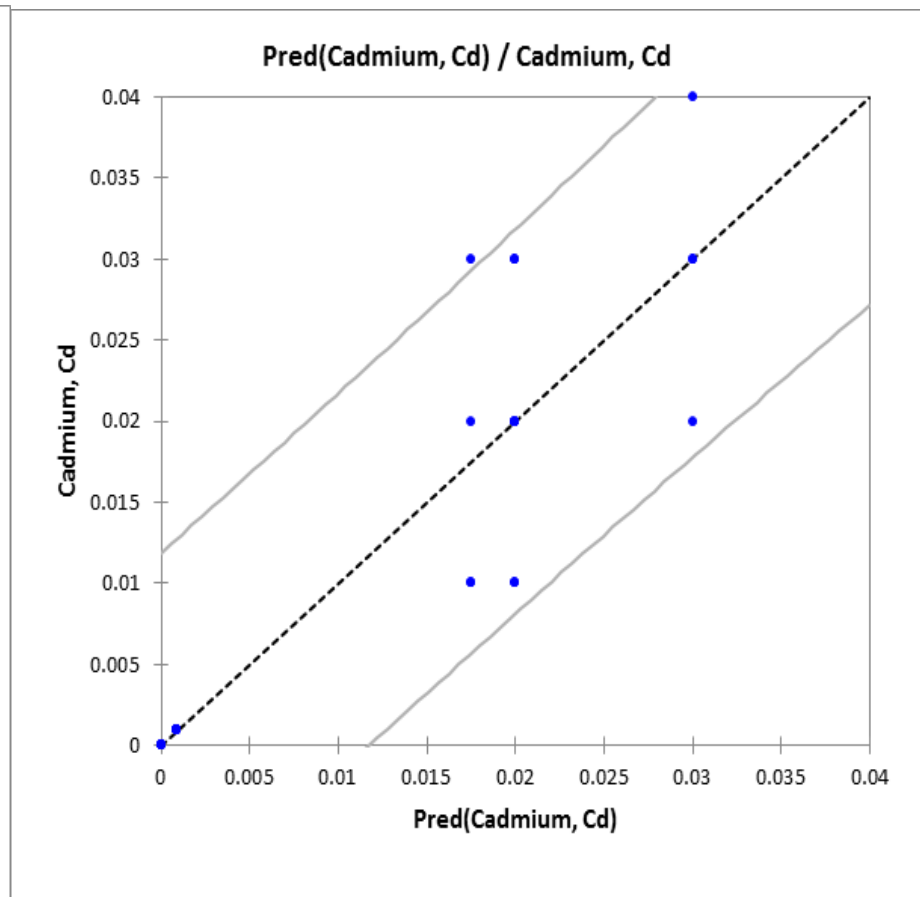


**Figure C.11b: Pred(Cadmium (Cd))/ cadmium**

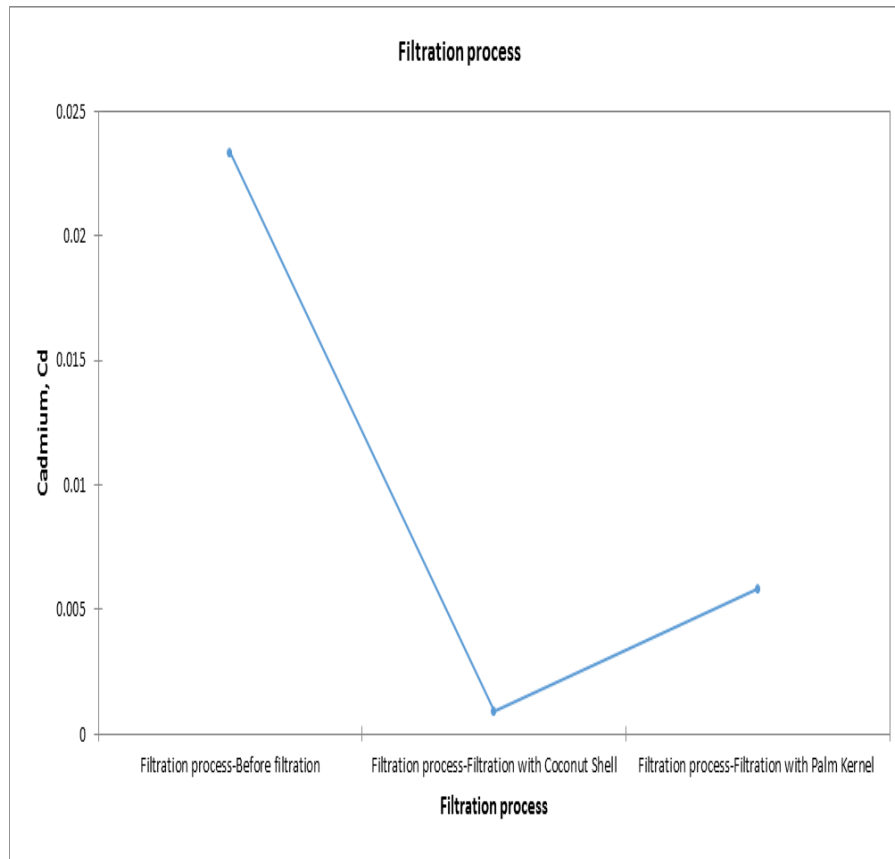


**Figure C.12a: Cadmium Samples**

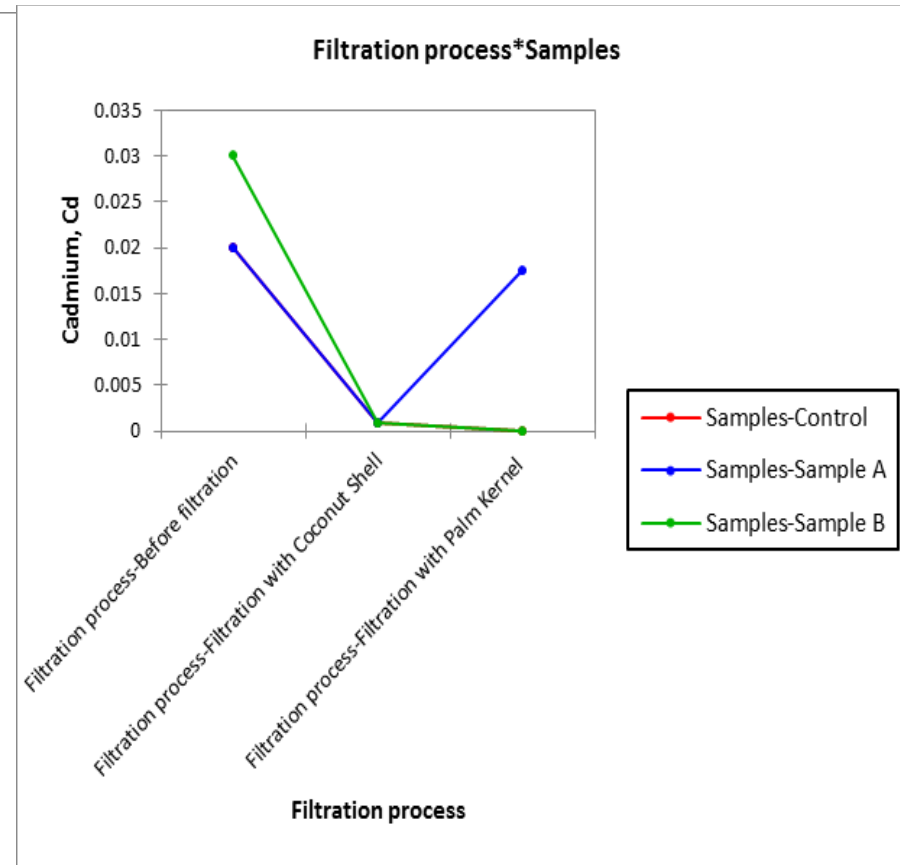


**Figure C.12b: Filtration process\* Cadmium Samples**



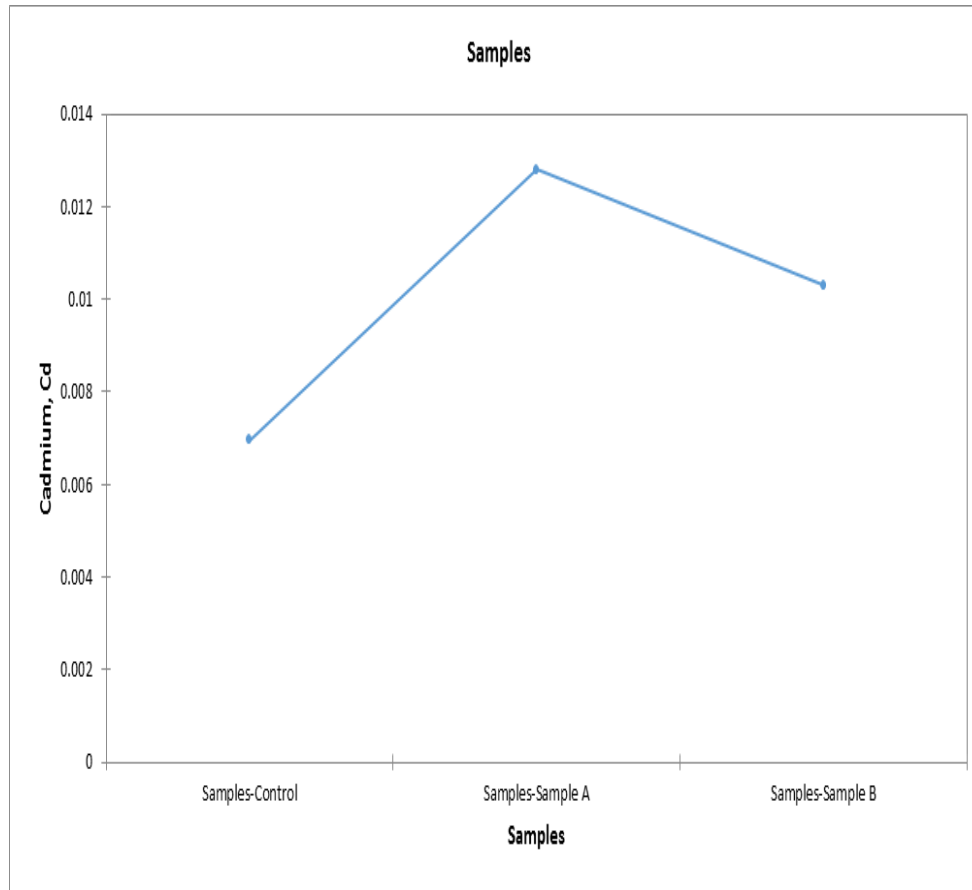


**Figure C.13a: Filtration process**

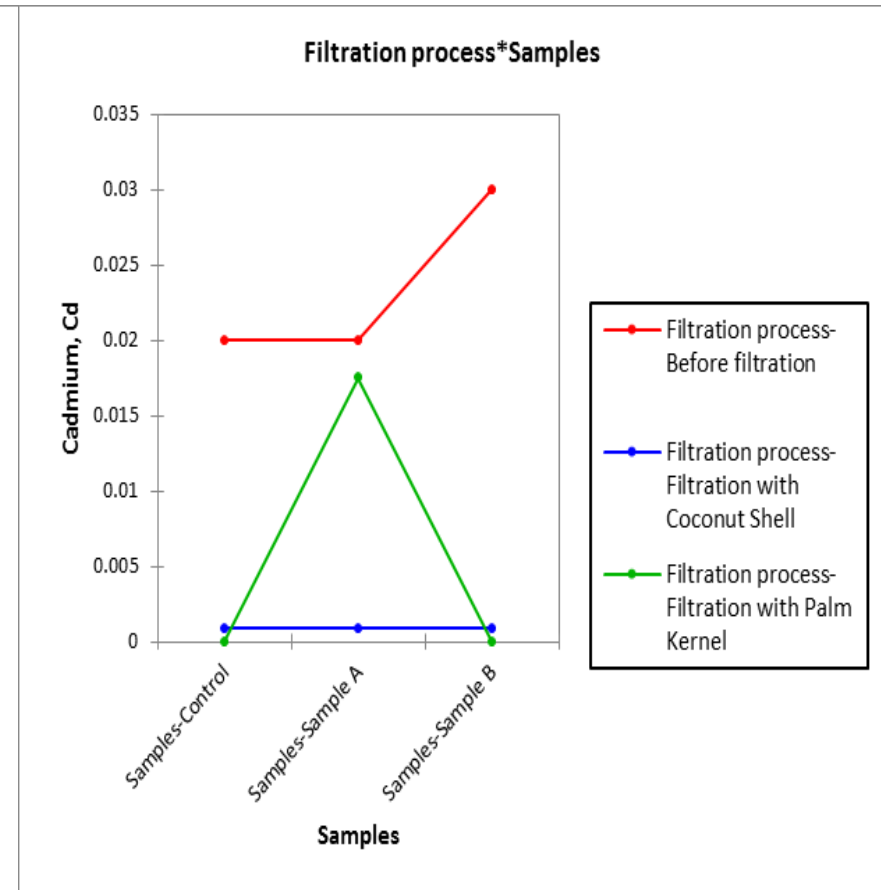


**Figure C.13b: Filtration process\* Cadmium Samples**

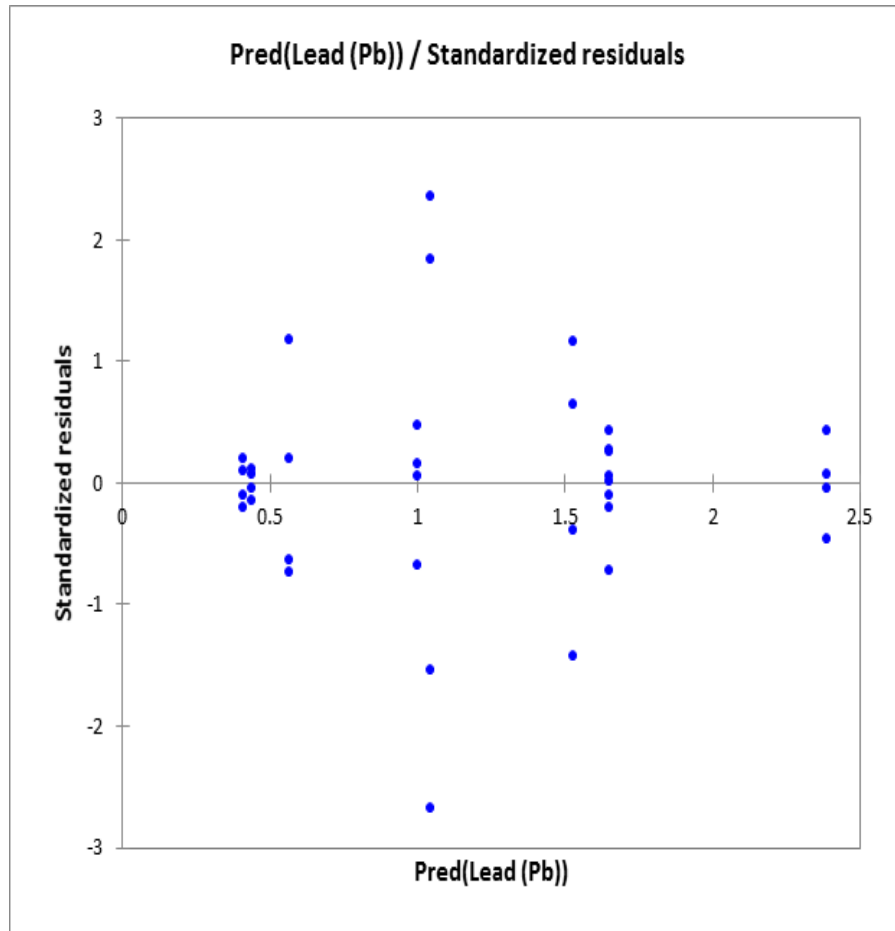


**Figure C.14a: Pred(Lead (Pb))/Standardized residuals**

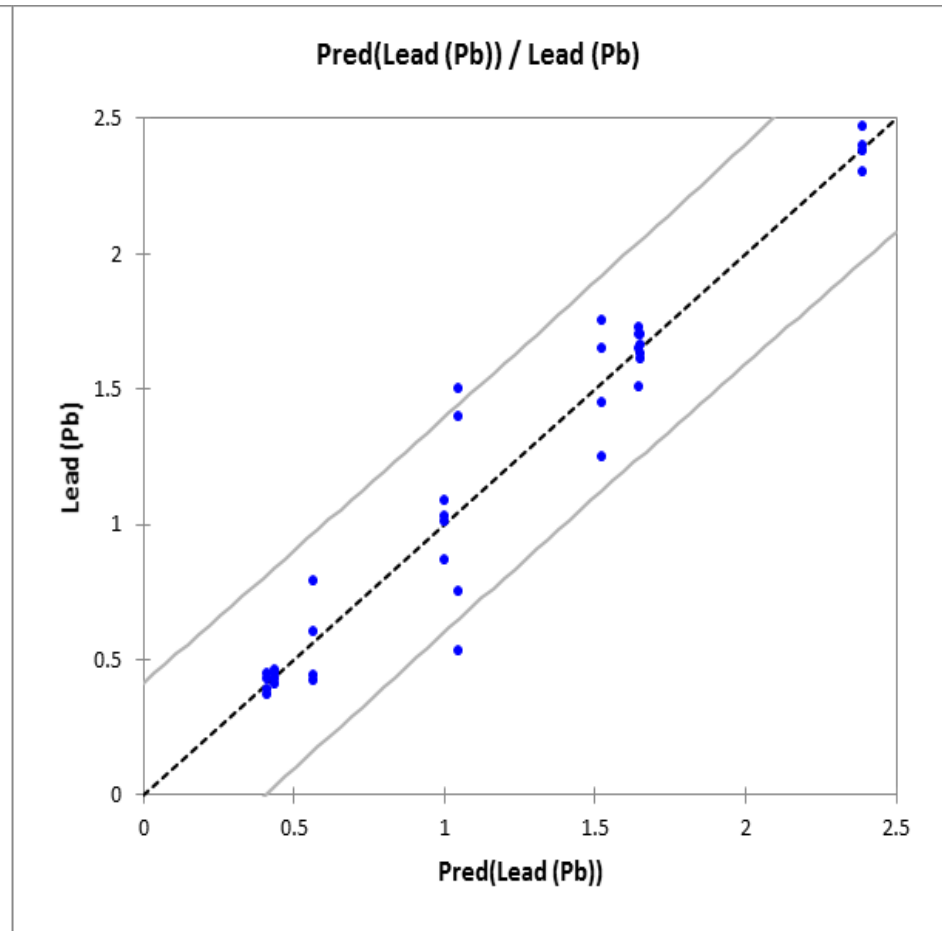


**Figure C.14b: Pred(Lead (Pb))/ lead**

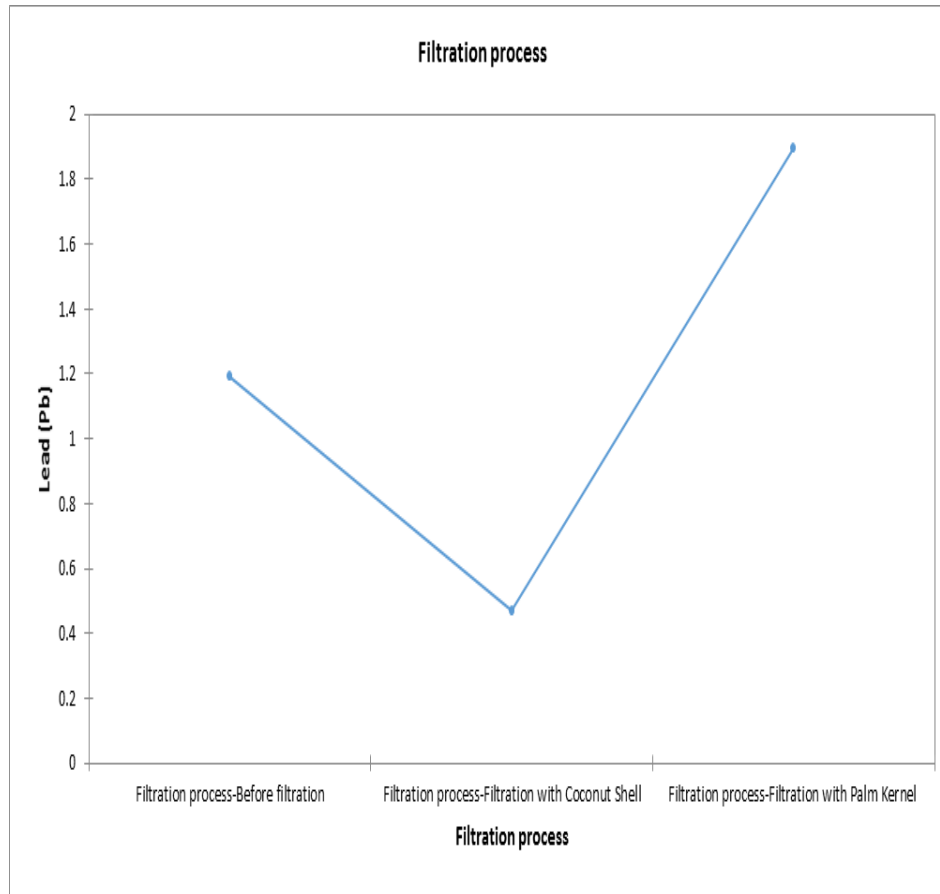


**Figure C.15a: Lead Samples**

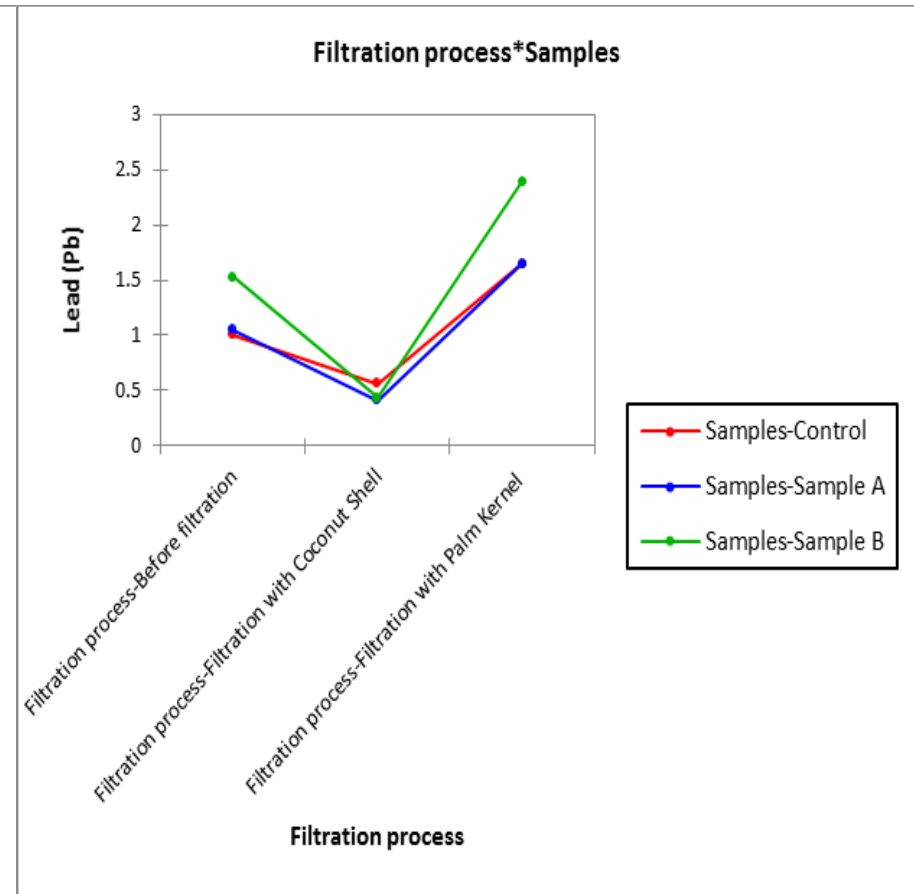


**Figure C.15b: Filtration process\* Lead Samples**

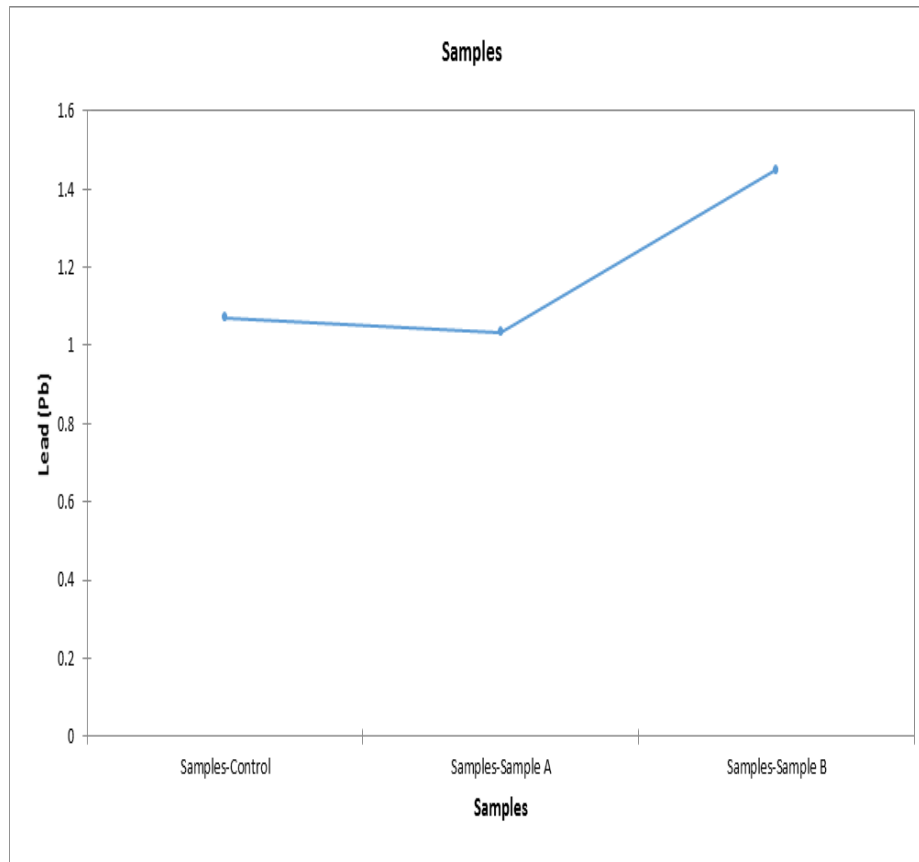


**Figure C.16a: Filtration process**

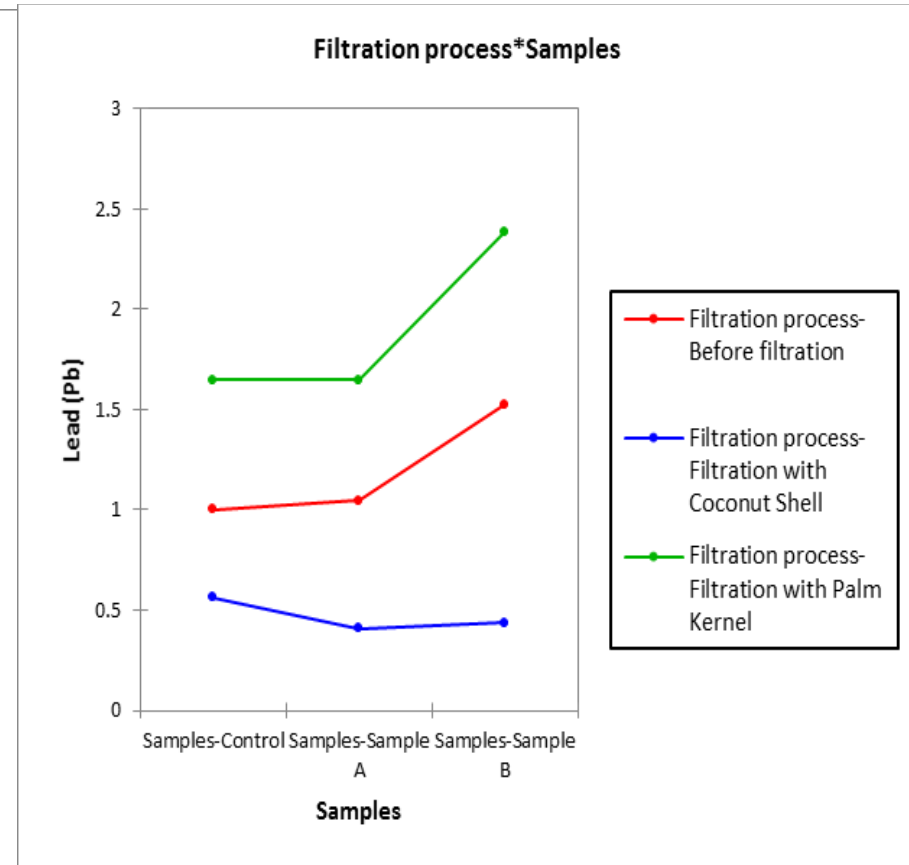


**Figure C.16b: Filtration process\* lead Samples**

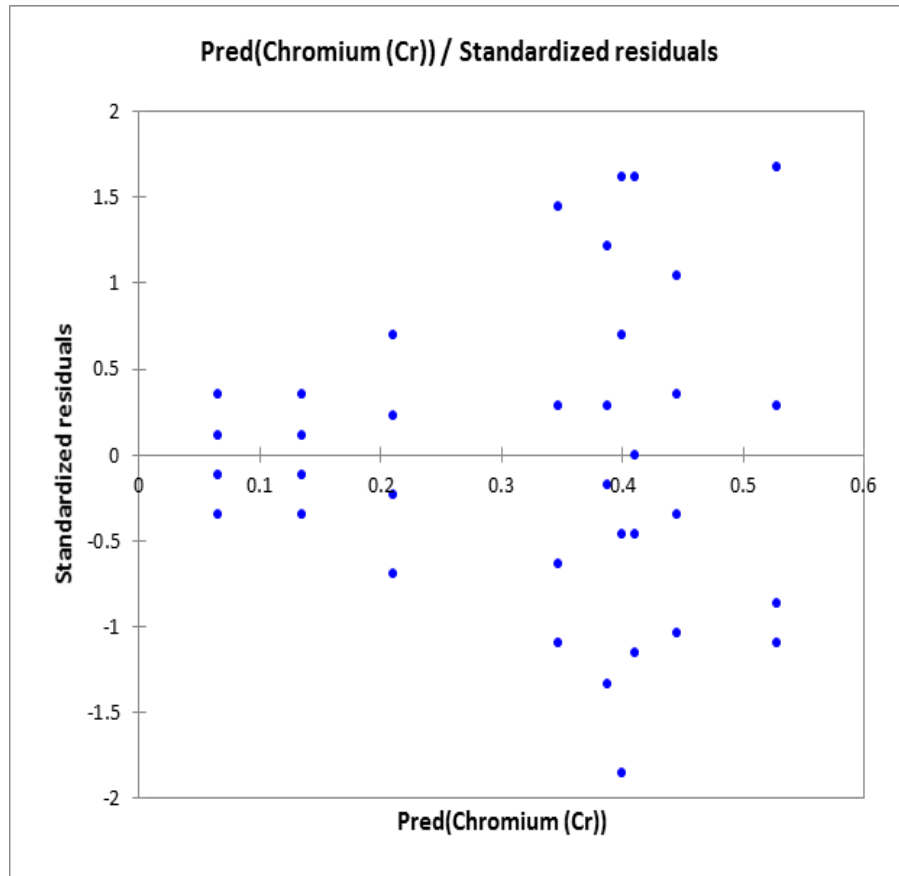


**Figure C.17a: Pred(Chromium (Cr))/Standardized residuals**

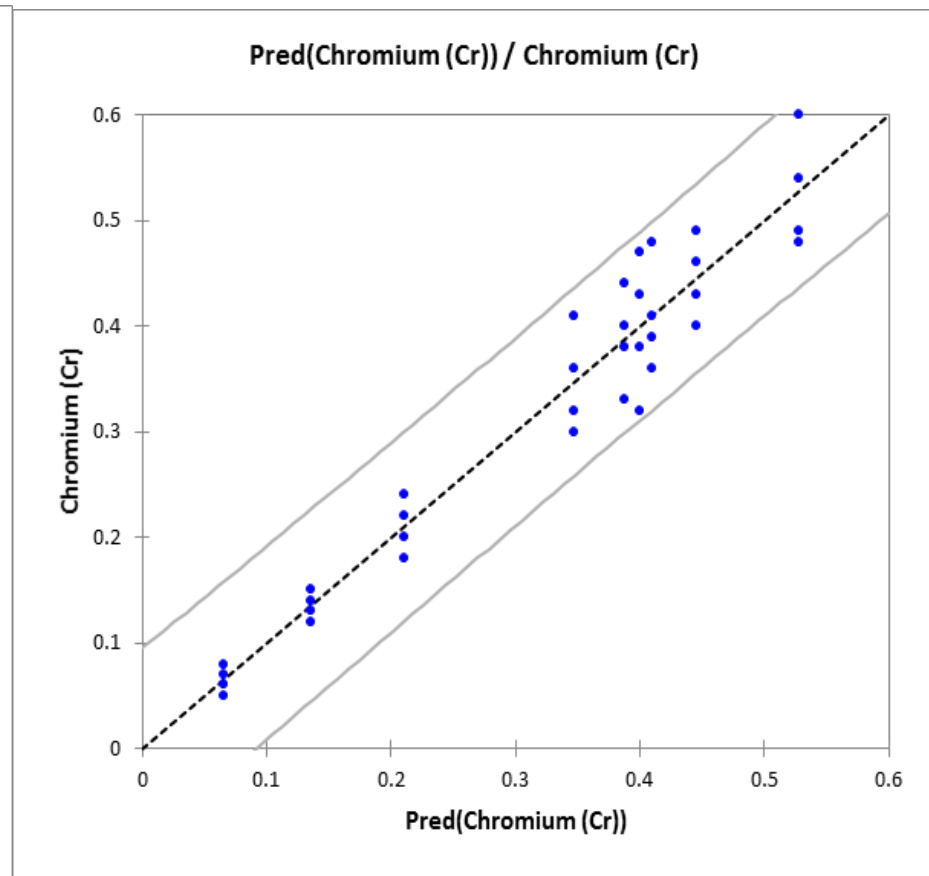


**Figure C.17b: Pred(Chromium (Cr))/ chromium**

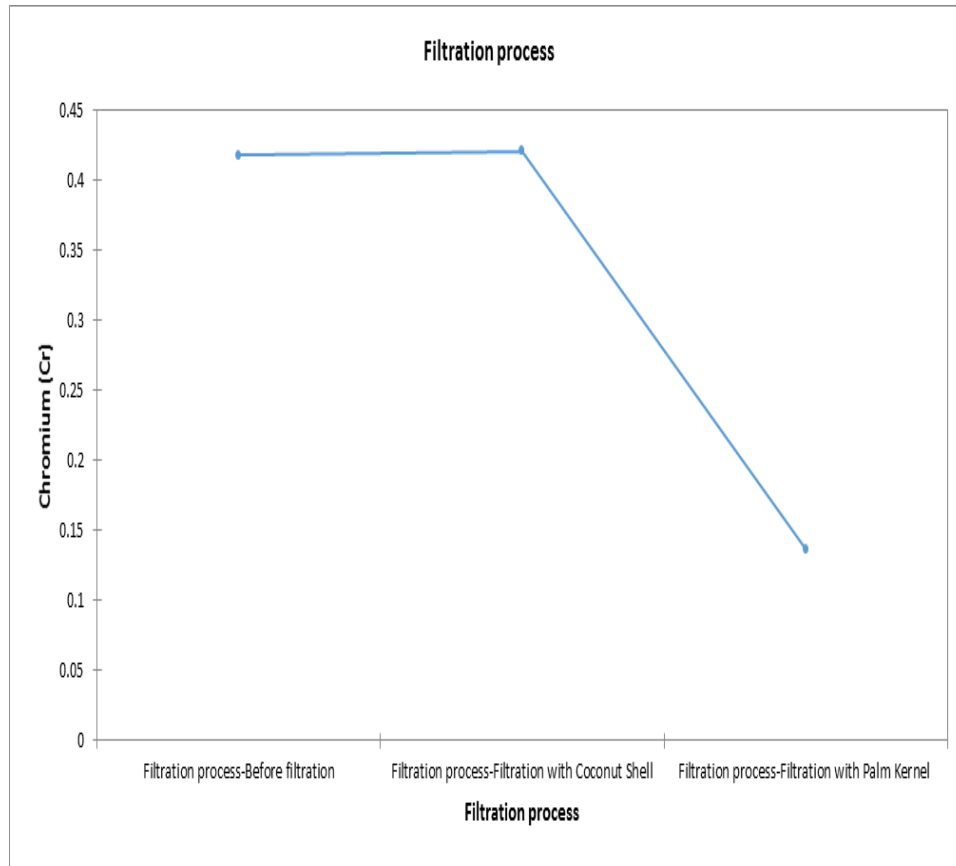


**Figure C.18a: Chromium Samples**

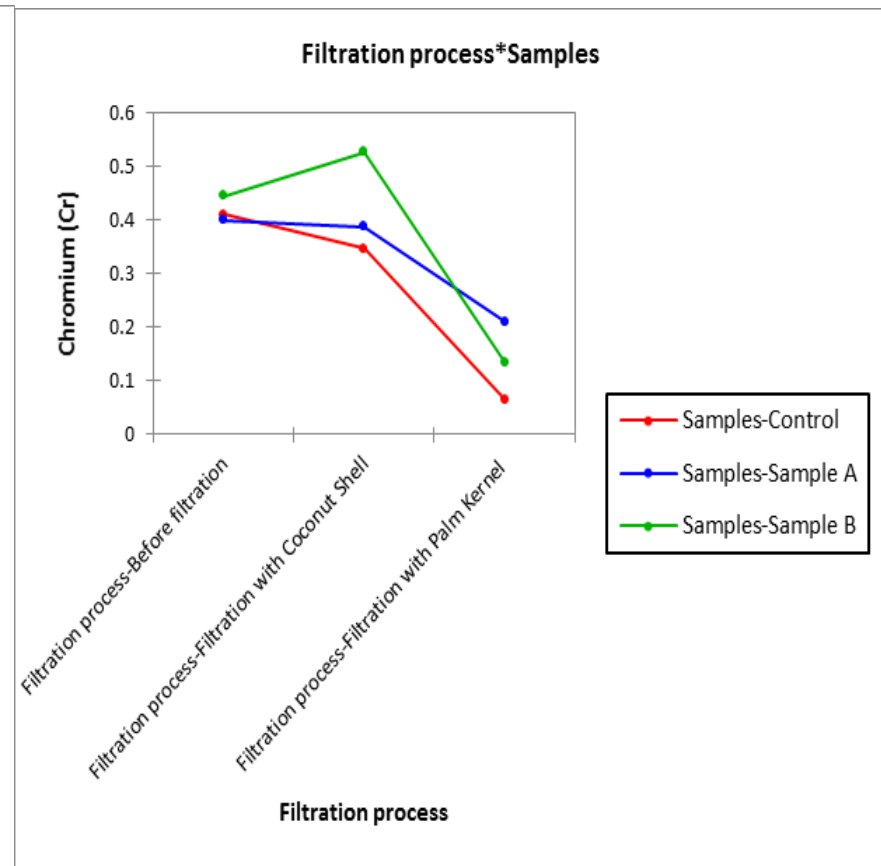


**Figure C.18b: Filtration process\* Chromium**

**Samples**

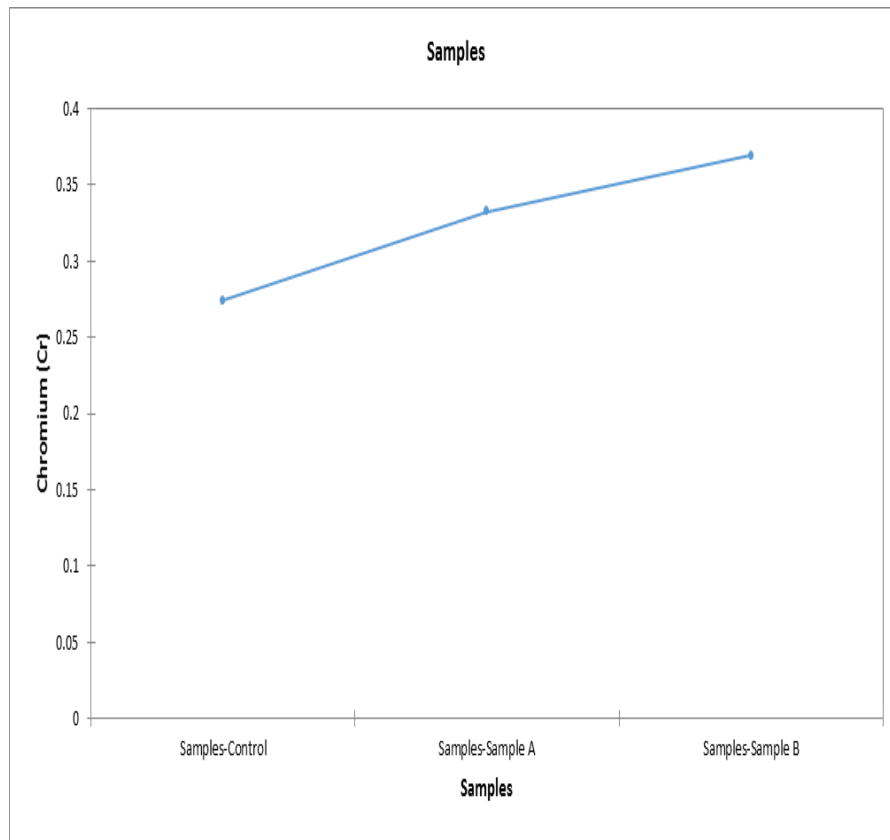


**Figure C.19a: Filtration process**

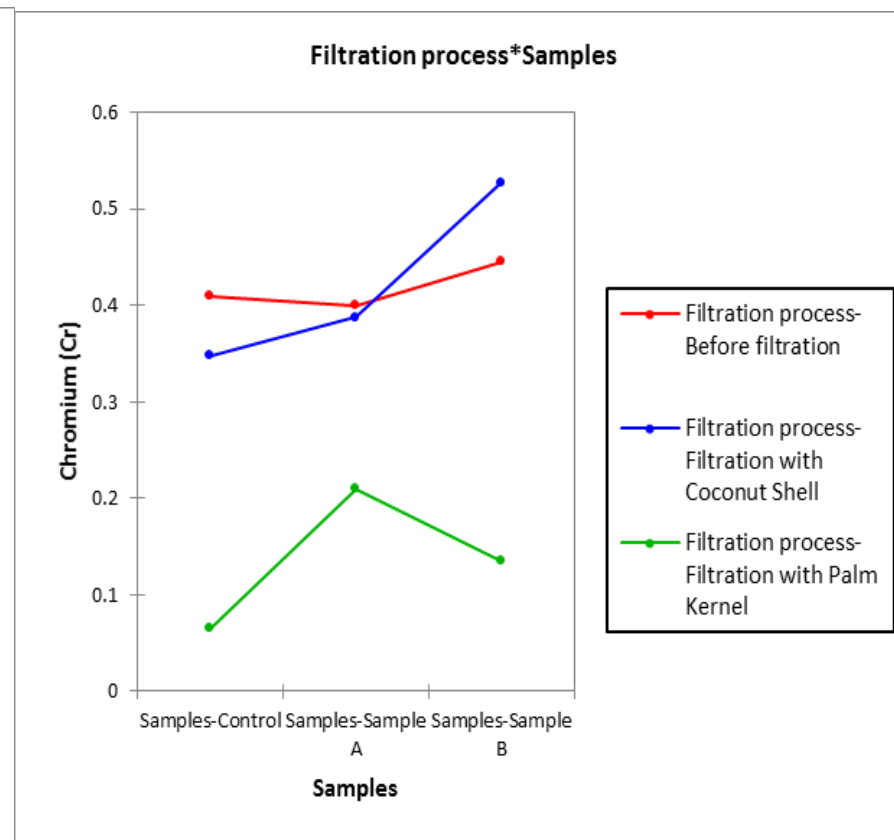


**Figure C.19b: Filtration process\* Chromium Samples**

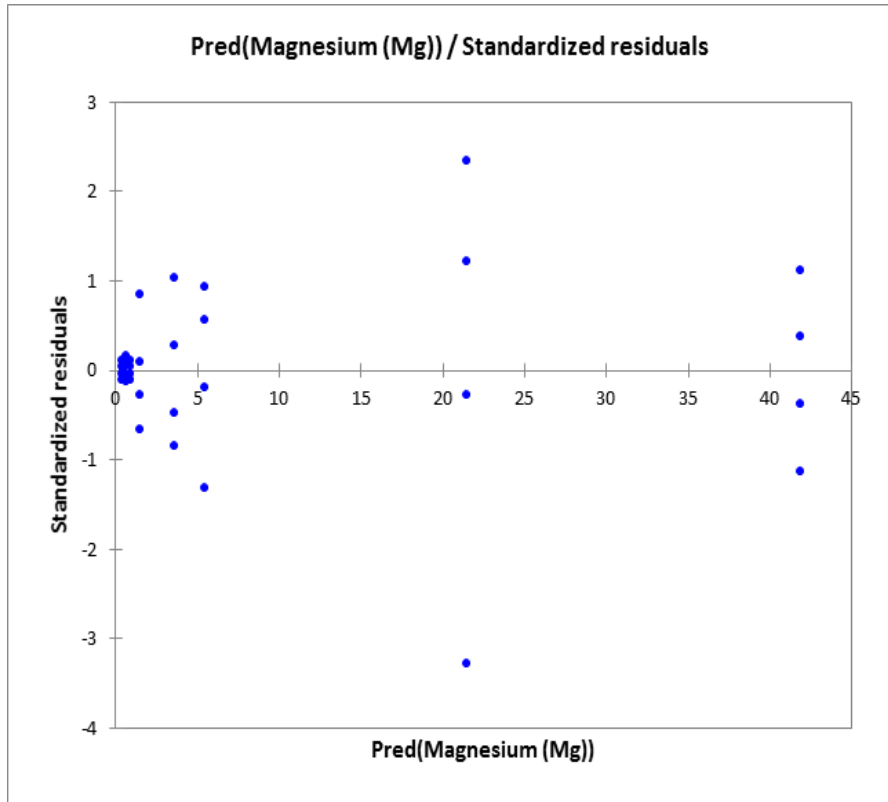


**Figure C.20a: Pred(Magnesium (Mg))/Standardized residuals**

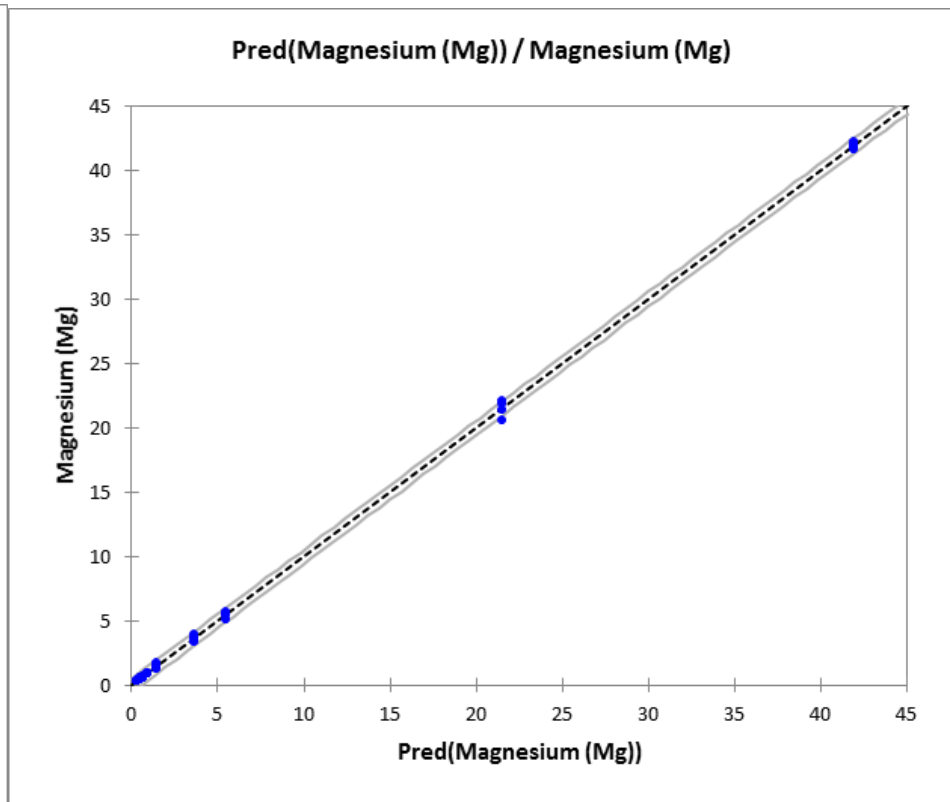


**Figure C.20b: Pred(Magnesium (Mg))/ chromium**



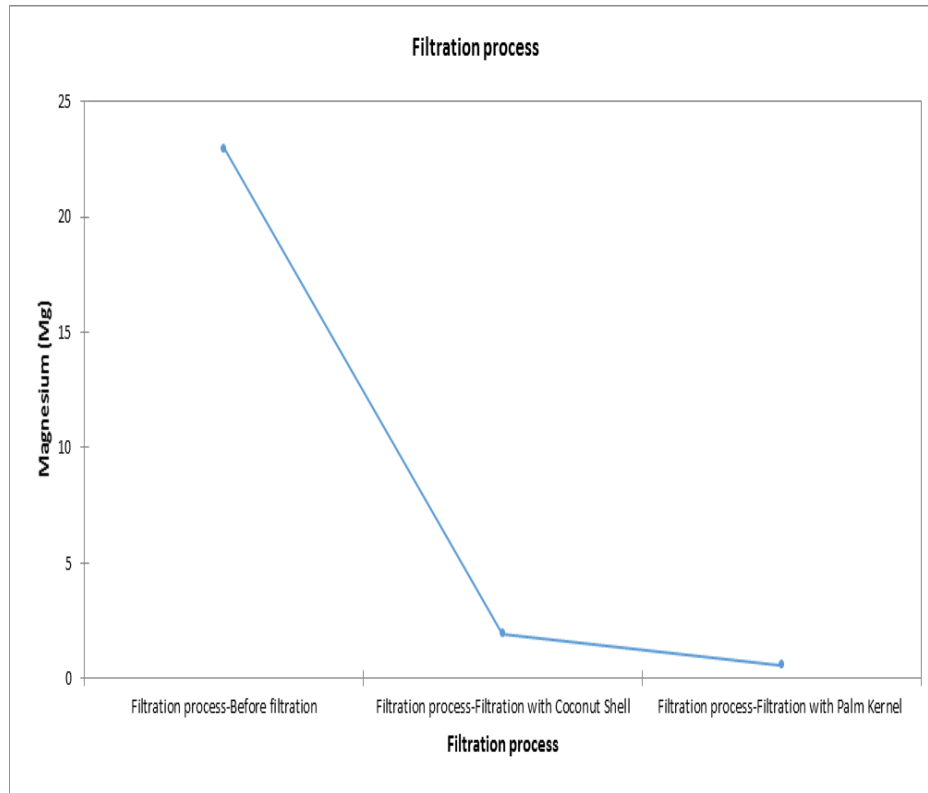


**Figure C.21a: Magnesium Samples**

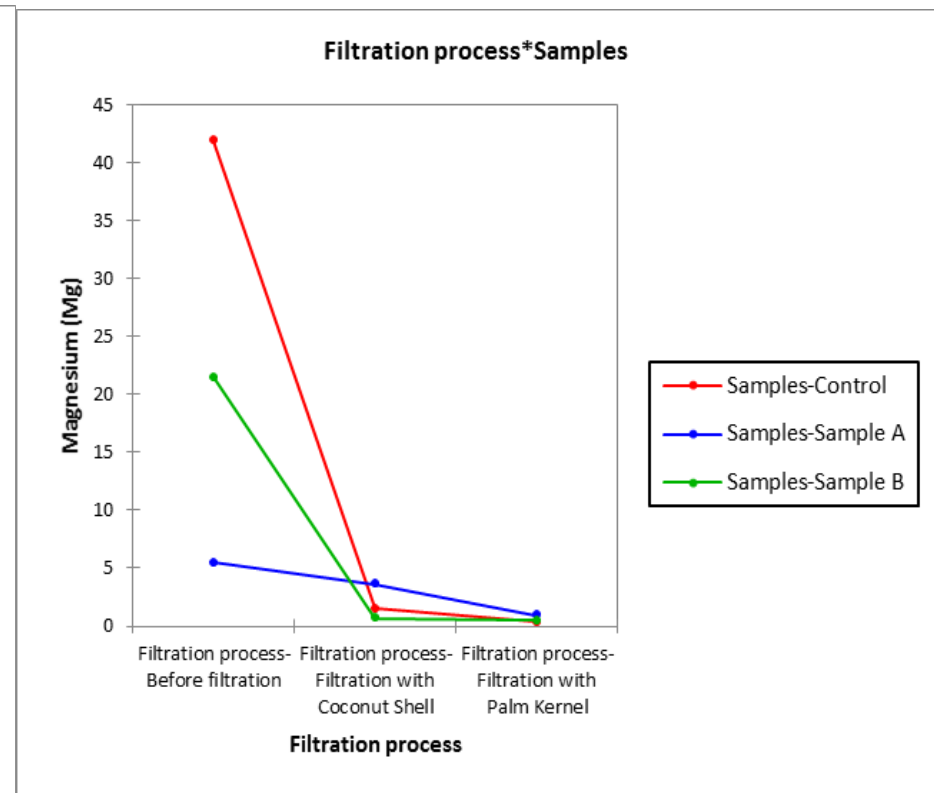


**Figure C.21b: Filtration process\* Magnesium Samples**

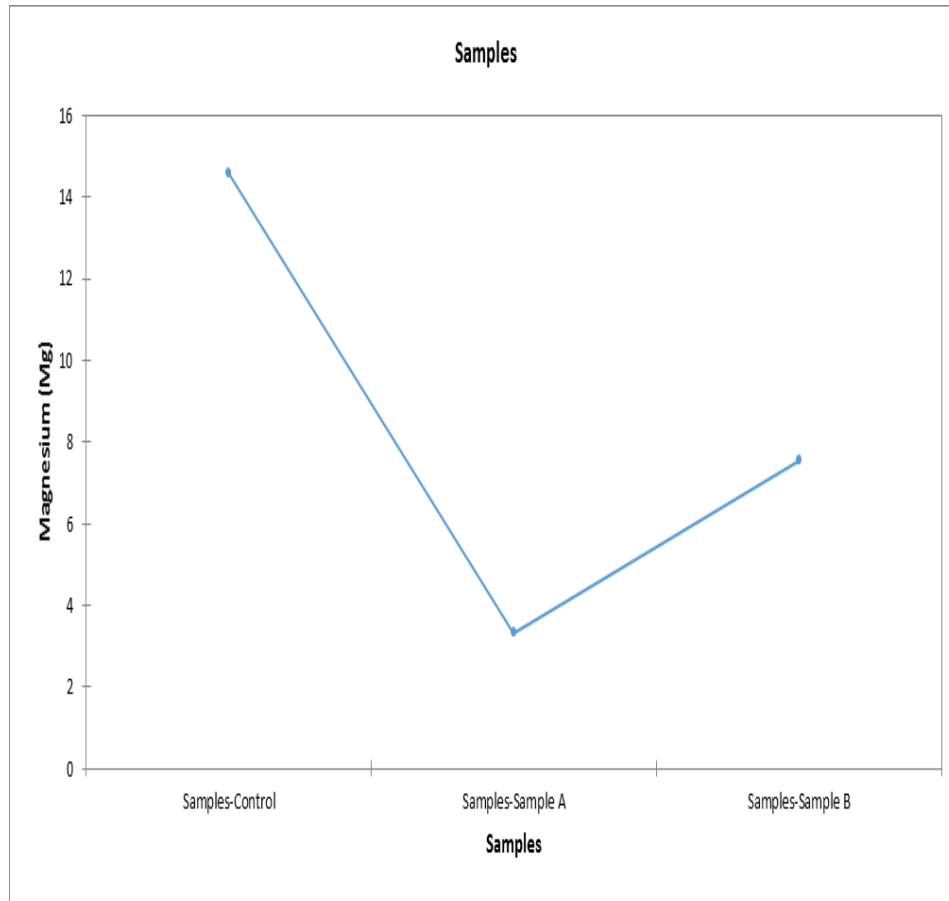


Figure C.22a: Filtration process

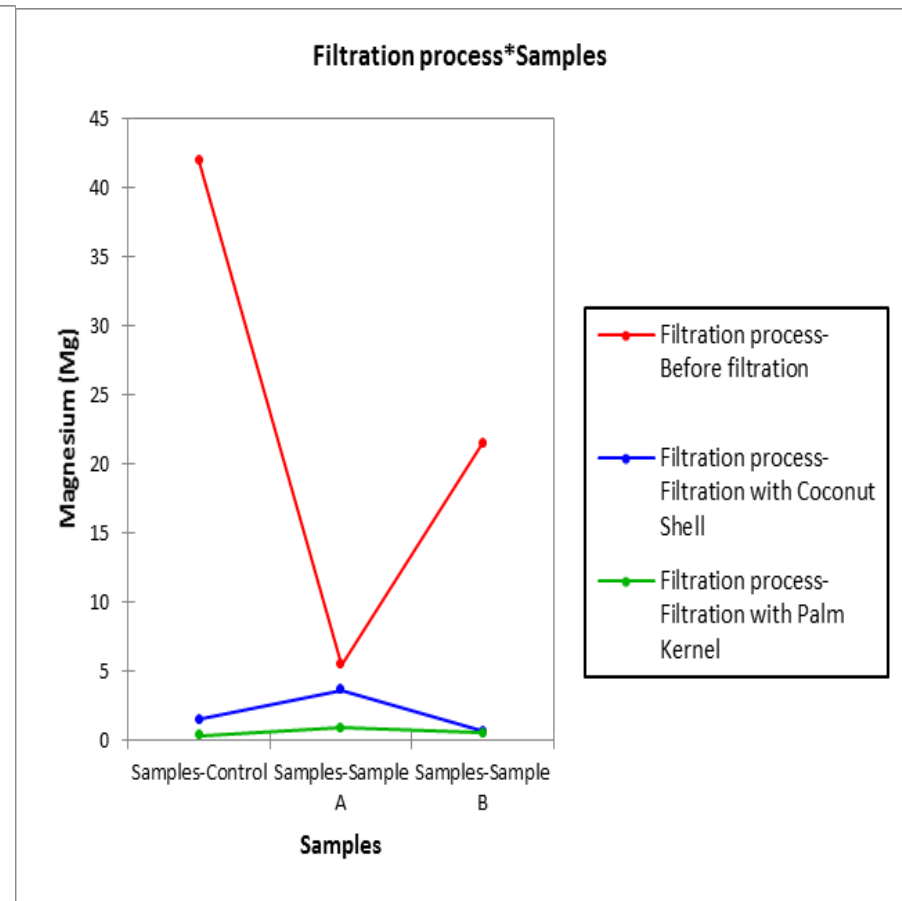


Figure C.22b: Filtration process\* Magnesium Samples

**APPENDIX D: EQUATION OF THE MODEL (HEAVY METALS)**

**D.1 Equation of the model (Variable Copper (Cu)):**

$$\text{Copper (Cu)} = 0.23000 - 0.01000 * \text{Filtration process-Before filtration} + 0.56000 * \text{Filtration process-Filtration with Coconut Shell} + 0.22750 * \text{Samples-Control} + 0.17000 * \text{Samples-Sample A} - 0.44660 * \text{Filtration process-Before filtration} * \text{Samples-Control} - 0.24000 * \text{Filtration process-Before filtration} * \text{Samples-Sample A} - 1.01660 * \text{Filtration process-Filtration with Coconut Shell} * \text{Samples-Control} - 0.18000 * \text{Filtration process-Filtration with Coconut Shell} * \text{Samples-Sample A}$$

**Table D.1.1: Model parameters (Variable Copper (Cu))**

Source	Value	Standard error	t	Pr >  t	Lower bound (95%)	Upper bound (95%)
Intercept	0.2300	0.0762	3.0203	0.0055	0.0738	0.3862
Filtration process-Before filtration	-0.0100	0.1077	-0.0929	0.9267	-0.2310	0.2110
Filtration process-Filtration with Coconut Shell	0.5600	0.1077	5.2000	< 0.0001	0.3390	0.7810
Filtration process-Filtration with Palm Kernel	0.0000	0.0000				
Samples-Control	0.2275	0.1077	2.1125	0.0440	0.0065	0.4485
Samples-Sample A	0.1700	0.1077	1.5786	0.1261	-0.0510	0.3910
Samples-Sample B	0.0000	0.0000				
Filtration process-Before filtration*Samples-Control	-0.4466	0.1523	-2.9324	0.0068	-0.7591	-0.1341
Filtration process-Before filtration*Samples-Sample A	-0.2400	0.1523	1.5758	0.1267	-0.5525	0.0725
Filtration process-Before filtration*Samples-Sample B	0.0000	0.0000				
Filtration process-Filtration with Coconut Shell*Samples-Control	-1.0166	0.1523	-6.6750	< 0.0001	-1.3291	-0.7041
Filtration process-Filtration with Coconut Shell*Samples-Sample A	-0.1800	0.1523	-1.1819	0.2476	-0.4925	0.1325
Filtration process-Filtration with Coconut Shell*Samples-Sample B	0.0000	0.0000				
Filtration process-Filtration with Palm Kernel *Samples-Control	0.0000	0.0000				
Filtration process-Filtration with Palm Kernel *Samples-Sample A	0.0000	0.0000				
Filtration process-Filtration with Palm Kernel *Samples-Sample B	0.0000	0.0000				

**Table D.1.2: Filtration process / Tukey (HSD) / Analysis of the differences between the categories with a confidence interval of 95%**

Contrast	Difference	Standardized difference	Critical value	Pr > Diff	Significant
Filtration with Coconut Shell vs Before filtration	0.4000	6.4333	2.4797	< 0.0001	Yes
Filtration with Coconut Shell vs Filtration with Palm Kernel	0.1611	2.5916	2.4797	0.0392	Yes
Filtration with Palm Kernel vs Before filtration	0.2389	3.8418	2.4797	0.0019	Yes
Tukey's d critical value:			3.5068		

Category	LS means	Standard error	Lower bound (95%)	Upper bound (95%)	Groups
Filtration with Coconut Shell	0.5236	0.0440	0.4334	0.6138	A
Filtration with Palm Kernel	0.3625	0.0440	0.2723	0.4527	B
Before filtration	0.1236	0.0440	0.0334	0.2138	C

**Table D.1.3: Samples / Tukey (HSD) / Analysis of the differences between the categories with a confidence interval of 95%**

Contrast	Difference	Standardized difference	Critical value	Pr > Diff	Significant
Sample A vs Control	0.2902	4.6679	2.4797	0.0002	Yes
Sample A vs Sample B	0.0300	0.4825	2.4797	0.8801	No
Sample B vs Control	0.2602	4.1854	2.4797	0.0008	Yes
Tukey's d critical value:			3.5068		

Category	LS means	Standard error	Lower bound (95%)	Upper bound (95%)	Groups
Sample A	0.4433	0.0440	0.3531	0.5335	A
Sample B	0.4133	0.0440	0.3231	0.5035	A
Control	0.1531	0.0440	0.0629	0.2433	B

## D.2 Equation of the model (Variable Iron, Fe):

**Iron, Fe = 3.40000-0.05000\*Filtration process-Before filtration+10.72500\*Filtration process-Filtration with Coconut Shell-2.25000\*Samples-Control+5.10000\*Samples-Sample A+0.40250\*Filtration process-Before filtration\*Samples-Control-3.80000\*Filtration process-Before filtration\*Samples-Sample A-8.22500\*Filtration process-Filtration with Coconut Shell\*Samples-Control-5.72500\*Filtration process-Filtration with Coconut Shell\*Samples-Sample A**

**TableD.2.1: Model parameters (Variable Iron, Fe)**

Source	Value	Standard error	t	Pr >  t	Lower bound (95%)	Upper bound (95%)
<b>Intercept</b>	3.4000	0.2293	14.8250	< 0.0001	2.9294	3.8706
<b>Filtration process-Before filtration</b>	-0.0500	0.3243	-0.1542	0.8786	-0.7155	0.6155
<b>Filtration process-Filtration with Coconut Shell</b>	10.7250	0.3243	33.0672	< 0.0001	10.0595	11.3905
<b>Filtration process-Filtration with Palm Kernel</b>	0.0000	0.0000				
<b>Samples-Control</b>	-2.2500	0.3243	-6.9372	< 0.0001	-2.9155	-1.5845
<b>Samples-Sample A</b>	5.1000	0.3243	15.7243	< 0.0001	4.4345	5.7655
<b>Samples-Sample B</b>	0.0000	0.0000				
<b>Filtration process-Before filtration*Samples-Control</b>	0.4025	0.4587	0.8775	0.3880	-0.5386	1.3436
<b>Filtration process-Before filtration*Samples-Sample A</b>	-3.8000	0.4587	-8.2846	< 0.0001	-4.7411	-2.8589
<b>Filtration process-Before filtration*Samples-Sample B</b>	0.0000	0.0000				
<b>Filtration process-Filtration with Coconut Shell*Samples-Control</b>	-8.2250	0.4587	-17.9317	< 0.0001	-9.1661	-7.2839
<b>Filtration process-Filtration with Coconut Shell*Samples-Sample A</b>	-5.7250	0.4587	-12.4813	< 0.0001	-6.6661	-4.7839
<b>Filtration process-Filtration with Coconut Shell*Samples-Sample B</b>	0.0000	0.0000				
<b>Filtration process-Filtration with Palm Kernel *Samples-Control</b>	0.0000	0.0000				
<b>Filtration process-Filtration with Palm Kernel *Samples-Sample A</b>	0.0000	0.0000				
<b>Filtration process-Filtration with Palm Kernel *Samples-Sample B</b>	0.0000	0.0000				

**Table D.2.2: Filtration process / Tukey (HSD) / Analysis of the differences between the categories with a confidence interval of 95%**

Contrast	Difference	Standardized difference	Critical value	Pr > Diff	Significant
Filtration with Coconut Shell vs Before filtration	7.2575	38.7568	2.4797	< 0.0001	Yes
Filtration with Coconut Shell vs Filtration with Palm Kernel	6.0750	32.4420	2.4797	< 0.0001	Yes
Filtration with Palm Kernel vs Before filtration	1.1825	6.3148	2.4797	< 0.0001	Yes
Tukey's d critical value:			3.5068		

Category	LS means	Standard error	Lower bound (95%)	Upper bound (95%)	Groups
Filtration with Coconut Shell	10.4250	0.1324	10.1533	10.6967	A
Filtration with Palm Kernel	4.3500	0.1324	4.0783	4.6217	B
Before filtration	3.1675	0.1324	2.8958	3.4392	C

**Table D.2.3: Samples / Tukey (HSD) / Analysis of the differences between the categories with a confidence interval of 95%**

Contrast	Difference	Standardized difference	Critical value	Pr > Diff	Significant
Sample A vs Control	6.7825	36.2202	2.4797	< 0.0001	Yes
Sample A vs Sample B	1.9250	10.2800	2.4797	< 0.0001	Yes
Sample B vs Control	4.8575	25.9403	2.4797	< 0.0001	Yes
Tukey's d critical value:			3.5068		

Category	LS means	Standard error	Lower bound (95%)	Upper bound (95%)	Groups
Sample A	8.8833	0.1324	8.6116	9.1550	A
Sample B	6.9583	0.1324	6.6866	7.2300	B
Control	2.1008	0.1324	1.8291	2.3725	C

**D.3 Equation of the model (Variable Zinc, Zn):**

$$\text{Zinc, Zn} = 5.45000 + 9.12500 * \text{Filtration process-Before filtration} - 0.05000 * \text{Filtration process-Filtration with Coconut Shell} + 2.87500 * \text{Samples-Control} + 4.92500 * \text{Samples-Sample A} - 14.61750 * \text{Filtration process-Before filtration} * \text{Samples-Control} - 3.02500 * \text{Filtration process-Before filtration} * \text{Samples-Sample A} - 7.60500 * \text{Filtration process-Filtration with Coconut Shell} * \text{Samples-Control} - 4.48750 * \text{Filtration process-Filtration with Coconut Shell} * \text{Samples-Sample A}$$

**Table D.3.1: Model parameters (Variable Zinc, Zn)**

Source	Value	Standard error	t	Pr >  t	Lower bound (95%)	Upper bound (95%)
Intercept	5.4500	0.1954	27.8909	< 0.0001	5.0491	5.8509
Filtration process-Before filtration	9.1250	0.2763	33.0205	< 0.0001	8.5580	9.6920
Filtration process-Filtration with Coconut Shell	-0.0500	0.2763	-0.1809	0.8578	-0.6170	0.5170
Filtration process-Filtration with Palm Kernel	0.0000	0.0000				
Samples-Control	2.8750	0.2763	10.4037	< 0.0001	2.3080	3.4420
Samples-Sample A	4.9250	0.2763	17.8220	< 0.0001	4.3580	5.4920
Samples-Sample B	0.0000	0.0000				
Filtration process-Before filtration * Samples-Control	-14.6175	0.3908	-37.4032	< 0.0001	-15.4194	-13.8156
Filtration process-Before filtration * Samples-Sample A	-3.0250	0.3908	-7.7404	< 0.0001	-3.8269	-2.2231
Filtration process-Before filtration * Samples-Sample B	0.0000	0.0000				
Filtration process-Filtration with Coconut Shell * Samples-Control	-7.6050	0.3908	-19.4596	< 0.0001	-8.4069	-6.8031
Filtration process-Filtration with Coconut Shell * Samples-Sample A	-4.4875	0.3908	-11.4826	< 0.0001	-5.2894	-3.6856
Filtration process-Filtration with Coconut Shell * Samples-Sample B	0.0000	0.0000				
Filtration process-Filtration with Palm Kernel * Samples-Control	0.0000	0.0000				
Filtration process-Filtration with Palm Kernel * Samples-Sample A	0.0000	0.0000				
Filtration process-Filtration with Palm Kernel * Samples-Sample B	0.0000	0.0000				

**Table D.3.2: Filtration process / Tukey (HSD) / Analysis of the differences between the categories with a confidence interval of 95%**

Contrast	Difference	Standardized difference	Critical value	Pr > Diff	Significant
Before filtration vs Filtration with Coconut Shell	7.3250	45.9112	2.4797	< 0.0001	Yes
Before filtration vs Filtration with Palm Kernel	3.2442	20.3336	2.4797	< 0.0001	Yes
Filtration with Palm Kernel vs Filtration with Coconut Shell	4.0808	25.5776	2.4797	< 0.0001	Yes
Tukey's d critical value:			3.5068		

Category	LS means	Standard error	Lower bound (95%)	Upper bound (95%)	Groups
Before filtration	11.2942	0.1128	11.0627	11.5256	A
Filtration with Palm Kernel	8.0500	0.1128	7.8185	8.2815	B
Filtration with Coconut Shell	3.9692	0.1128	3.7377	4.2006	C

**Table D.3.3: Samples / Tukey (HSD) / Analysis of the differences between the categories with a confidence interval of 95%**

Contrast	Difference	Standardized difference	Critical value	Pr > Diff	Significant
Sample A vs Control	6.9533	43.5817	2.4797	< 0.0001	Yes
Sample A vs Sample B	2.4208	15.1732	2.4797	< 0.0001	Yes
Sample B vs Control	4.5325	28.4086	2.4797	< 0.0001	Yes
Tukey's d critical value:			3.5068		

Category	LS means	Standard error	Lower bound (95%)	Upper bound (95%)	Groups
Sample A	10.8958	0.1128	10.6644	11.1273	A
Sample B	8.4750	0.1128	8.2435	8.7065	B
Control	3.9425	0.1128	3.7110	4.1740	C



#### D.4 Equation of the model (Variable Cadmium, Cd):

**Cadmium, Cd = 0.03000\*Filtration process-Before filtration+0.00090\*Filtration process-Filtration with Coconut Shell+0.01750\*Samples-Sample A-0.01000\*Filtration process-Before filtration\*Samples-Control-0.02750\*Filtration process-Before filtration\*Samples-Sample A-0.01750\*Filtration process-Filtration with Coconut Shell\*Samples-Sample A**

**Table D.4.1: Model parameters (Variable Cadmium, Cd)**

Source	Value	Standard error	t	Pr >  t	Lower bound (95%)	Upper bound (95%)
Intercept	0.0000	0.0028	0.0000	1.0000	-0.0058	0.0058
Filtration process-Before filtration	0.0300	0.0040	7.4527	< 0.0001	0.0217	0.0383
Filtration process-Filtration with Coconut Shell	0.0009	0.0040	0.2236	0.8248	-0.0074	0.0092
Filtration process-Filtration with Palm Kernel	0.0000	0.0000				
Samples-Control	0.0000	0.0040	0.0000	1.0000	-0.0083	0.0083
Samples-Sample A	0.0175	0.0040	4.3474	0.0002	0.0092	0.0258
Samples-Sample B	0.0000	0.0000				
Filtration process-Before filtration*Samples-Control	-0.0100	0.0057	-1.7566	0.0903	-0.0217	0.0017
Filtration process-Before filtration*Samples-Sample A	-0.0275	0.0057	-4.8307	< 0.0001	-0.0392	-0.0158
Filtration process-Before filtration*Samples-Sample B	0.0000	0.0000				
Filtration process-Filtration with Coconut Shell*Samples-Control	0.0000	0.0057	0.0000	1.0000	-0.0117	0.0117
Filtration process-Filtration with Coconut Shell*Samples-Sample A	-0.0175	0.0057	-3.0741	0.0048	-0.0292	-0.0058
Filtration process-Filtration with Coconut Shell*Samples-Sample B	0.0000	0.0000				
Filtration process-Filtration with Palm Kernel *Samples-Control	0.0000	0.0000				
Filtration process-Filtration with Palm Kernel *Samples-Sample A	0.0000	0.0000				
Filtration process-Filtration with Palm Kernel *Samples-Sample B	0.0000	0.0000				

**Table D.4.2: Filtration process / Tukey (HSD) / Analysis of the differences between the categories with a confidence interval of 95%**

Contrast	Difference	Standardized difference	Critical value	Pr > Diff	Significant
Before filtration vs Filtration with Coconut Shell	0.0224	9.6527	2.4797	< 0.0001	<b>Yes</b>
Before filtration vs Filtration with Palm Kernel	0.0175	7.5299	2.4797	< 0.0001	<b>Yes</b>
Filtration with Palm Kernel vs Filtration with Coconut Shell	0.0049	2.1227	2.4797	0.1040	<b>No</b>
<b>Tukey's d critical value:</b>			3.5068		

Category	LS means	Standard error	Lower bound (95%)	Upper bound (95%)	Groups
Before filtration	0.0233	0.0016	0.0200	0.0267	<b>A</b>
Filtration with Palm Kernel	0.0058	0.0016	0.0025	0.0092	<b>B</b>
Filtration with Coconut Shell	0.0009	0.0016	-0.0025	0.0043	<b>B</b>

**Table D.4.3: Samples / Tukey (HSD) / Analysis of the differences between the categories with a confidence interval of 95%**

Contrast	Difference	Standardized difference	Critical value	Pr > Diff	Significant
Sample A vs Control	0.0058	2.5100	2.4797	0.0468	<b>Yes</b>
Sample A vs Sample B	0.0025	1.0757	2.4797	0.5370	<b>No</b>
Sample B vs Control	0.0033	1.4343	2.4797	0.3380	<b>No</b>
Tukey's d critical value:			3.5068		

Category	LS means	Standard error	Lower bound (95%)	Upper bound (95%)	Groups
Sample A	0.0128	0.0016	0.0094	0.0162	<b>A</b>
Sample B	0.0103	0.0016	0.0069	0.0137	<b>A</b> <b>B</b>
Control	0.0070	0.0016	0.0036	0.0103	<b>B</b>

**D.5 Equation of the model (Variable Lead (Pb)):**

**Lead (Pb) = 2.38750-0.86250\*Filtration process-Before filtration-1.95000\*Filtration process-Filtration with CoconutShell-0.73750\*Samples-Control-0.74000\*Samples-Sample A+0.21250\*Filtration process-Before filtration\*Samples-Control+0.26000\*Filtrationprocess-Before filtration\*Samples-Sample A+0.86250\*Filtration process-Filtration with Coconut Shell\*Samples-Control+0.71250\*Filtration process-Filtration with Coconut Shell\*Samples-SampleA**

**Table D.5.1: Model parameters (Variable Lead (Pb))**

Source	Value	Standard error	t	Pr >  t	Lower bound (95%)	Upper bound (95%)
Intercept	2.3875	0.0962	24.8054	< 0.0001	2.1900	2.5850
Filtration process-Before filtration	-0.8625	0.1361	-6.3365	< 0.0001	-1.1418	-0.5832
Filtration process-Filtration with Coconut Shell	-1.9500	0.1361	-14.3259	< 0.0001	-2.2293	-1.6707
Filtration process-Filtration with Palm Kernel	0.0000	0.0000				
Samples-Control	-0.7375	0.1361	-5.4181	< 0.0001	-1.0168	-0.4582
Samples-Sample A	-0.7400	0.1361	-5.4365	< 0.0001	-1.0193	-0.4607
Samples-Sample B	0.0000	0.0000				
Filtration process-Before filtration*Samples-Control	0.2125	0.1925	1.1039	0.2794	-0.1825	0.6075
Filtration process-Before filtration*Samples-Sample A	0.2600	0.1925	1.3507	0.1880	-0.1350	0.6550
Filtration process-Before filtration*Samples-Sample B	0.0000	0.0000				
Filtration process-Filtration with Coconut Shell*Samples-Control	0.8625	0.1925	4.4806	0.0001	0.4675	1.2575
Filtration process-Filtration with Coconut Shell*Samples-Sample A	0.7125	0.1925	3.7013	0.0010	0.3175	1.1075
Filtration process-Filtration with Coconut Shell*Samples-Sample B	0.0000	0.0000				
Filtration process-Filtration with Palm Kernel *Samples-Control	0.0000	0.0000				
Filtration process-Filtration with Palm Kernel *Samples-Sample A	0.0000	0.0000				
Filtration process-Filtration with Palm Kernel *Samples-Sample B	0.0000	0.0000				

**Table D.5.2: Filtration process / Tukey (HSD) / Analysis of the differences between the categories with a confidence interval of 95%**

Contrast	Difference	Standardized difference	Critical value	Pr > Diff	Significant
Filtration with Palm Kernel vs Filtration with Coconut Shell	1.4250	18.1328	2.4797	< 0.0001	Yes
Filtration with Palm Kernel vs Before filtration	0.7050	8.9709	2.4797	< 0.0001	Yes
Before filtration vs Filtration with Coconut Shell	0.7200	9.1618	2.4797	< 0.0001	Yes
Tukey's d critical value:			3.5068		

Category	LS means	Standard error	Lower bound (95%)	Upper bound (95%)	Groups
Filtration with Palm Kernel	1.8950	0.0556	1.7810	2.0090	A
Before filtration	1.1900	0.0556	1.0760	1.3040	B
Filtration with Coconut Shell	0.4700	0.0556	0.3560	0.5840	C

**Table D.5.3: Samples / Tukey (HSD) / Analysis of the differences between the categories with a confidence interval of 95%**

Contrast	Difference	Standardized difference	Critical value	Pr > Diff	Significant
Sample B vs Sample A	0.4158	5.2914	2.4797	< 0.0001	Yes
Sample B vs Control	0.3792	4.8248	2.4797	0.0002	Yes
Control vs Sample A	0.0367	0.4666	2.4797	0.8874	No
Tukey's d critical value:			3.5068		

Category	LS means	Standard error	Lower bound (95%)	Upper bound (95%)	Groups
Sample B	1.4500	0.0556	1.3360	1.5640	A
Control	1.0708	0.0556	0.9568	1.1849	B
Sample A	1.0342	0.0556	0.9201	1.1482	B

**D.6 Equation of the model (Variable Chromium (Cr)):**

**Chromium (Cr) = 0.13500+0.31000\*Filtration process-Before filtration+0.39250\*Filtration process-Filtration with Coconut Shell-0.07000\*Samples-Control+0.07500\*Samples-Sample A+0.03500\*Filtration process-Before filtration\*Samples-Control-0.12000\*Filtration process-Before filtration\*Samples-Sample A-0.11000\*Filtration process-Filtration with Coconut Shell\*Samples-Control-0.21500\*Filtration process-Filtration with Coconut Shell\*Samples-Sample A**

**Table D.6.1: Model parameters (Variable Chromium (Cr))**

Source	Value	Standard error	t	Pr >  t	Lower bound (95%)	Upper bound (95%)
Intercept	0.1350	0.0216	6.2539	< 0.0001	0.0907	0.1793
Filtration process-Before filtration	0.3100	0.0305	10.1547	< 0.0001	0.2474	0.3726
Filtration process-Filtration with Coconut Shell	0.3925	0.0305	12.8571	< 0.0001	0.3299	0.4551
Filtration process-Filtration with Palm Kernel	0.0000	0.0000				
Samples-Control	-0.0700	0.0305	-2.2930	0.0299	-0.1326	-0.0074
Samples-Sample A	0.0750	0.0305	2.4568	0.0207	0.0124	0.1376
Samples-Sample B	0.0000	0.0000				
Filtration process-Before filtration*Samples-Control	0.0350	0.0432	0.8107	0.4246	-0.0536	0.1236
Filtration process-Before filtration*Samples-Sample A	-0.1200	0.0432	-2.7795	0.0098	-0.2086	-0.0314
Filtration process-Before filtration*Samples-Sample B	0.0000	0.0000				
Filtration process-Filtration with Coconut Shell*Samples-Control	-0.1100	0.0432	-2.5479	0.0168	-0.1986	-0.0214
Filtration process-Filtration with Coconut Shell*Samples-Sample A	-0.2150	0.0432	-4.9800	< 0.0001	-0.3036	-0.1264
Filtration process-Filtration with Coconut Shell*Samples-Sample B	0.0000	0.0000				
Filtration process-Filtration with Palm Kernel *Samples-Control	0.0000	0.0000				
Filtration process-Filtration with Palm Kernel *Samples-Sample A	0.0000	0.0000				
Filtration process-Filtration with Palm Kernel *Samples-Sample B	0.0000	0.0000				

**Table D.6.2: Filtration process / Tukey (HSD) / Analysis of the differences between the categories with a confidence interval of 95%**

Contrast	Difference	Standardized difference	Critical value	Pr > Diff	Significant
Filtration with Coconut Shell vs Filtration with Palm Kernel	0.2842	16.1227	2.4797	< 0.0001	Yes
Filtration with Coconut Shell vs Before filtration	0.0025	0.1418	2.4797	0.9890	No
Before filtration vs Filtration with Palm Kernel	0.2817	15.9809	2.4797	< 0.0001	Yes
<b>Tukey's d critical value:</b>			3.5068		

Category	LS means	Standard error	Lower bound (95%)	Upper bound (95%)	Groups
Filtration with Coconut Shell	0.4208	0.0125	0.3953	0.4464	A
Before filtration	0.4183	0.0125	0.3928	0.4439	A
Filtration with Palm Kernel	0.1367	0.0125	0.1111	0.1622	B

**Table D.6.3: Samples / Tukey (HSD) / Analysis of the differences between the categories with a confidence interval of 95%**

Contrast	Difference	Standardized difference	Critical value	Pr > Diff	Significant
Sample B vs Control	0.0950	5.3900	2.4797	< 0.0001	Yes
Sample B vs Sample A	0.0367	2.0804	2.4797	0.1129	No
Sample A vs Control	0.0583	3.3097	2.4797	0.0073	Yes
Tukey's d critical value:			3.5068		

Category	LS means	Standard error	Lower bound (95%)	Upper bound (95%)	Groups
Sample B	0.3692	0.0125	0.3436	0.3947	A
Sample A	0.3325	0.0125	0.3069	0.3581	A
Control	0.2742	0.0125	0.2486	0.2997	B

**D.7 Equation of the model (Variable Magnesium (Mg)):**

**Magnesium (Mg) = 0.50500+20.97000\*Filtration process-Before filtration+0.14000\*Filtration process-Filtration with Coconut Shell-0.15500\*Samples-Control+0.39500\*Samples-Sample A+20.58000\*Filtration process-Before filtration\*Samples-Control-16.42000\*Filtration process-Before filtration\*Samples-Sample A+0.98500\*Filtration process-Filtration with Coconut Shell\*Samples-Control+2.58500\*Filtration process-Filtration with Coconut Shell\*Samples-Sample A**

**Table D.7.1: Model parameters (Variable Magnesium (Mg))**

Source	Value	Standard error	t	Pr >  t	Lower bound (95%)	Upper bound (95%)
Intercept	0.5050	0.1334	3.7864	0.0008	0.2313	0.7787
Filtration process-Before filtration	20.9700	0.1886	111.1784	< 0.0001	20.5830	21.3570
Filtration process-Filtration with Coconut Shell	0.1400	0.1886	0.7422	0.4643	-0.2470	0.5270
Filtration process-Filtration with Palm Kernel	0.0000	0.0000				
Samples-Control	-0.1550	0.1886	-0.8218	0.4184	-0.5420	0.2320
Samples-Sample A	0.3950	0.1886	2.0942	0.0458	0.0080	0.7820
Samples-Sample B	0.0000	0.0000				
Filtration process-Before filtration*Samples-Control	20.5800	0.2667	77.1529	< 0.0001	20.0327	21.1273
Filtration process-Before filtration*Samples-Sample A	-16.4200	0.2667	-61.5574	< 0.0001	-16.9673	-15.8727
Filtration process-Before filtration*Samples-Sample B	0.0000	0.0000				
Filtration process-Filtration with Coconut Shell*Samples-Control	0.9850	0.2667	3.6927	0.0010	0.4377	1.5323
Filtration process-Filtration with Coconut Shell*Samples-Sample A	2.5850	0.2667	9.6910	< 0.0001	2.0377	3.1323
Filtration process-Filtration with Coconut Shell*Samples-Sample B	0.0000	0.0000				
Filtration process-Filtration with Palm Kernel *Samples-Control	0.0000	0.0000				
Filtration process-Filtration with Palm Kernel *Samples-Sample A	0.0000	0.0000				
Filtration process-Filtration with Palm Kernel *Samples-Sample B	0.0000	0.0000				

**Table D.7.2: Filtration process / Tukey (HSD) / Analysis of the differences between the categories with a confidence interval of 95%**

Contrast	Difference	Standardized difference	Critical value	Pr > Diff	Significant
Before filtration vs Filtration with Palm Kernel	22.3567	205.3003	2.4797	< 0.0001	Yes
Before filtration vs Filtration with Coconut Shell	21.0267	193.0870	2.4797	< 0.0001	Yes
Filtration with Coconut Shell vs Filtration with Palm Kernel	1.3300	12.2133	2.4797	< 0.0001	Yes
Tukey's d critical value:			3.5068		

Category	LS means	Standard error	Lower bound (95%)	Upper bound (95%)	Groups
Before filtration	22.9417	0.0770	22.7837	23.0997	A
Filtration with Coconut Shell	1.9150	0.0770	1.7570	2.0730	B
Filtration with Palm Kernel	0.5850	0.0770	0.4270	0.7430	C

**Table D.7.3: Samples / Tukey (HSD) / Analysis of the differences between the categories with a confidence interval of 95%**

Contrast	Difference	Standardized difference	Critical value	Pr > Diff	Significant
Control vs Sample A	11.2500	103.3083	2.4797	< 0.0001	Yes
Control vs Sample B	7.0333	64.5868	2.4797	< 0.0001	Yes
Sample B vs Sample A	4.2167	38.7215	2.4797	< 0.0001	Yes
Tukey's d critical value:			3.5068		

Category	LS means	Standard error	Lower bound (95%)	Upper bound (95%)	Groups
Control	14.5750	0.0770	14.4170	14.7330	A
Sample B	7.5417	0.0770	7.3837	7.6997	B
Sample A	3.3250	0.0770	3.1670	3.4830	C

**APPENDIX E: BET DATA AND THEORY**



**Table E.1: Brunauer, Emmett and Teller (BET) Summary**

<b>Parameters</b>	<b>Palm Kernel shell</b>	<b>Coconut shells</b>
<b>Surface area (m<sup>2</sup>/g)</b>	717.142	1177.524
<b>Correlation coefficient (r)</b>	0.9994	0.9963
<b>Slope</b>	3.063	2.121
<b>Intercept</b>	1.793e+00	8.361e-01
<b>Constant</b>	2.706	3.537

**Table E.2: Langmuir Summary**

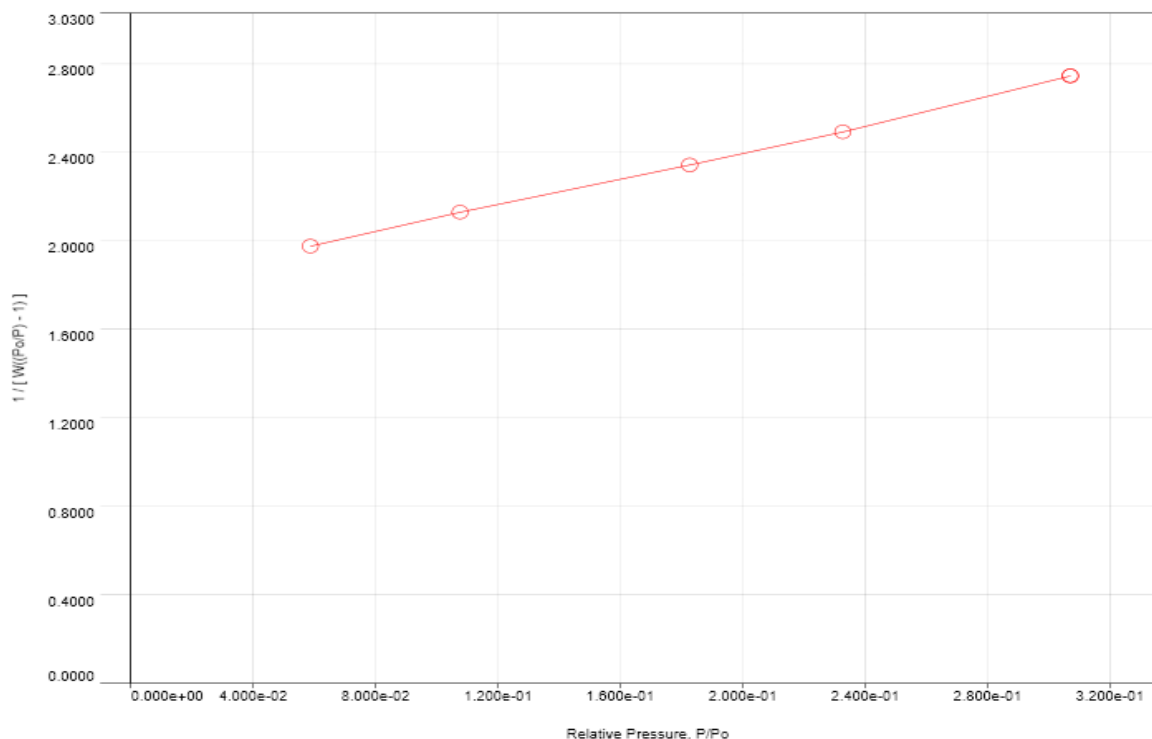
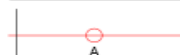
<b>Parameters</b>	<b>Palm Kernel shell</b>	<b>Coconut shells</b>
<b>Surface area (m<sup>2</sup>/g)</b>	23038.720	6641.996
<b>Correlation coefficient (r)</b>	0.663	0.864
<b>Slope</b>	0.15116	0.52432
<b>Intercept</b>	1.87129	0.88741



<b>Analysis</b>		<b>Report</b>	
Operator:	Abdulrahman Abdulkareem	Date:	2008/03/12
Sample ID:	Palmkernel Shell	Operator:	Abdulrahman Abdulkareem
Sample Desc:		Date:	2018/10/19
Sample weight:	0.07 g	Filename:	Palmkernel Shell.qps
Outgas Time:	3.0 hrs	Comment:	
Analysis gas:	Nitrogen	Sample Volume:	1 cc
Press. Tolerance:	0.100/0.100 (ads/des)	OutgasTemp:	250.0 C
Analysis Time:	114.9 min	Bath Temp:	273.0 K
Cell ID:	2	Equil time:	60/60 sec (ads/des)
		End of run:	2008/03/12 21:36:04
		Equil timeout:	240/240 sec (ads/des)
		Instrument:	Nova Station B

**Multi-Point BET Plot**

<b>Adsorbate</b>	Nitrogen	Data Reduction Parameters	
	Molec. Wt.: 28.013	Temperature: 77.350K	Liquid Density: 0.808 g/cc
		Cross Section: 16.200 Å²	



<b>BET summary</b>	
Slope =	3.063
Intercept =	1.793e+00
Correlation coefficient, r =	0.999392
C constant =	2.708
Surface Area =	717.142 m²/g

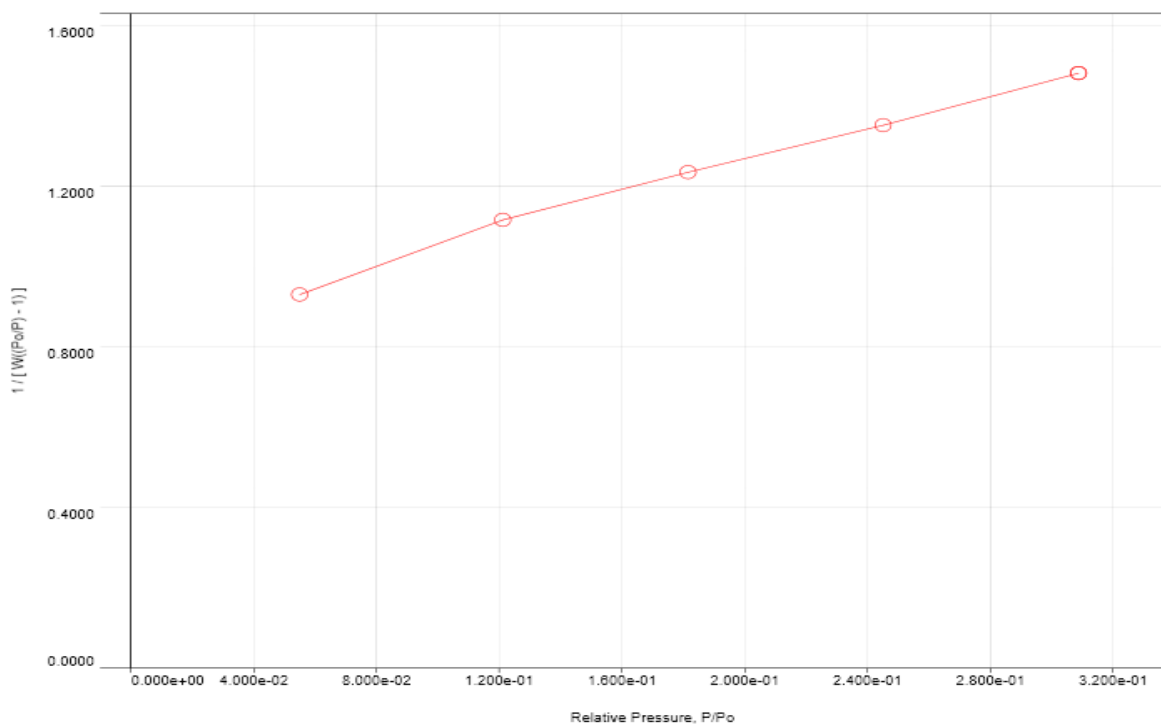
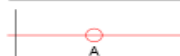
**E.4. Multi-Point BET Plot of Palm kernel Shell**



<b>Analysis</b>		<b>Report</b>	
Operator:	Abdulrahman Abdulkareem	Date:	2008/03/12
Sample ID:	Coconut hell	Filename:	Coconut hell.qps
Sample Desc:		Comment:	
Sample weight:	0.04 g	Sample Volume:	1 cc
Outgas Time:	3.0 hrs	Outgas Temp:	250.0 C
Analysis gas:	Nitrogen	Bath Temp:	273.0 K
Press. Tolerance:	0.100/0.100 (ads/des)	Equil time:	60/60 sec (ads/des)
Analysis Time:	109.8 min	End of run:	2008/03/12 0:53:41
Cell ID:	2	Equil timeout:	240/240 sec (ads/des)
		Instrument:	Nova Station B

**Multi-Point BET Plot**

<b>Adsorbate</b>	Nitrogen	<b>Data Reduction Parameters</b>	
	Molec. Wt.: 28.013	Temperature: 77.350K	Liquid Density: 0.808 g/cc
		Cross Section: 16.200 Å²	



<b>BET summary</b>	
Slope =	2.121
Intercept =	8.361e-01
Correlation coefficient, r =	0.996314
C constant =	3.537
Surface Area =	1177.524 m²/g

**E.5 Multi-Point BET Plot of Coconut Shell**

## **E.6 BET (Brunauer, Emmett and Teller)**

By BET (Brunauer, Emmett and Teller) the specific surface area of a sample is measured including the pore size distribution. This information is used to predict the dissolution rate, as this rate is proportional to the specific surface area. Thus, the surface area can be used to predict bioavailability. Further, it is useful in the evaluation of product performance and manufacturing consistency.

The specific surface determined by BET relates to the total surface area (reactive surface) as all porous structures adsorb the small gas molecules. The surface area determined by BET is thus usually more extensive than the surface area defined by air permeability. The method used complies with Ph. Eu.2.9.26 Method II.

### **Instrument and measuring principle, BET**

The BET instrument applied by Particle Analytical (Micromeritics Gemini 2375 and Gemini V) determines the specific surface area ( $\text{m}^2/\text{g}$ ) of pharmaceutical samples. The samples are dried with nitrogen purging or in a vacuum applying elevated temperatures. Unless otherwise instructed, we use P/P<sub>0</sub> of 0,1, 0,2 and 0,3 as standard measurement points. The volume of gas adsorbed to the surface of the particles was measured at the boiling point of nitrogen (-196°C). The amount of adsorbed gas was correlated to the total surface area of the particles, including pores in the surface. The calculation was based on the BET theory. Traditionally nitrogen is used as adsorbate gas. Gas adsorption also enables the determination of size and volume distribution of micropores (0.35 – 2.0 nm).

## Technical info

Instrument	Micromeritics Gemini 2375 and Gemini V
Sample requirement	Samples dried with Micromeritics Flowprep 060
Measuring range	Micropores (0.35 – 2.0 nm)
Result	The specific surface area in m <sup>2</sup> /g or m <sup>2</sup> /cm <sup>3</sup> .
Sample amount	1 – 2 g of dry substance is typically required for analysis.

## BET theory

The specific surface area of a powder sample was determined by physical adsorption of a gas on the surface of the solid and by calculating the amount of adsorbate gas corresponding to a monomolecular layer on the surface. Physical adsorption results from relatively weak forces (van der Waals forces) between the adsorbate gas molecules and the adsorbent surface area of the test powder sample. The determination is usually carried out at the temperature of liquid nitrogen. The amount of gas adsorbed can be measured by a volumetric or continuous flow procedure.

## Multi-point measurements

The data are treated according to the Brunauer, Emmett and Teller (BET) adsorption isotherm equation:

$$\left[ \frac{1}{V_a \left( \frac{P_0}{P} - 1 \right)} \right] = \frac{C-1}{V_m C} \times \frac{P}{P_0} + \frac{1}{V_m C}$$

$P$  = partial vapour pressure of adsorbate gas in equilibrium with the surface at

77.4 K (b.p. of liquid nitrogen), in pascals,

$P_o$  = saturated pressure of adsorbate gas, in pascals,

$V_a$  = the volume of gas adsorbed at standard temperature and pressure (STP) [273.15 K and atmospheric pressure ( $1.013 \times 10^5$  Pa)], in millilitres,

$V_m$  = the volume of gas adsorbed at STP to produce an apparent monolayer on the sample surface, in millilitres,

$C$  = the dimensionless constant that is related to the enthalpy of adsorption of the adsorbate gas on the powder sample.

A value of  $V_a$  is measured at each of not less than 3 values of  $P/P_o$ . Then the BET value:

$$\frac{1}{V_a \left( \frac{P_o}{P} - 1 \right)}$$

was plotted against  $P/P_o$  according to equation (1). This plot should yield a straight line usually in the approximate relative pressure range 0.05 to 0.3. The data are considered acceptable if the correlation coefficient,  $r$ , of the linear regression is not less than 0.9975; that is,  $r^2$  is not less than 0.995. From the resulting linear plot, the slope, which is equal to  $(C - 1)/V_m C$ , and the intercept, which is equal to  $1/V_m C$ , are evaluated by linear regression analysis. From these values,  $V_m$  is calculated as  $1/(\text{slope} + \text{intercept})$ , while  $C$  is calculated as  $(\text{slope}/\text{intercept}) + 1$ . From the value of  $V_m$  so determined, the specific surface area,  $S$ , in  $\text{m}^2 \cdot \text{g}^{-1}$ , is calculated by the equation:

$N$  = Avogadro constant ( $6.022 \times 10^{23} \text{ mol}^{-1}$ ),

$A$  = the effective cross-sectional area of one adsorbate molecule, in square

metres (0.162 nm<sup>2</sup> for nitrogen and 0.195 nm<sup>2</sup> for krypton),

$M$  = mass of test powder, in grams,

22400 = the volume occupied by 1 mole of the adsorbate gas at STP allowing for minor departures from the ideal, in millilitres.

A minimum of 3 data points is required. Additional measurements may be carried out, primarily when non-linearity is obtained at a P/Po value close to 0.3. Because non-linearity is often achieved at a P/Po value below 0.05, values in this region are not recommended. The test for linearity, the treatment of the data, and the calculation of the specific surface area of the sample are described above.

### Single point measurement

Usually, at least 3 measurements of  $V_a$  each at different values of P/Po are required for the determination of specific surface area by the dynamic flow gas adsorption technique (Method I) or by volumetric gas adsorption (Method II). However, under certain circumstances described below, it may be acceptable to determine the specific surface area of a powder from a single value of  $V_a$  measured at a single value of P/Po such as 0.300 (corresponding to 0.300 moles of nitrogen or 0.001038 mole fraction of krypton), using the following equation for calculating  $V_m$ :

$$S = \frac{V_m N_a}{m \times 22400}$$

The specific surface area is then calculated from the value of  $V_m$  by equation (2) given above.



The single-point method may be employed directly for a series of powder samples of a given material for which the material constant  $C$  is much higher than unity. These circumstances may be verified by comparing values of the specific surface area determined by the single-point method with that specified by the multiple-point method for the series of powder samples. The close similarity between the single-point values and multiple-point values suggests that  $1/C$  approaches zero.

The single-point method may be employed indirectly for a series of very similar powder samples of a given material for which the material constant  $C$  is not infinite but may be assumed to be invariant. Under these circumstances, the error associated with the single-point method can be reduced or eliminated by using the multi-point method to evaluate  $C$  for one of the samples of the series from the BET plot, from which  $C$  is calculated as  $(1 + slope/intercept)$ . Then  $V_m$  is derived from the single value of  $V_a$  measured at a different amount of  $P/P_o$  by the equation:

$$V_m = V_a \left( 1 - \frac{P}{P_0} \right)$$

The specific surface area is calculated from  $V_m$  by equation (2) given above.

The following section describes the methods to be used for the sample preparation, the dynamic flow gas adsorption technique (*Method I*) and the volumetric gas adsorption technique (*Method II*).

**Sample preparation:** Outgassing: Before the specific surface area of the sample can be determined, it is necessary to remove gases and vapours that may have become physically adsorbed onto the surface after manufacture and during treatment, handling and storage. If

outgassing is not achieved, the specific surface area may be reduced or maybe variable because a common region of the surface is covered with molecules of the previously adsorbed gases or vapours. The outgassing conditions are critical for obtaining the required precision and accuracy of specific surface area measurements on pharmaceuticals because of the sensitivity of the surface of the materials.

**Conditions:** The outgassing conditions must be demonstrated to yield reproducible BET plots, a constant weight of test powder, and no detectable physical or chemical changes in the test powder. The outgassing conditions defined by the temperature, pressure and time should be chosen so that the original surface of the solid is reproduced as carefully as possible. Outgassing of many substances is often achieved by applying a vacuum, by purging the sample in a flowing stream of a non-reactive, dry gas, or by using a desorption-adsorption cycling method. In either case, elevated temperatures are sometimes referred to increase the rate at which the contaminants leave the surface. Caution should be exercised when outgassing powder samples using high temperatures to avoid affecting the nature of the surface and the integrity of the sample.

If heating is employed, the recommended temperature and time of outgassing are as low as possible to achieve reproducible measurement of specific surface area in an acceptable time. For outgassing sensitive samples, other outgassing methods such as the desorption-adsorption cycling method may be employed.

### **The volumetric method (Ph. Eu.2.9.26 Method II)**

**Principle:** In a volumetric way (see Figure 2.9.26.-2), recommended adsorbate gas is nitrogen which is admitted into the evacuated space above the previously outgassed powder sample to give a defined equilibrium pressure,  $P$ , of the gas. The use of a diluent gas, such as

helium, is therefore unnecessary, although helium may be employed for other purposes, such as to measure the dead volume.

Since only pure adsorbate gas, instead of a gas mixture, is employed, interfering effects of thermal diffusion are avoided in this method.

**Procedure:** Admit a small amount of dry nitrogen into the sample tube to prevent contamination of the clean surface, remove the sample tube, insert the stopper, and weigh it. Calculate the weight of the sample. Attach the sample tube to the volumetric apparatus. Cautiously evacuate the sample down to the specified pressure (e.g. between 2 Pa and 10 Pa). Alternatively, some instruments operate by evacuating to a defined rate of pressure change (e.g. less than 13 Pa/30 s) and holding for a specified period before commencing the next step.

If the principle of operation of the instrument requires the determination of the dead volume in the sample tube, for example, by the admission of a non-adsorbed gas, such as helium, this procedure is carried out at this point, followed by evacuation of the sample. The determination of dead volume may be avoided using difference measurements, that is, utilising reference and sample tubes connected by a differential transducer. The adsorption of nitrogen gas is then measured as described below.

Raise a Dewar vessel containing liquid nitrogen at 77.4 K up to a defined point on the sample cell. Admit a sufficient volume of adsorbate gas to give the lowest desired relative pressure. Measure the volume adsorbed,  $V_a$ . For multi-point measurements, repeat the analysis of  $V_a$  at successively higher  $P/P_o$  values. When nitrogen is used as the adsorbate gas,  $P/P_o$  values of 0.10, 0.20, and 0.30 are often suitable.

**Reference materials:** Periodically verify the functioning of the apparatus using appropriate reference materials of known surface area, such as  $\alpha$ -alumina, which should have a specific surface area similar to that of the sample to be examined.

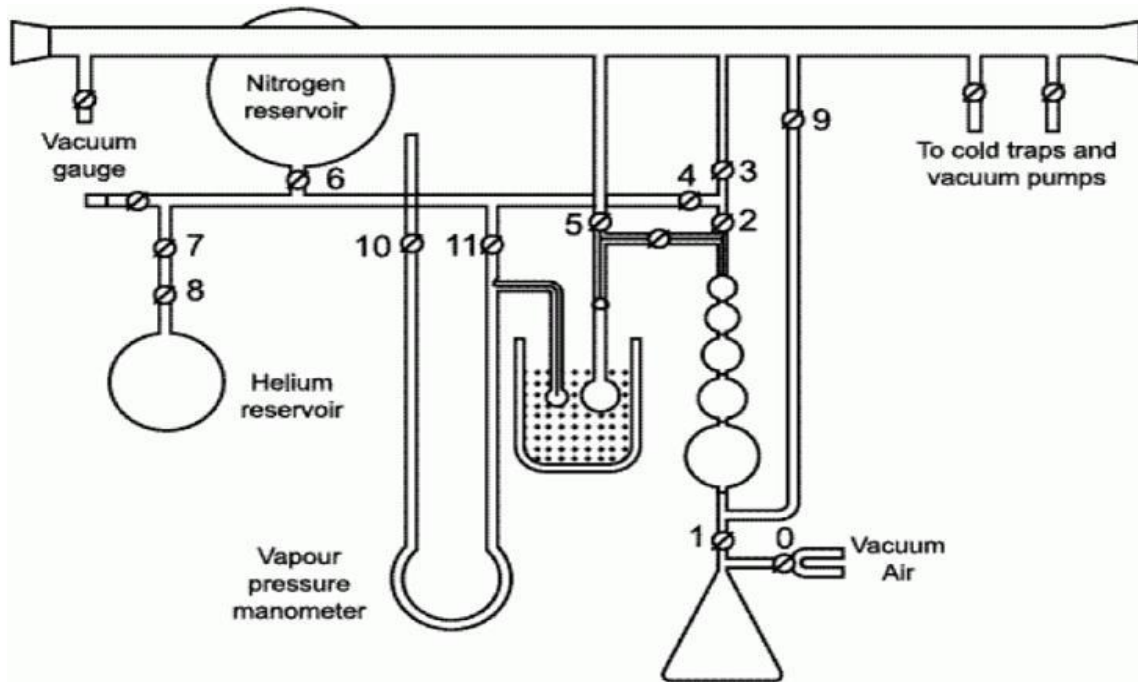
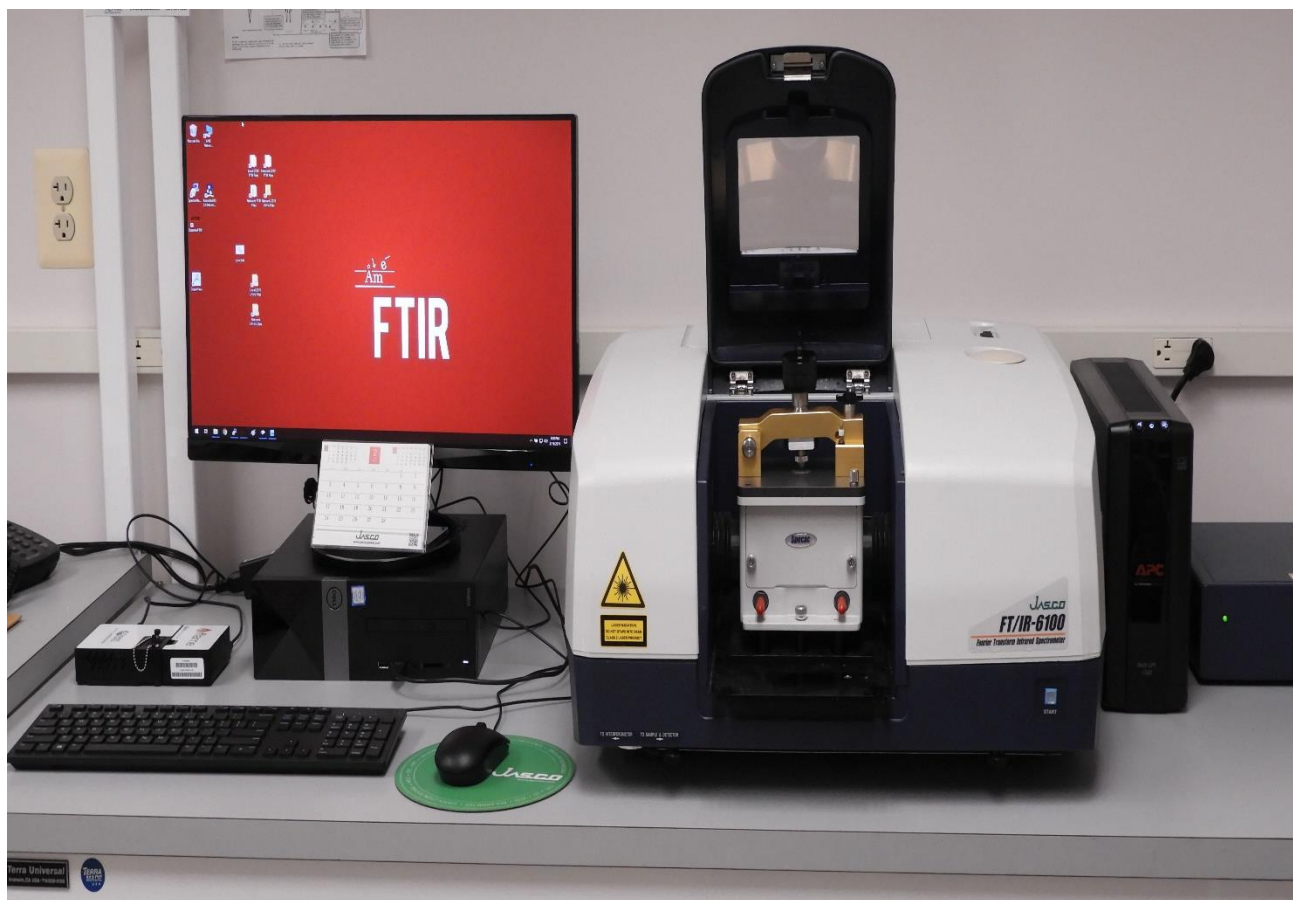


**Figure 1. Schematic diagram of the dynamic flow method apparatus dynamic flow method apparatus**

## APPENDIX F: FTIR SPECTROSCOPY



### JASCO-6100-FTIR-with-Ocean-Systems-FLAME-UV-Vis

#### Principles of FTIR

Fourier Transform-Infrared **Spectroscopy (FTIR)** is an analytical technique **used** to identify organic (and in some cases, inorganic) materials. This technique measures the absorption of infrared radiation by the sample material versus wavelength. The infrared absorption bands identify molecular components and structures.

#### **Advantages of FTIR** are:-

This spectroscopy gives a better signal to noise ratio compared to the dispersive instrument.

With **FTIR**, a spectrum can be obtained very quickly and saves time. Gases, solids as well as the liquid can be analysed with **FTIR**. By using **FTIR**, no external calibration is required and gives accurate results.

## APPENDIX G: SCANNING ELECTRON MICROSCOPY (SEM)



JSM-7610F is an ultra-high resolution Schottky Field Emission Scanning Electron Microscope which has a semi-in-lens objective lens. High power optics can provide high throughput and high-performance analysis. It's also suitable for high spatial resolution analysis. Furthermore, Gentle Beam mode can reduce the incident electron penetration to the specimen, enabling you to observe its topmost surface by using a few hundred landing energy.

### **High-resolution imaging and high-performance analysis by a semi-in-lens objective lens**

The JSM-7610F combines two proven technologies – an electron column with a semi-in-lens objective lens which can provide high resolution imaging by low accelerating voltage and an in-lens Schottky FEG which can offer stable large probe current – to deliver ultrahigh-

resolution with wide range of probe currents for all applications (A few pA to more than 200 nA).

The in-lens Schottky FEG is a combination of a Schottky FEG and the first condenser lens and is designed to collect the electrons from the emitter efficiently.

### **The topmost surface imaging at low accelerating voltage by Gentle Beam mode (GB)**

The Gentle Beam (GB) model applies a negative voltage to a specimen and decelerates incident electrons just before they irradiate the sample; thus, the resolution is improved at an extremely low accelerating voltage.

Therefore, 7610F is possible to observe a topmost surface by a few hundred eV which were challenging to find conventionally and nonconductive samples such as ceramics and semiconductor etc.

### **High throughput and high-performance analysis by High Power Optics**

The High Power Optics produces fine electron probe for both observation and analysis.

The aperture angle control lens maintains a small probe diameter even at a larger probe current.

Using both techniques, the 7610F is suitable for a wide variety of analysis with EDS, WDS, and CL etc

## APPENDIX H: ATOMIC ABSORPTION SPECTROSCOPY (AAS)



### **Buck Scientific 210 VGP Atomic Absorption Spectrophotometer**

Atomic absorption spectroscopy and atomic emission spectroscopy is a spectroanalytical procedure for the quantitative determination of chemical elements using the absorption of optical radiation by free atoms in the gaseous state. Atomic absorption spectroscopy is based on the absorption of light by free metallic ions.

### **Uses of Flame Atomic Absorption Spectrometry**

**Flame Atomic Absorption Spectrometry** is a sensitive technique for the quantitative determination of more than sixty metals. As it is used for determining the concentration of metals it can be applied in Environmental Analysis.